秋田県立大学大学院博士学位論文

Preparation of Functionally Integrated Device with Superwettability and its Applications

（超湿潤性を有する機能統合デバイスの創製とその応用）

陳　柏屹

2017 年 3 月

Abstract

To handle serious oil spills, many strategies have been proposed to design novel materials for oil–water separation. In the past decades, bioinspired surfaces with superwettability have been explored and utilized in oil-water separation. The underwater superoleophobic and superhydrophobic-superoleophilic materials were usually used for oil-water separation. However, their application has been limited because the complex fabricating process, fragile roughness structure, easy to be polluted and lose efficacy. Therefore, this study has aimed on developing simple and versatile strategies to fabricate low cost and robust oil-water separation devices with superwettability.

In Chapter 1, the research backgrounds, fundamental understandings of superwettability, research significance and research purpose were particularly described.

In Chapter 2, the experimental section was presented. The experimental materials, methods and characterizations were particularly described in this chapter.

In Chapter 3, the author has developed a facile method for fabricating underwater low adhesive hydrogel-coated functionally integrated device to separate oil from mixtures with water. The wettability of device surface before and after modification was studied and the oil-water separation efficiency was also investigated. The results showed that the device has realized the effective separation of oil-water mixtures and can be reused. What is more, it also can be used for selective removal of little water from oil surface by means of a magnetic field.

In Chapter 4, the author has developed a versatile and simple strategy to fabricate robust, self-cleaning and superhydrophobic surfaces for both soft and hard substrates by a straightforward spraying method. The wettability of substrate surface before and after modification was studied. The results showed that the superhydrophobic surface was successfully fabricated through the method. Meanwhile, the superhydrophobic surface showed remarkable robustness against knife scratch and sandpaper abrasion. Further, it

could be used for oil-water separation as well as showed excellent separation efficiency and reusability.

In Chapter 5, the author has developed a facile way to make robust, transparent and superhydrophobic surface. Candle soot was used as rough surface template and then the roughness structure was reinforced through chemical vapor deposition method. Further, the surface was modified into superhydrophobic and used for oil-water separation. The wettability of substrate surface before and after modification was tested. Meanwhile, the robustness and oil-water separation efficiency were investigated. The results revealed that the robust, transparent and superhydrophobic surface was successfully fabricated and showed excellent separation efficiency and reusability in oil-water separation.

In chapter 6, general conclusions of the research were made.

Content

Chapter 1 Introduction

1.1 Background

Textile industries, petrochemical, food industries and oil pollution accidents on marine transportation of oil productions have caused extensively oil pollution and has become a serious global environmental problem.[1] For example, the “Deepwater Horizon” oilrig belonging to BP exploded in 2010 and leaked at least 210 million gallons of oil into the Gulf of Mexico, this was the most serious pollution of the last decade.[2] The leaked oil usually polluted the water source people used, the polluted water often contained toxic chemicals, which would threaten people’s health or even made a destructive impact on the ecosystem. Therefore, the development of technique for separation and collection oil pollutions from water is become more and more urgent.

Traditional separation techniques generally include combustion method, solidification method and biodegradation method. Combustion method is simple and direct, which ignite the oil component directly to remove oil from mixture. However, this method has caught further environment pollution and a destruction of ecological environment. Solidification method has been also used in oil-water separation constantly, this method utilizes chemical coagulator to congeal oil component in oil-water mixture. However, this process takes long time and unable to completely congeal oil content, meanwhile, chemical coagulator polluted the environment secondly. Biodegradation method utilize microorganism and enzyme to degrade oil content from oil-water mixture which would completely remove oil content, but this method suffers from high cost. Therefore, these techniques suffer from the limits of high operation cost, low efficiency and secondary pollution. Besides, they are very hard to apply to the separation of oil-water emulsions.[2] Although traditional physical separation materials such as hydrophobic/oleophilic adsorption materials and filtration membranes are widely used in practical applications because of their low cost and high efficiency,[3] they still have two important problems:[6]

First, they are very easy to be polluted by oil which leads to the loss of function. Also, the pores of the material are easy to be clogged and the material surface are very easy to be fouled by organic oil, this would usually lead to a serious reduction of separation efficiency and fluid flow rate. Second, because of the poor mechanical property the separation materials are very difficult to reuse and thus cause secondary contamination to the environment.[4] Furthermore, the safe handling of the oil sorbent waste is challenging, as is the recovery of the absorbed oil.[5]

Therefore, advanced oil-water separation techniques and materials should be develop. The oil-water separation material which can selectively permeate or absorb oil (or water) but repelling water (or oil) would be highly desirable.[7] Because oils and water are intrinsically immiscible, materials with superwettability which have extremely affinities to water or oil are remarkable promising for increasing oil-water separation efficiency.[73, 74] Until now, two different types of oil-water separation materials with superwettability, superhydrophobic/superoleophilic (SHBOI) material and underwater superoleophobic (UWSOB) material have been widely designed, fabricated and used in oil-water separation (Fig. 1-1).

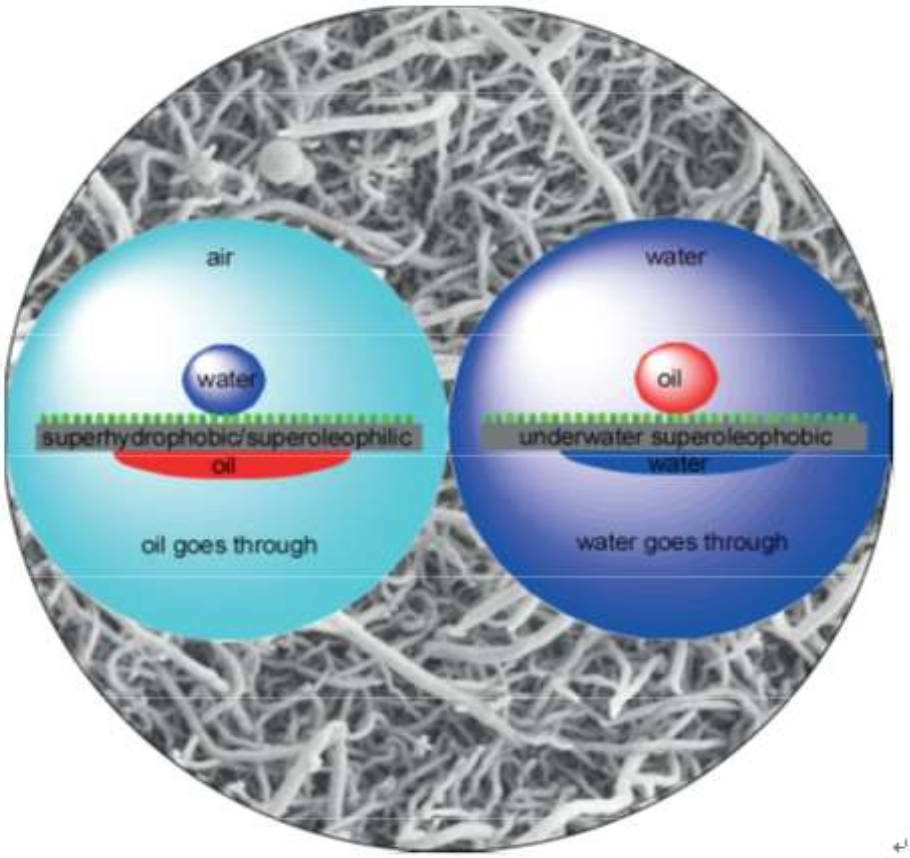

Fig. 1-1 Oil-water separation with SHBOI and UWSOB materials.[5]

Among this two kinds of separation materials, SHBOI surfaces have received broad attention in recent years because they can separate oil-water emulsions or mixtures effectively by selective adsorption or permeation.[73] SHBOI polymeric textiles and metal meshes can be successfully designed and used for oil-water separation, because they can remove the oil selectively by absorption or filtration as membrane. Additionally, UWSOB materials can also be used for oil-water separation, because the materials shows extremely high water affinity while repelling oil.[70]

1.2 Wettability of solid surfaces

Wettability is a very important character of solid surfaces, it has attracted extensive attention for a long time, from cave painting in the ancient to microfluidic devices in the modern. Several superwettability have been disclosed in Fig. 1-2,[4] including superhydrophilic (SHL), superhydrophobic (SHB), superoleophilic (SOL), and

superoleophobic (SOB). When air is changed to water or oil, several other superwettabilities underwater superoleophobic (WSOB), underwater superoleophilic (WSOL), underoil superhydrophobic (OSHB), and underoil superhydrophilic (OSHL) appear. Among these terms, superhydrophobicity is the most typical example of wettability which has been investigated widely.

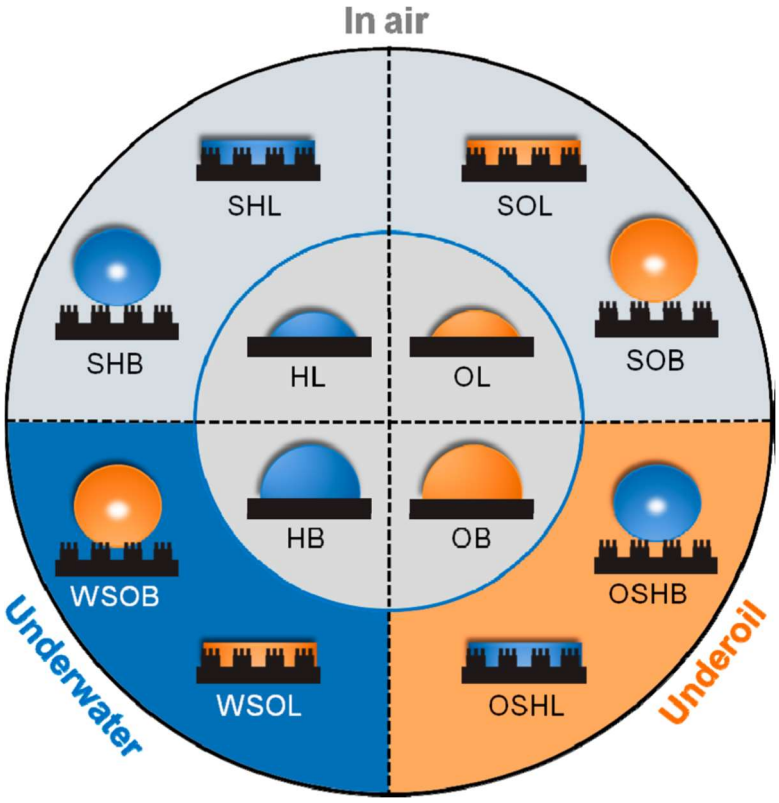

Fig. 1-2 Several different superwettabilities. Surface wettability on a flat solid surface commonly shows four basic states in air (inside inner circle), including hydrophilic (HL), hydrophobic (HB), oleophilic (OL), and oleophobic (OB). Their combination will generate four possible extreme states in air, that is, superhydrophilic (SHL), superhydrophobic (SHB), superoleophilic (SOL), and superoleophobic (SOB). When air is changed to water or oil, there are four possible extreme states: underwater superoleophobic (WSOB), underwater superoleophilic (WSOL), underoil superhydrophobic (OSHB), and underoil superhydrophilic (OSHL).[4]

Historically, as the father of contact angle (CA) and wettability, Thomas Young first described CA in 1804 and 1805.[1] Wenzel explained the contribution of roughness to

hydrophobicity in 1936[2] and 1949.[3] In the following half acentury, most efforts focused on theoretical studies and analytical techniques.[4,5] In 1997, the self-cleaning property of lotus leaves was explained as a result of the microscaled papillae and the epicuticular wax by Barthlott and Neinhuis, they provided a monomicrostructure model.[6] Following, Jiang and his cooperators found the lotus leaf surface possess micro and nanoscaled hierarchical structures, this kind of structure is branch-like nanostructures on the top of micropapillae and results in superhydrophobicity.[7] Thus, the origin of lotus leaf's superhydrophobicity become clear, which was explained from a monoscaled model of microstructures to a dual-scaled model of hierarchical structures. These researches about the lotus leaf activated the field of wettability from surface chemistry, biomimetic study, fundamental theory, and material science. In the following decade, a mass of surfaces with superwettability have been fabricated, besides superhydrophobic surfaces, and have shown promising applications in anti-ice, antibiofouling, self-cleaning, antifogging, microfluidic devices oil-water separation, sensor and smart membrane.

1.2.1 Definition of hydrophobicity and hydrophilicity

Generally, solid surfaces which possess contact angle CA $\theta < 90°$ are defined as hydrophilic. The solid surfaces which possess contact angle CA $> 90°$ are defined as hydrophobic. The CA limit of 90° between hydrophilicity and hydrophobicity originates from Young's equation:[8]

$$\gamma_{SV} = \gamma_{SL} + \gamma_{LV}\cos\theta \rightarrow \cos\theta = \frac{\gamma_{SV} - \gamma_{SL}}{\gamma_{LV}}$$

where γ_{SV}, γ_{SL}, and γ_{LV} represent solid-gas, solid-liquid, and liquid-gas interface tensions, respectively. θ is the balance CA or the intrinsic CA of the materials and can be written as θ_e. The CA is determined by the interactions across the three interfaces on the smooth surface. It is an ideal and simple mathematics and physical model. Here, the solid surface should be an ideally smooth surface which is isotropic, homogeneous and undeformed. Meanwhile, the water droplet is defined as a mathematic entity which has

consistent bulk phase and surface.

In comparison to hydrophobic and hydrophilic surfaces, there are not many efforts devoted to the study of oleophobic and oleophilic surfaces probably because of the complexity and diversity of the oil phase. In a pervasive understanding, solid surfaces with oil CAs $\theta < 90°$ are considered to be oleophilic, and those with oil CAs $\theta > 90°$ are oleophobic. There remain some difficult conundrums, for example, the influence of surface chemical structure of oil droplets, the influence of oil types, surface chemistry, and topography of solid materials.

1.2.2 Definition of superhydrophobicity and superhydrophilicity

Superhydrophobicity was found by Reick in 1976, he found that the shape of water on surface of hydrophobic fumed silicon dioxide particle coatings remained almost spherical and the force of adhesion is negligible.The finding of the lotus effect accelerates the wide use of superhydrophobicity, especially in the past decade. According to the general definition, a superhydrophobic surface has a CA $\theta > 150°$. Surface chemistry and surface roughness are two critical factors to obtain the superhydrophobicity. However, the maximized CA on the flat surfaces is around 118° that depends on the modification of hydrophobic fluoride. The role of surface roughness has been further discussed in the following two main models.

In 1936, to explain the superwettability on rough surfaces, Wenzel modified Young's equation by introducing a factor of surface roughness, r, which is defined as the ratio of the actual area of a rough surface to the geometric projected area.[2,3] Assuming θ^* to be the apparent angle on the rough solid surface, it can be evaluated by considering a small displacement dx of the contact line along the parallel direction of the surface. The total free energy difference dF can be written as

$$dF = r(\gamma SL - \gamma SV)\, dx + \gamma LV \cos \theta^*$$

As F is a minimum, the system will reach a thermodynamic equilibrium. Thus, the

equilibrium condition yields Young's equation when r is equal to 1 and leads to Wenzel's equation for r is larger than 1:

$$\cos \theta^* = r \cos \theta e$$

As r is always larger than 1, surface roughness will enhance surface wettability. That is, (a) when $\theta < \pi/2$, θ^* decreases with the increase of surface roughness and the surface becomes more hydrophilic; and (b) when $\theta > \pi/2$, θ^* increases with the increase of surface roughness and the surface becomes more hydrophobic.

In 1944, Cassie and Baxter derived an equation describing CA hysteresis for composite smooth surfaces with varying degrees of heterogeneity:[9]

$$\cos \theta^* = \Sigma f_i \cos \theta_i$$

where f_i is the fractional area of the surface with a CA of θ_i and $\Sigma f_i = 1$.

Roughness makes it possible for a droplet to have more than one metastable position of equilibrium, and the drop can transfer from one metastable equilibrium to the other, provided that the energy barrier can be overcome.

On the other side, the water contact angle on a superhydrophilic surface should be less than 5° or 10°. We believe that a superhydrophilic surface should have a CA of 0°. A fresh cleaved mica surface or clean glass is simply naturally hydrophilic, but not superhydrophilic, although water seems to spread over them with a CA of a few degrees. Superhydrophilicity of CA 0° cannot be realized on flat homogeneous surface, but it can be achieved on a heterogeneous surface such as TiO_2 surface.[12] Moreover, Drelich and Chibowski suggested to refer to surfaces as superhydrophilic surfaces only for structured surfaces (rough and/or porous) possessing a roughness factor defined by a Wenzel equation larger than 1 ($r > 1$), on which water spreads completely.[13] Also, it can be deducted from the Wenzel equation. Superhydrophilic surfaces cannot be obtained without manipulation of surface roughness of hydrophilic materials.

1.2.3 Measurements of surfaces with superwettability

The static contact angle measurement is often used to characterize the superwettability. Generally the water droplets of different volume from 2 to 5 μL were used to monitor the values of CAs. Importantly, the different fitting modes of the static CA also were used to fit the shapes of water droplets on the surfaces, such as ellipse fitting, circle fitting, tangent searching, and Laplace Young fitting. These differences always result in different observed values of the CAs from around 150° even to 179° with similar shape.[14] For a water droplet of 5 μL, the CA is about 156° by using ellipse fitting; however, the CA can be more than 179° under the Laplace-Young fitting mode. Therefore, the fitting mode should be clearly noted with static CAs to reflect the real situation of solid surface wettability.

When comparing the superhydrophobicity of different surfaces, the CA must be measured using a water droplet with the same volume. Because the CA is affected by the volume of water droplets and the gravity force, 2 or 3 μL might be a suitable volume when measuring CA of water droplet on solid surfaces. However, it is very difficult to obtain a water droplet with volume lower than 4 μL, because of the low water adhesion of many superhydrophobic surfaces.[15] To reduce the influence of the deformation of the water droplet caused by the gravity force, Zhang et al.[14] proposed the new method to measure the CAs by using a much smaller water droplet. First, a 5 μL water droplet is dropped on a superhydrophobic surface with CA around 154°. The volume of the water droplet reached 0.3 μL with a CA of 173° after vaporization for 40 min under ambient conditions.[16]

1.2.4 Nature example with superwettability

After billions of years of evolution, nature has created countless mysterious livings which exhibit excellent functions.[17] To take wettability as an example, people have found many functional natural interfacial materials. These findings have brought us many excellent methods to design and fabricate functional interfacial materials with

superwettability.

As a symbol of purity in many cultures, the lotus leaf is famous for its low-adhesive superhydrophobicity and self-cleaning property. In 1997, W. Barthlott and C. Neihuis discovered that the microstructures and wax materials on the lotus leaf surface contribute to its self-cleaning properties.[6,19] When a water droplet falls on the lotus leaf, the complementary role of micropapillae and hydrophobic wax keeps the droplet with a CA of about 160°. This droplet can easily roll off the surface immediately taking away the adherent dirt particles, the “lotus effect”. Later, Jiang et al. discovered the synergetic effect of micro-nano hierarchical structures on the superhydrophobic lotus leaf.[7] Hierarchical structures in the form of branch-like nanostructures on each papilla are observed. These multiscale structures effectively prevent the underside of pallillae from being wetted.

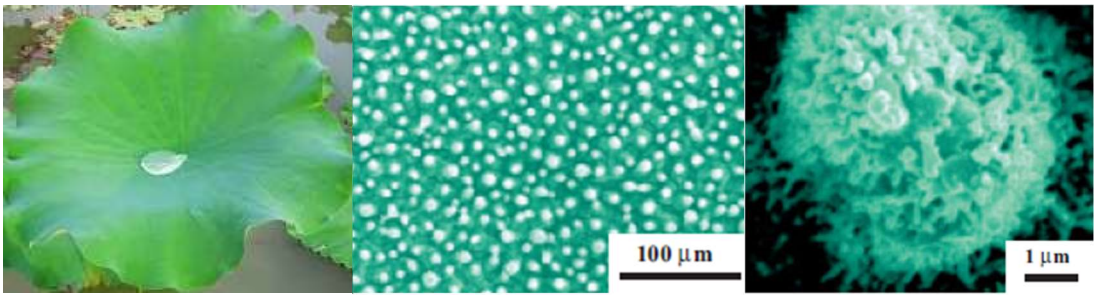

Fig. 1-3 Typical biological materials with superwettability and corresponding multiscale structures. Lotus leaves demonstrate low adhesive, superhydrophobic, and self-cleaning properties, due to randomly distributed micropapillae covered by branch-like nanostructures.[7]

Water strider is famous for its ability of walking freely on the surface of ponds, marshes, and slow streams. Previous investigators thought that the water strider’s leg was hydrophobic and its weight was supported by the surface tension generated by the curvature of the free surface. The hydrodynamic propulsion of the water strider was assumed to rely on momentum transfer by surface waves. This assumption results in Denny’s paradox: the infant water strider, whose legs are too slow to generate waves,

should be impossible to propel itself along the water surface. In 2003, Bush et al. resolved this paradox,[20] and captured the walking process of different insects on the water surface. Their results indicated that capillary waves do not play a critical role in the propulsion of the strider. The strider transferred momentum to the underlying fluid mainly through hemispherical vortices shed by its hairy driving legs. In 2004, Jiang et al. further revealed that the secret of water strider standing effortlessly on the water surface lies in the huge superhydrophobic force of its legs.[21] It is remarkable that the leg does not pierce the water surface until a dimple of ca. 4 mm depth is formed. This robust and durable repellency force from just one leg is enough to support 15 times the total body weight of the water strider. Therefore, the water strider can move freely on the water surface even in a violent storm or torrent.

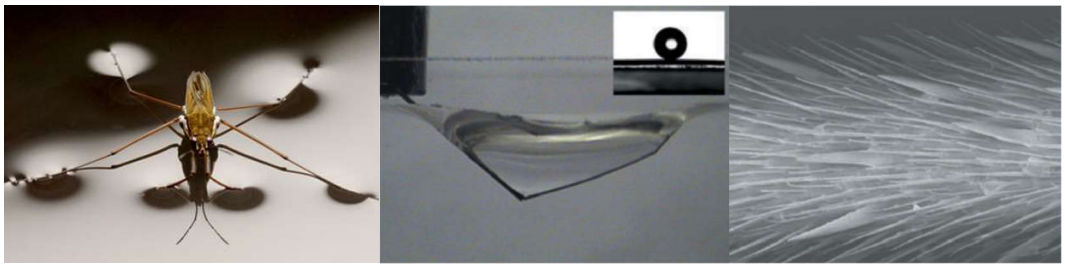

Fig. 1-4 Typical biological materials with superwettability and corresponding multiscale structures. Non-wetting leg of a water strider. Typical side view of a maximal-depth dimple just before the leg pierces the water surface. Scanning electron microscope images of a leg showing numerous oriented spindly microsetae.[21]

Fish scales exhibit a self-cleaning property underwater, in addition to the drag-reducing function.[26] Jiang et al. revealed that fish scales (Crucian Carp, Carassius carassius) have superoleophilicity in air and superoleophobicity underwater.[26] Fish scales are usually covered by a thin layer of mucus, which results in their hydrophilic nature. The fan-shaped fish scales with oriented micropapillae have diameters of 4-5 mm, they are densely arranged on fish body. Each micropapillea has a length of 100-300 μm and a width of 30-40 μm. Surface with micropapillae can be observed nanoscale roughness. These

multiscale structures absorb water and form a water-solid interface which would repell oil, this may be the most important reason of the underwater superoleophobicity of fish scales.[18,27]

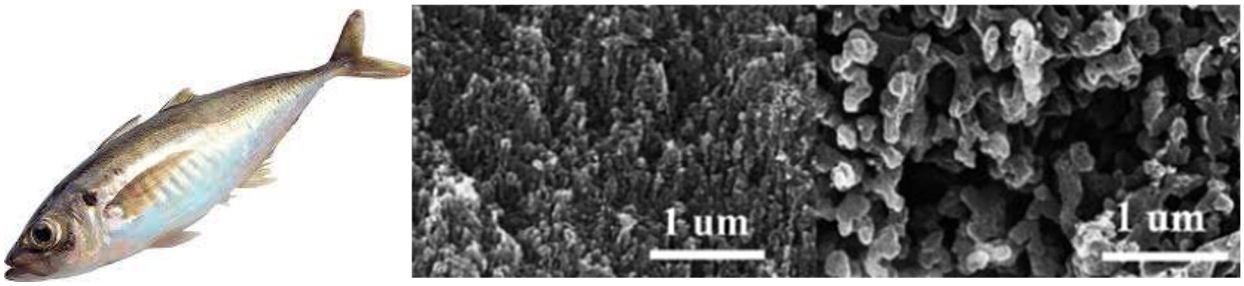

Fig. 1-5 Typical biological materials with superwettability and corresponding multiscale structures. Fish scales present drag reduction, superoleophilicity in air, and superoleophobicity in water due to oriented micropapillae covered by nanostructures.[26]

1.3 Fabrication of SHBOI materials

Recently, more attention has been paid to the control of surface wettability by mimicking the structures of creature surface, the fabrication of SHBOI materials, and extending their potential functional applications in diverse fields. Chemical composition and surface roughness are the two main factors to govern surface wettability. According to biological inspiration (e.g., lotus effect) and the previous bionic research results, there are two ways to prepare SHBOI materials: one is to roughen the surface of low-surface-energy materials, that is, hydrophobic materials, and the other is to modify the rough surface with low-surface-energy materials. Clearly, it is focused on the effective construction of rough surface structures and low-surface-energy coating modification to prepare superhydrophobic surfaces. Many methods including physical, chemical, and the combination of physical and chemical methods have currently been developed to obtain superhydrophobic surfaces in a simple and environment-friendly way. Herein, I will summarize the progress in the preparation of SHBOI materials and their related functions.

1.3.1 Vapor deposition methods

Vapor deposition methods including CVD and PVD can produce perfectly aligned nanostructures with controlled height and diameter. For example, Jiang et al. have prepared various kinds of ACNTs films on quartz-glass substrates by the method of CVD[29,30] such as honeycomb-like, island-like, and postlike. The prepared films behave superhydrophobic with CA higher than 160° and SA lower than 5° due to the micro-nanostructure arrays of the surface.

Since then, superhydrophobic transparent films with nanostructures were prepared by microwave plasma-enhanced CVD on glass, silicon, and PMMA substrates, respectively, by employing TMMOS $(CH_3)_3Si(OCH_3)$) as starting materials.[34,35] Furthermore, the mechanical properties and optical transparence of the films were improved using CO_2 as an additive gas instead of Ar through the combination of microwave plasma-enhanced CVD and oxygen-plasma treatment.

A single-step PVD has also been used to fabricate superhydrophobic surfaces. Miller et al. prepared PTFE thin films with nanoasperities by a vacuum-deposited method, exhibiting the superhydrophobic property with a CA of ~150°.[35] Moreover, Amirfazli et al. reported a SHBOI material with robust chemical stability from the low surface energy of n-hexatriacontane together with therandomly distributed micro-nanostructures.[36]

1.3.2 Spraying methods

The spraying deposition is one of the most well-developed approaches for painting, graphicarts, and industrial coating.[37-41] Zhang et al. fabricated a SHBOI coating through spraying ethanol dispersion of metal alkylcarboxylate on any substrate.[42] This dispersion was prepared through the reaction of metal salt and alkylcarboxyl acid in an ethanol solution. The resultant coating with flower-like hierarchical structures exhibited a stable superrepellent behavior for several oil liquids. Using the spraying process, they

also fabricated the superhydrophobic perfluorooctanoic acid-modified TiO_2-polystyrene nanocomposites coatings[38] and superhydrophobic CNT nanocomposite films.[42] Recently, Park et al. spin-coated a SHBOI surface used a new-developed copolymer. The polymer material is transparent, easy to prepare, low cost, simple and applicable to rough substrates.[43] This process is applicable for a variety of substrates and is not limited to small areas and flat substrates. The superhydrophobicity of those coatings can be easily repaired by spraying the dispersion again when the coating surfaces are damaged by using the cheap coating materials at any time and almost anywhere.

1.3.3 Layer-by-Layer methods

The layer-by-layer (LbL) technique is easy and wide to tune various micro-nanostructures and fabricate SHBOI materials by electrostatic interactions between the different layers such as polyanion and polycation. Shiratori et al. have presented a SHBOI film by the LBL technique.[44] They assembled a polyelectrolyte multilayer containing SiO_2 nanoparticles, and then created a suitable surface morphology for superhydrophobicity by heating the multilayer film to 650 °C.

However, hydrophobic modification is a necessary step in most fabrication processes of superhydrophobic coating via the LBL technique. For example, Rubner et al. prepared a honeycomb-like PAH/PAA multilayer film by the LBL technique, subsequently coated it with silica nanoparticles, and finally modified with semifluorinated silane by CVD.[45] The honeycomb-like structure was fabricated by the suitable acid treatment of polyelectrolyte multilayer films. A single acid treatment produced small pores with diameter of 0.5-2 μm. In comparison, a combined acid treatment led to big pores with a diameter of 10 μm. Thus, they obtained stable superhydrophobic multilayer coating.

The LBL technique can feasibly combine with other techniques together to control surface structures. Zhang et al.[46] fabricated gold-cluster-covered polyelectrolyte multilayer films on indium tin oxide (ITO) by a combination of LBL technique and electrochemical deposition. The film behaved as a stable SHBOI material after further

modification of n-dodecanethiol. The CAs increased gradually with the electrochemical deposition time.

1.4 Fabrication of UWSOB mterials

UWSOB materials appeared as an opposite term to SHBOI materials. A general definition of superhydrophilic surfaces is the surfaces with CAs close to 0°. Similar to the SHBOI materials, surface roughness is a necessary feature of superhydrophilic surfaces, according to the basic principle developed by Wenzel[2] and Cassie and Baxter.[4] For a hydrophilic rough surface, the water can fill in the troughs on the rough surface, resulting in the decrease of apparent CA even to 0° (a superhydrophilic state). Although most efforts have been focused on the fabrication of UWSOB materials, the superhydrophilic surfaces have also received much attention because of their wide practical applications, such as antifogging, antifouling, and self-cleaning. Here, I briefly introduce the recent progress in the fabrication of superhydrophilic surfaces.

In general, any kind of solid surface could be treated to superhydrophilic by chemical and physical approaches. One common approach is to coat hydrophilic inorganic meso- or nanoparticles onto solid surfaces. Because of the attractive self-cleaning capability, titanium oxide[48] and zinc oxide[49] are most studied among inorganic materials because of their photoinduced superhydrophilicity. Moreover, silica nanocoating[48] is well studied due to its highly hydrophilicity and easy availability. Nanoparticles have been coated onto substrates through various methods such as inkjet printing,[50] spin coating,[51] sputtering,[49] sol-gel techniques,[48] solution growth,[52] lithographic techniques,[53] and electrochemical deposition.[54] On the other hand, hydrophilic polymers act as a big group of coating materials for superhydrophilic surfaces. To make the hydrophilic polymer surface rough or to conjugate hydrophilic group onto rough polymer surface are the two main ways make polymer superhydrophilic. Many techniques, such as ion irradiation,[55] electron beam,[56] and plasma treatment,[57] have been widely used to improve the hydrophilicity of polymer surfaces.

It must be pointed out that several kinds of surfaces aroused much attention because of their capability to go from superhydrophobic to superhydrophilic states responding to external stimuli. For example, UV and ozone treatment made carbon nanotube films transform from superhydrophobic to superhydrophilic, and heating in a vacuum recovered the films.[59] Zhang et al.[60] showed that the superhydrophilic micro-nanostructured nylon6,6 surface can be reversed to superhydrophobic after treatment with formic acid and ethanol. A reversible switch between superhydrophilicity and superhydrophobicity was tuned by controlling the adsorption- desorption process of n-dodecanethiol associated with the lightinduced silver nanoparticles on WO_3 nanostructured film.[61]

1.5 Application in oil-water separation

Separation of water and oil mixture is considered a worldwide challenge due to frequent oil spill accidents and the increasing industrial oily wastewater. For example, the flood of oil in the Gulf of Mexico in 2010 is one of the most serious pollution accidents of the last decades. Recently, functional surfaces integrated with both superhydrophobicity and superoleophilicity were proved to be effective in the separation of oil and water mixture. Utilizing different synthesis strategies, a series of SHBOI and UWSOB materials (such as metal mesh, carbon nanotube sponge, polymer film, etc.) have been fabricated and used in oil and water mixture separation, which provide an important avenue for the development of advanced separation techniques.

1.5.1 Oil-water separation with SHBOI materials

Copper meshes and stainless-steel meshes, these kinds of metal meshes made of connected metal strands are used as pore-structured metal membrane. These metal meshes surfaces can be modified into superhydrophobic-superoleophilic. And then, due to the superwettability and pore-structure of meshes, they can be used into oil-water separation. Jiang and his cooperators firstly created the oil-water separation by materials with

superwettability, meanwhile they developed a series of SHBOI materials used for oil-water separation.[73] In 2004, they created an easy, low cost and facile spray-and-dry method to fabricate superhydrophobic and superoleophilic metal meshes used for oil-water separation.[73] Briefly, they prepared a homogeneous polytetrafluoroethylene (PTFE) emulsion which was a low surface energy material. Following, they used water and polyvinyl acetate which was a anionic surfactant sodium dodecyl benzene sulfonate, to fabricate a spay adhesive and then spay onto stainless-steel-mesh substrates. Then the spayed substrates were dried to evaporate water. Finally, the surfactant which was used as an adhesive obtained a PTFE backbone rough surface with micro-nanostructure. The contact angle CA of water on this surface was measured, it showed a result of superhydrophobicity, more than 150°. However, the contact angle CA of oil was about 0° which showed a superoleophilicity. These phenomenons were due to the nano-microscale hierarchical roughness structures combined with the hydrophobic chemical composition of the metal meshes. Because of the superhydrophobicity and superoleophilicity, the modified meshes allowed oil permeating but did not allow spreading and passing through the mesh. As a result, the oil-water mixtures were effectively separated, the oil-water separation by SHBOI material was realized.

Wang and his cooperators[77] created a novel electrospinning method to fabricate the SHBOI materials with a bead-on-string morphology from thermoplastic polyurethane (TPU). Briefly, TPU was added into the mixture of N,N-dimethylformamide and tetrahydrofuran to create a solution, then, this solution was electrospun onto a copper-mesh substrate. This electrospun TPU bead-on-string was hydrophobic, however, after the treatment through hydrophobic silica nanoparticles prepared by heating nano-silica at reflux in toluene in the presence of hexadecyltrimethoxysilane, the modified meshes realized superhydrophobicity and superoleophilicity. Finally, the prepared SHBOI TPU modified copper meshes was used into oil-water separation and showed a high efficiency.

On the other hand, Wang and Guo and their cooperators used a pH responsive material

to modify copper meshes and they obtained a superhydrophobic mesh film.[78] Then, the modified meshes were used into oil-water separation successfully. Biriefly, a thin layer of gold was sputter-coated onto a copper mesh using a facile electrochemical deposition method, then the gold coated mesh got a roughness structure. Following, a mixture of decane-1-thiol and 11-mercaptoundecanoic acid was used to modified the surface of gold coated copper mesh, the mixture possessed a pH-sensitive carboxylic group at one end and a thiol group at the other. A thiol-gold complex formed on the gold surface by bonding with the two thiols. Changing pH value of medium environment can control the carboxylic groups' deprotonation and protonation, therefore, the modified copper mesh surface became a pH-switchable surface, the wettability of the surface can be controlled by the pH value of environment. Meanwhile, the mesh can be successfully used in oil-water separation. They poured an acidic water solution and oil into the upper bottle, the modified mesh allowed the oil pass through and went down to the bottom bottle, but did not allow the water pass through. On the other hand, when they poured a alkaline water solution and oil into the upper bottle, the modified mesh allowed water pass through but not water.

Seeger and Zhang[79] and their cooperators created the novel oil-water separation used SHBOI textiles firstly, they developed an easy one-step chemical vapor deposition method with trichloromethylsilane.[80-82] They used the polyester fabric as a substrate and a dense layer of silicone nanofilaments observed by SEM measurement was coated on the substrate. This chemical vapor deposition coating has changed the wettability of the substrate. [79, 80-83] When the substrate was not coated by silicone nanofilaments, it can be wetted by both oil and water, however, when the substrate was coated by silicone nanofilaments it can be wetted by oil but not water, it showed superhydrophobicity and superoleophilicity simultaneously. Finally, this modified substrate was used for oil-water separation, the substrate was flexible, superhydrophobic and superoleophilic, meanwhile, it showed high separation efficiency and remarkable reusable.

In latest studies,[84, 85] researchers devoted to fabricate robust and more durable superhydrophobic materials for oil-water separations by simple and facile methods. This kind of materials allowed oil pass through or absorb but did not allow water pass through.

1.5.2 Oil-water separation with UWSOB materials

UWSOB materials achieved from combining roughness structure and low surface energy substance can also be used in oil-water separation. A novel UWSOB polyacrylamide-hydrogel modified metal mesh has been proposed by Feng and his cooperators[70]. With this excellent material, water can be separated from oil-water mixtures effectively and selectively because of its water absorption, such as the mixture of water and diesel, crude oil, vegetable oil, gasoline. What is more, this kind of surface cannot be contaminated by oils thus presented a disaffinity for oil droplets, which capacitates the material to realize a high recyclability for repeated separation. As this new material successfully eliminates the weakness of being polluted and hard to be reusable that usually happened in using SHBOI materials, it shows a promising property for applying to the oil spills cleaning up and oil polluted water treatment. In latest researches, a stainless-steel mesh was created by depcositing the sodium silicate and TiO_2 nanoparticles on it, then, it became a self-cleaning UWSOB mesh and can be applied in oil-water separation.[75] With ultraviolet illumination, those TiO_2 nanoparticles can make the contaminants removed conveniently and easily from the mesh and then the pacific recovery ability was achieved. Intelligent surfaces have an ability to change wettability between superoleophilicity and superoleophobicity, we can produce them by utilizing common materials.[76] Through grafting a block copolymer onto those substrates, the intelligent coatings were generated. With protonation and deprotonation, the contained blocks of pH-responsive poly(2-vinylpyridine) (PVP) and oleophilic-hydrophobic polydimethylsiloxane can change its characteristics, such as their wettability and conformation, through changing the value of pH of the aqueous medium, for the purpose to achieve the switchable oil wettability under water. Such materials are also

replaceable to the highly controllable oil-water separation as mentioned by the researchers.

In recent years, UWSOB materials were often used to separate oil-water emulsions successfully. For example, UWSOB materials can be fabricated to a separation film, and the water was allowed to pass through but the oil was remained in upper bottle. Meanwhile, the separation film made by UWSOB materials showed high separation efficiency. Under the driven of gravity force, the UWSOB separation film separated the oil-water emulsion efficiently and showed high water flow rate.

1.6 Purpose of this research

The application of superwetting materials in oil-water separation has been limited because the complex fabricating process, fragile roughness structure, easy to be polluted and lose efficacy. Therefore, this study has aimed on developing simple and versatile strategies to fabricate simple and robust oil-water separation devices with superwettability.

In Chapter 1, the research backgrounds, fundamental understandings of superwettability, research significance and research purpose were particularly described.

In Chapter 2, the experimental section was presented. The experimental materials, methods and characterizations were particularly described in this chapter.

In Chapter 3, I have developed a facile method for fabricating underwater low adhesive hydrogel-coated functionally integrated device to separate oil from mixtures with water. The wettability of device surface before and after modification was studied and the oil-water separation efficiency was also investigated. The results showed that the device has realized the effective separation of oil-water mixtures and can be reused. What is more, it also can be used for selective removal of little water from oil surface by means of a magnetic field.

In Chapter 4, I have developed a versatile and simple strategy to fabricate robust, self-cleaning and superhydrophobic surfaces for both soft and hard substrates by a straightforward spraying method. The wettability of substrate surface before and after modification was studied. The results showed that the superhydrophobic surface was successfully fabricated through the method. Meanwhile, the superhydrophobic surface showed remarkable robustness against knife scratch and sandpaper abrasion. Further, it could be used for oil-water separation as well as showed excellent separation efficiency and reusability.

In Chapter 5, I have developed a facile way to make robust, transparent and superhydrophobic surface. Candle soot was used as rough surface template and then the roughness structure was reinforced through chemical vapor deposition. Further, the surface was used for oil-water separation. The results revealed that the robust, transparent and superhydrophobic surface was successfully fabricated and showed excellent separation efficiency and reusability in oil-water separation.

In chapter 6, general conclusions of the research were made.

Finally, the overall structure of the present research was shown in Fig. 1-6.

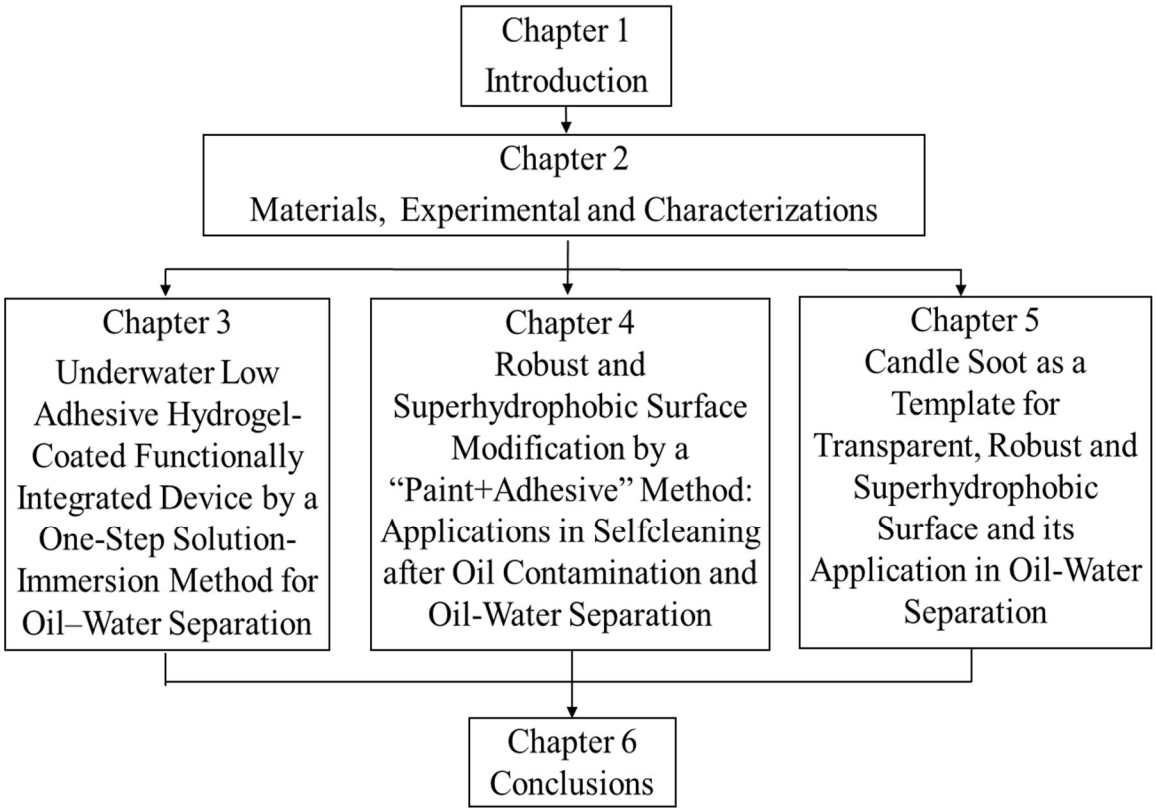

Fig. 1-6 The overall structure of the present research

References

[1] French, R. H. Origins and applications of London dispersion forces and Hamaker constants in ceramics. J. Am. Ceram. Soc. 2000, 83, 2117-2146.

[2] Wenzel, R. N. Resistance of solid surfaces to wetting by water. Ind. Eng. Chem. 1936, 28, 988-994.

[3] Wenzel, R. N. Surface Roughness and Contact Angle. J. Phys. Colloid Chem. 1949, 53, 1466-1467.

[4] Wang, S. T.; Liu, K. S.; Yao, X,; Jiang, L. Bioinspired Surfaces with Superwettability: New Insight on Theory, Design, and Applications. Chem. Rev. 2015, 115, 8230−8293.

[5] (a) Bartell, F. E.; Shepard, J. W. Surface Roughness as Related to Hysteresis of Contact Angles 0.2. The Systems Paraffin-3 Molar Calcium Chloride Solution-Air and Paraffin-Glycerol-Air. J. Phys. Chem. 1953, 57, 455-458. (b) Chu, Z. L.; Feng, Y. J.; Seeger, S. Oil/Water Separation with Selective Superantiwetting/Superwetting Surface Materials. Angew. Chem. Int. Ed. 2015, 54, 2328-2338

[6] Barthlott, W.; Neinhuis, C. Purity of the sacred lotus, or escape from contamination in biological surfaces. Planta. 1997, 202, 1-8.

[7] Feng, L.; Li, S. H.; Li, Y. S.; Li, H. J.; Zhang, L. J.; Zhai, J.; Song, Y. L.; Liu, B. Q.; Jiang, L.; Zhu, D. B. Super-hydrophobic surfaces: From natural to artificial. Adv. Mater. 2002, 14, 1857-1860.

[8] Adamson, A. W.; Gast, A. P. Physical Chemistry of Surfaces, 6th ed. John Wiley & Sons, Inc.: New York. 1997, 353-389.

[9] Johnson, R. E.; Dettre, R. H. Contact Angle Hysteresis. III. Study of an Idealized Heterogeneous Surface. J. Phys. Chem. 1964, 68, 1744-1750.

[12] Wang, R.; Hashimoto, K.; Fujishima, A.; Chikuni, M.; Kojima, E.; Kitamura, A.; Shimohigoshi, M.; Watanabe, T. Light-induced amphiphilic surfaces. Nature. 1997, 388, 431-432.

[13] Drelich, J.; Chibowski, E. Superhydrophilic and superwetting surfaces: Definition and mechanisms of control. Langmuir. 2010, 26, 18621-18623.

[14] Zhang, X.; Shi, F.; Yu, X.; Liu, H.; Fu, Y.; Wang, Z.; Jiang, L.; Li, X. Polyelectrolyte Multilayer as Matrix for Electrochemical Deposition of Gold Clusters: Toward Super-Hydrophobic Surface. J. Am. Chem. Soc. 2004, 126, 3064-3065.

[15] Ferrari, M.; Ravera, F.; Rao, S.; Liggieri, L. Surfactant adsorption at superhydrophobic surfaces. Appl. Phys. Lett. 2006, 89, 053104.

[16] Liu, K.; Du, J.; Wu, J.; Jiang, L. Superhydrophobic gecko feet with high adhesive forces towards water and their bio-inspired materials. Nanoscale. 2012, 4, 768-772.

[17] Aizenberg, J.; Fratzl, P. Biological and Biomimetic Materials. Adv. Mater. 2009, 21, 387-388.

[19] Neinhuis, C.; Barthlott, W. Characterization and distribution of water-repellent, self-cleaning plant surfaces. Ann. Bot. 1997, 79, 667-677.

[20] Hu, D. L.; Chan, B.; Bush, J. W. M. The hydrodynamics of water strider locomotion. Nature. 2003, 424, 663-666.

[21] Gao, X. F.; Jiang, L. Water-repellent legs of water striders. Nature. 2004, 432, 36.

[22] Feng, L.; Zhang, Y.; Xi, J.; Zhu, Y.; Wang, N.; Xia, F.; Jiang, L. Petal effect: a superhydrophobic state with high adhesive force. Langmuir. 2008, 24, 4114-4119.

[23] Bhushan, B.; Her, E. K. Fabrication of Superhydrophobic Surfaces with High and Low Adhesion Inspired from Rose Petal. Langmuir. 2010, 26, 8207-8217.

[24] Feng, L.; Zhang, Y. A.; Li, M. Z.; Zheng, Y. M.; Shen, W. Z.; Jiang, L. The Structural Color of Red Rose Petals and Their Duplicates. Langmuir. 2010, 26, 14885-14888.

[25] Yang, S.; Ju, J.; Qiu, Y.; He, Y.; Wang, X.; Dou, S.; Liu, K.; Jiang, L. Peanut Leaf Inspired Multifunctional Surfaces. Small. 2014, 10, 294-299.

[26] Liu, M. J.; Wang, S. T.; Wei, Z. X.; Song, Y. L.; Jiang, L. Bioinspired Design of a Superoleophobic and Low Adhesive Water/ Solid Interface. Adv. Mater. 2009, 21, 665-669.

[27] Nosonovsky, M.; Bhushan, B. Multiscale effects and capillary interactions in functional biomimetic surfaces for energy conversion and green engineering. Philos. Trans. R. Soc., A. 2009, 367, 1511-1539.

[28] Liu, X.; Zhou, J.; Xue, Z.; Gao, J.; Meng, J.; Wang, S.; Jiang, L. Clam's Shell Inspired High-Energy Inorganic Coatings with Underwater Low Adhesive Superoleophobicity. Adv. Mater. 2012, 24, 3401-3405.

[29] Du, X.; He, J. A self-templated etching route to surface-rough silica nanoparticles for superhydrophobic coatings. ACS Appl. Mater. Interfaces. 2011, 3, 1269-1276.

[30] (a) Li, S.; Feng, L.; Li, H.; Zhai, J.; Song, Y.; Jiang, L.; Zhu, D. B. Super-hydrophobicity of Post-like Aligned Carbon Nanotube Films. Chem. J. Chin. Univ. 2003, 24, 340-342. (b) Li, S.; Li, H.; Wang, X.; Song, Y.; Liu, Y.; Jiang, L.; Zhu, D. Super-Hydrophobicity of Large-Area Honeycomb-Like Aligned Carbon Nanotubes. J. Phys. Chem. B. 2002, 106, 9274-9276.

[31] Hozumi, A.; Takai, O. Preparation of ultra water-repellent films by microwave plasma-enhanced CVD. Thin Solid Films. 1997, 303, 222-225.

[35] Miller, J. D.; Veeramasuneni, S.; Drelich, J.; Yalamanchili, M. R.; Yamauchi, G. Effect of roughness as determined by atomic force microscopy on the wetting properties of PTFE thin films. Polym. Eng. Sci. 1996, 36, 1849-1855.

[36] Tavana, H.; Amirfazli, A.; Neumann, A. Fabrication of superhydrophobic surfaces of n-hexatriacontane. Langmuir. 2006, 22, 5556-5559.

[37] Liu, B.; Fu, Y. Q.; Ruan, W. Q.; He, Y. N.; Wang, X. G. Preparation of super-hydrophobic surfaces by using elastomer templates and UV-curable resin. Acta Polym. Sin. 2008, 2, 155-160.

[38] Bartell, F. E.; Shepard, J. W. Surface Roughness as Related to Hysteresis of Contact Angles 0.1. The System Paraffin Water Air. J. Phys. Chem. 1953, 57, 211-215.

[39] Feng, L.; Li, S.; Li, H.; Zhai, J.; Song, Y.; Jiang, L.; Zhu, D. Super-Hydrophobic Surface of Aligned Polyacrylonitrile Nanofibers. Angew. Chem. 2002, 114, 1269-1271.

[40] Cao, X. P.; Qu, M. N.; Zhao, G. Y.; Wang, Q.; Zhang, J. Y. Fabrication of superhydrophobic surfaces by a Pt nanowire array on Ti/Si substrates. Nanotechnology 2008, 19, 055707.

[41] Kim, D.-H.; Kim, Y.; Kim, B. M.; Ko, J. S.; Cho, C.-R.; Kim, J.- M. Uniform superhydrophobic surfaces using micro/nano complex structures formed spontaneously

by a simple and cost-effective nonlithographic process based on anodic aluminum oxide technology. J. Micromech. Microeng. 2011, 21, 045003.

[42] Johnson Rulon, E.; Dettre Robert, H. Contact Angle Hysteresis II. Contact Angle Measurements on Rough Surfaces In Contact Angle, Wettability, and Adhesion. Adv. Chem. Ser. 1964, 43, 136-144.

[43] Zhang, H.; Zeng, X.; Gao, Y.; Shi, F.; Zhang, P.; Chen, J.-F. A Facile Method To Prepare Superhydrophobic Coatings by Calcium Carbonate. Ind. Eng. Chem. Res. 2011, 50, 3089-3094.

[44] Soeno, T.; Inokuchi, K.; Shiratori, S. Shiratori. Ultra Water-Repellent Surface Resulting from Complicated Microstructure of SiO2 nano particles. Trans. Mater. Res. Soc. Jpn. 2003, 28, 1207.

[45] Zhai, L.; Cebeci, F. C.; Cohen, R. E.; Rubner, M. F. Stable superhydrophobic coatings from polyelectrolyte multilayers. Nano Lett. 2004, 4, 1349-1353.

[47] Zhang, X.; Shi, F.; Yu, X.; Liu, H.; Fu, Y.; Wang, Z.; Jiang, L.; Li, X. Polyelectrolyte multilayer as matrix for electrochemical deposition of gold clusters: toward super-hydrophobic surface. J. Am. Chem. Soc. 2004, 126, 3064-3065.

[48] (c) Permpoon, S.; Houmard, M.; Riassetto, D.; Rapenne, L.; Berthome, G.; Baroux, B.; Joud, J. C.; Langlet, M. Natural and persistent superhydrophilicity of SiO_2/TiO_2 and TiO_2/SiO_2 bi-layer films. Thin Solid Films. 2008, 516, 957-966.

[49] Liu, H.; Feng, L.; Zhai, J.; Jiang, L.; Zhu, D. B. Reversible wettability of a chemical vapor deposition prepared ZnO film between superhydrophobicity and superhydrophilicity. Langmuir. 2004, 20, 5659-5661.

[50] Nakata, K.; Nishimoto, S.; Yuda, Y.; Ochiai, T.; Murakami, T.; Fujishima, A. Rewritable Superhydrophilic-Superhydrophobic Patterns on a Sintered Titanium Dioxide Substrate. Langmuir. 2010, 26,11628-11630.

[51] Song, S.; Jing, L. Q.; Li, S. D.; Fu, H. G.; Luan, Y. B. Superhydrophilic anatase TiO2 film with the micro- and nanometerscale hierarchical surface structure. Mater. Lett. 2008, 62, 3503-3505.

[52] Vernardou, D.; Kalogerakis, G.; Stratakis, E.; Kenanakis, G.; Koudoumas, E.;

Katsarakis, N. Photoinduced hydrophilic and photocatalytic response of hydrothermally grown TiO2 nanostructured thin films. Solid State Sci. 2009, 11, 1499-1502.

[53] Lai, Y.; Lin, C.; Wang, H.; Huang, J.; Zhuang, H.; Sun, L. Superhydrophilic-superhydrophobic micropattern on TiO2 nanotube films by photocatalytic lithography. Electrochem. Commun. 2008, 10, 387-391.

[54] Ye, J. M.; Yin, Q. M.; Zhou, Y. L. Superhydrophilicity of anodic aluminum oxide films: From ″honeycomb″ to ″bird's nest″. Thin Solid Films. 2009, 517, 6012-6015.

[55] Choi, W.-K. Superhydrophilic polymer surface modification by low energy reactive ion beam irradiation using a closed electron Hall drift ion source. Surf. Coat. Technol. 2007, 201, 8099-8104.

[56] Chan, C. M.; Ko, T. M.; Hiraoka, H. Polymer surface modification by plasmas and photons. Surf. Sci. Rep. 1996, 24,1-54.

[57] Kim, H.; Jung, S. J.; Han, Y. H.; Lee, H. Y.; Kim, J. N.; Jang, D. S.; Lee, J. J. The effect of inductively coupled plasma treatment on the surface activation of polycarbonate substrate. Thin Solid Films. 2008,516, 3530-3533.

[59] Wang, H. Z.; Huang, Z. P.; Cai, Q. J.; Kulkarni, K.; Chen, C.L.; Carnahan, D.; Ren, Z. F. Reversible transformation of hydrophobicity and hydrophilicity of aligned carbon nanotube arrays and buckypapers by dry processes. Carbon. 2010, 48, 868-875.

[60] Zhang, L.; Zhang, X. Y.; Dai, Z.; Wu, J. J.; Zhao, N.; Xu, J. Micro-nano hierarchically structured nylon 6,6 surfaces with unique wettability. J. Colloid Interface Sci. 2010, 345, 116-119.

[61] Gu, C.; Zhang, J.; Tu, J. A strategy of fast reversible wettability changes of WO3 surfaces between superhydrophilicity and superhydrophobicity. J. Colloid Interface Sci. 2010, 352, 573-579.

[62] Jin, M. H.; Wang, J.; Yao, X.; Liao, M. Y.; Zhao, Y.; Jiang, L. Adv. Mater. 2011, 23, 2861-2864;

[63] Cheng, P.-C.; Xu, Z.-K. Sci. Rep. 2013, 3, 2776.

[64] (a) Bi, H. C.; Xie, X.; Yin, K. B.; Zhou, Y. L.; Wan, S.; He, L. B.; Xu, F.; Banhart, F. L.; Sun, T.; Ruoff, R. S. Adv. Funct. Mater. 2012,22, 4421-4425; (b) Zhu, Q.; Pan, Q.

M.; Liu, F. T. J. Phys. Chem. C 2011, 115, 17464-17470; (c) Dong, X. C.; Chen, J.; Ma, Y. W.; Wang, J.; Chan-Park, M. B.; Liu, X. M.; Wang, L. H.; Huang, W.; Chen, P. Chem. Commun. 2012, 48, 10660-10662.

[65] Kajitvichyanukul, P.; Hung, Y.-T.; Wang, L. in Handbook of Environmental Engineering, Vol. 13 (Eds.: L. Wang, J. Chen, Y.-T. Hung, N. Shammas), Humana, New York, 2011, 639-668.

[66] Su, C.; Xu, Y.; Zhang, W.; Liu, Y.; Li, J. Appl. Surf. Sci. 2012, 258,2319-2323.

[67] Wang, F.; Lei, S.; Xue, M.; Ou, J.; Li, W. Langmuir. 2014, 30, 1281-1289.

[68] Zhang, W.; Zhu, Y.; Liu, X.; Wang, D.; Li, J.; Jiang, L.; Jin, J. Angew. Chem. Int. Ed. 2014, 53, 856 – 860; Angew. Chem. 2014, 126, 875-879.

[69] Deng, D.; Prendergast, D. P.; MacFarlane, J.; Bagatin, R.; Stellacci, F.; Gschwend, P. M. ACS Appl. Mater. Interfaces. 2013, 5,774-781.

[70] Xue, Z.; Wang, S.; Lin, L.; Chen, L.; Liu, M.; Feng, L.; Jiang, L. Adv. Mater. 2011, 23, 4270-4273.

[71] Sun, T.; Feng, L.; Gao, X.; Jiang, L. Acc. Chem. Res. 2005, 38, 644-652.

[72] Zhang, J.; Seeger, S. Adv. Funct. Mater. 2011, 21, 4699-4704.

[73] Feng, L.; Zhang, Z.; Mai, Z.; Ma, Y.; Liu, B.; Jiang, L.; Zhu, D. Angew. Chem. Int. Ed. 2004, 43, 2012-2014; Angew. Chem. 2004, 116, 2046-2048.

[74] Tu, C.-W.; Tsai, C.-H.; Wang, C.-F.; Kuo, S.-W.; Chang, F.-C. Macromol. Rapid Commun. 2007, 28, 2262-2266.

[75] Zhang, L.; Zhong, Y.; Cha, D.; Wang, P. A self-cleaning underwater superoleophobic mesh for oil-water separation. Sci. Rep. 2013, 3, 2326.

[76] Zhang, L.; Zhang, Z.; Wang, P. Smart surfaces with switchable superoleophilicity and superoleophobicity in aqueous media: toward controllable oil/water separation. NPG Asia Mater. 2012, 4, e8 (DOI: 10.1038/am.2012.14).

[77] Wang, L.; Yang, S.; Wang, J.; Wang, C.; Chen, L. Fabrication of superhydrophobic TPU film for oil–water separation based on electrospinning route Mater. Lett. 2011, 65, 869-872.

[78] Wang, B.; Guo, Z. pH-responsive bidirectional oil–water separation material. Chem.

Commun. 2013, 49, 9416-9418.

[79] Zhang, J.; Seeger, S. Polyester materials with superwetting silicone nanofilaments for oil/water separation and selective oil absorption. Adv. Funct. Mater. 2011, 21, 4699-4704.

[80] Artus, G. R. J.; Jung, S.; Zimmermann, J.; Gautschi, H. P.; Marquardt, K. Silicone nanofilaments and their application as superhydrophobic coatings. Adv. Mater. 2006, 18, 2758-2762.

[81] Zimmermann, J.; Reifler, F. A.; Fortunato, G.; Gerhardt, L. C.; Seeger, S. One-Step Approach to Durable and Robust Superhydrophobic Textiles Adv. Funct. Mater. 2008, 18, 3662-3669.

[82] Zimmermann, J.; Rabe, M.; Artus, G. R. J.; Seeger, S. Patterned superfunctional surfaces based on a silicone nanofilament coating. Soft Matter Soft Mater 2008, 4, 450-452.

[83] Zhang, J.; Seeger, S. Superoleophobic coatings with ultralow sliding angles based on silicone nanofilaments. Angew. Chem. Int. Ed. 2011, 50, 6652-6656.

[84] Wu, L.; Zhang, J.; Li, B.; Wang, A. Mimic nature, beyond nature: facile synthesis of durable superhydrophobic textiles using organosilanes. J. Mater. Chem. B 2013, 1, 4756-4763.

[85] Wu, L.; Zhang, J.; Li, B.; Wang, A. Mechanical-and oil-durable superhydrophobic polyester materials for selective oil absorption and oil/water separation J. Colloid Interface Sci. 2014, 413, 112-117.

Chapter 2 Materials, Experiment and Characterizations

2.1 Materials

2.1.1 Fabrication of the underwater low adhesive hydrogel-coated surface and its applications

Oil Blue 35 (Askul Co., Ltd., Japan), canola oil (Nisshin Oillio Co., Ltd., Japan), nickel foam (Anping Huirui Wire Mesh Manufacture Co., Ltd., China). Toluene, dichloromethane, n-hexane, alcohol, acrylamide (C3H5NO, 97%), N,N'-methylenebisacrylamide ($C_7H_{10}N_2O_2$), ammonium persulfate ($H_8N_2O_8S_2$) and N,N,N',N'-tetramethylethylenediamine ($C_6H_{16}N_2$) were purchased from Nacalai tesque and Alfa Aesar, used as received.

2.1.2 Fabrication of the robust and superhydrophobic surface and its applications

Calcium carbonate nanoparticles with 80 nm in diameter (Shiraishikogyo Co., Ltd., Japan), Oil blue 35 (Askful Co., Ltd., Japan), Scarlet 4GE (Askful Co., Ltd., Japan), 3M spray adhesive 55 (Sumitomo3M Co., Ltd., Japan), gasoline (Komeri Co., Ltd., Japan), sandpaper (standard glasspaper, Grit No. 150, Marumotostruers Co., Ltd., Japan), stainless steel mesh (Anpinghuirui wire mesh Co., Ltd, China). 1H, 1H, 2H, 2H-perfluorooctyltriethoxysilane ($C_8F_{13}H_4Si(OCH_2CH_3)_3$) were purchased from Sigma-Aldrich, laboratory solvents were obtained from Nacalai tesque. All chemicals were analytical grade reagents and were used as received.

2.1.3 Fabrication of the robust, transparent and superhydrophobic surface and its applications

Candle (Kameyama Co.,Ltd., Japan), Oil blue 35 (Askful Co., Ltd., Japan), Scarlet 4GE (Askful Co., Ltd., Japan), gasoline (Komeri Co., Ltd., Japan), stainless steel mesh (Anpinghuirui wire mesh Co., Ltd, China) and sea sand. Trichloro(1H, 1H, 2H, 2H-perfluorooctyl)silane was purchased from Sigma-Aldrich, laboratory solvents and

silicon tetrachloride were obtained from Nacalai tesque. All chemicals were analytical grade reagents and were used as received.

2.2 Experimental methods

2.2.1 Fabrication of the underwater low adhesive hydrogel-coated surface and its applications

a) Fabrication of the surface. The nickel foam was folded into an open and rectangular box with an edge length of 3 cm×3 cm×1 cm. The as-prepared box was ultrasonicated in ethanol and deionised water for three times, and dried in oven.

A mixed aqueous solution were prepared by adding acrylamide (35 mmol), N, N'-Methylenebisacrylamide (0.2 mmol), ammonium persulfate (0.1 mmol) and N,N,N',N'-Tetramethylethylenediamine (10 μl) in order. And then, the as-prepared box was immersed into the mixture aqueous solution for 5 min. Finally, it was taken out and rinsed three times by deionised water.

b) Separation of dichloromethane from oil–water mixture. In order to distinguish dichloromethane from oil–water mixture, we dyed the layer with Oil Blue 35 to indicate the directional delivery. The labeled dichloromethane (5 mL) and 5 mL of water were added into a beaker forming the oil–water mixture solution. After the as-prepared device put on the top of the supporting beaker, water was allowed to penetrate the surface rapidly while dyed dichloromethane was prevented. Then the dichloromethane was collected and measured its volume.

c) Magnetically driven floating device for the removal of little water from oil. The system was constructed by adding water, whose density is lighter than dichloromethane, at different places on the surface of watch glass. We dyed the water to a blue color, to distinguish the dichloromethane from water. Afterwards, the as-prepared device was placed on the surface of the system, which floated due to its underwater superoleophobicity. By employing an external magnetic field, the as-prepared device can

be driven and directionally clean up dyed water.

2.2.2 Fabrication of the robust and superhydrophobic surface and its applications

a) Fabrication of the surface. 500 mg of 1H, 1H, 2H, 2H-perfluorooctyltriethoxysilane was placed into 49.5 g of absolute ethanol, and the solution was magnetically stirred for 0.5 h. To the resulting solution, 6 g of calcium carbonate were added and stirred for 3 h to make a paint-like suspension. In the following experiments, spray adhesive was used to promote the robustness of the painted superhydrophobic coatings. For all kinds of substrates, adhesive was directly coated onto the abluent surfaces, and then the "substrates + adhesive" surface was treated with the paint by spay-coating, the paint was dried in air for at least 10min before testing.

b) Superhydrophobicity test in air and oil. The superhydrophobic paint treated surfaces on glass slide, PTFE pad, wood, aluminium sheet, stainless steel mesh, paper and gauze substrates were tested in air. Water droplets were dropped from a height of 10 mm (tip to surface) using a dropper fitted with a 3 ml dimension. The water droplets were around 19.7± 0.2 μL in size and were left to detach under their own weight. Scarlet 4GE was added to the water to aid visualization; this did not change the behavior of the water droplets on the surface. The superhydrophobicity test in oil (hexane) was similar as those in air. A spray-coated glass slide was immersed in oil, and then water was dropped onto the surface to test the superhydrophobicity in oil.

c) Self-cleaning test immersed in oil. The glass slide sample after superhydrophibicity test was following used to measurement the self-cleaning property immersed in oil. Soil and dust was used as dirt and placed onto the painted surface, water was then dropped onto the surface to remove dirt from the surface under oil immersion.

d) Robustness test. Both hard (glass slide, PTFE pad, wood, aluminium sheet and stainless steel mesh) and soft (gauze and paper) substrates were involved in the robustness tests, such as knife-scratch and sandpaper abrasion. For knife-scratch tests, water was firstly dropped on painted surfaces to test the wettability, and then a knife (box cutter)

was used to scratched the “paint + adhesive” treated surfaces along a meshy path, followed by the water dropping test to confirm the robustness of the superhydrophobic surfaces.

To further demonstrate the robustness, a glass slide sample was tested via sandpaper-abrasion method. The “paint + adhesive” treated surface was placed facedown to the sandpaper. This surface was longitudinally and transversely (10 cm for each direction) abraded by the sandpaper under a weight at 100 g, respectively, this process is defined as 1 cycle. 30 cycles of mechanical abrasion tests were carried out on the glass slide sample, and water contact angles were measured after each cycle’s abrasion test.

e) Separation of oil phase from oil-water mixture. In order to investigate the oil-water separation application of the painted surface, dichloromethane-water mixture was used as a representative to distinguish the oil phase. We dyed the oil layer with Solvent Blue 35 and water layer with Scarlet 4GE to indicate the directional flowage. An oil-water mixture was formed by adding blue dichloromethane (5 mL) and red water (5 mL) into a graduated cylinder. Meanwhile, a rounded painted stainless steel mesh was placed between a split type funnel formed an oil-water separation device, and then the device was placed on the top of a flask. Following, the dichloromethane-water mixture was poured rapidly into the device, dichloromethane was allowed to penetrated through the painted mesh while water was prevented. Finally, the oil phase in graduated cylinder was measured its water content to study oil-water separation efficiency of the device.

2.2.3 Fabrication of the robust, transparent and superhydrophobic surface and its applications

a) Fabrication of the surface. In order to obtain a robust, transparent and superhydrophobic surface in the end, firstly, a quartz wafer was washed by dry ethanol/ethanol – deionized water (v/v 1:1)/deionized water sequentially for 15 min each time, following a drying process in an oven at 60°C. Then, the abluent wafer was held in the flame of a candle until a candle soot layer a few micrometers thick was deposited. Subsequently, the soot coated substrate was placed in a desiccator together with an open

glass dish containing about 1ml of $SiCl_4$. The desiccator was closed again and chemical vapor deposition of $SiCl_4$ was carried out for 2 h. Similar to a Stöber reaction, a silica shell was formed as a coating on candle soot by hydrolysis and condensation of $SiCl_4$. Consequently, the quartz wafer coated by candle soot and silica shell was calcinated in air at 600°C for 30 min, candle soot composed of carbon polymer thermally degraded and diffused through the silica coating and a hollow and superhydrophilic silica shell was obtained on the quartz wafer. To transform it into superhydrophobic, the silica shell coated substrate with abundant hydroxyl was performed chemical vapor deposition in a desiccator together with an open glass dish containing about 1ml of Trichloro(1H, 1H, 2H, 2H-perfluorooctyl)silane, stable oxane bonds between silane and silica shell formed by left for 2h at 60°C, the silica shell finally achieved superhydrophobicity.

b) Robustness tests. For the robustness tests, sea sands grained 300 to 500 um in diameter were used to impact the surface from a height of 40 cm, while the substrate was held at 30° to the horizontal surface. After a certain time of impact, the silica shell coated substrate was observed and contact angle was performed on the surface.

c) Oil-water separation. In order to investigate the oil-water separation application of the painted surface, dichloromethane-water mixture was used as a representative to distinguish the oil phase. We dyed the oil layer with Solvent Blue 35 and water layer with Scarlet 4GE to indicate the directional flowage. An oil-water mixture was formed by adding blue dichloromethane (5 mL) and red water (5 mL) into a graduated cylinder. Meanwhile, a rounded painted stainless steel mesh was placed between a split type funnel formed an oil-water separation device, and then the device was placed on the top of a flask. Following, the dichloromethane-water mixture was poured rapidly into the device, dichloromethane was allowed to penetrated through the painted mesh while water was prevented. Finally, the oil phase in graduated cylinder was measured its water content to study oil-water separation efficiency of the device.

2.3 Characterizations

2.3.1 Surface modification

Morphology of the surfaces before and after modification was observed using a scanning electron microscope (S-4300, Hitachi Co., Ltd., Tokyo, Japan) at 20.0 kV. Photographic images were taken with a Nikon camera (D5000). The CA was characterized on the OCA20 instrument (Data Physics Instruments Gmbh, Filderstadt).

2.3.2 Oil-water separation

The oil contents in water was measured by a total organic carbon analyzer (TOC-V CPH, Shimazu Co., Ltd., Tokyo, Japan). Moistures in solvents were analyzed by Karl Fischer Moisture Titrator (MKC-610 Kyotoelectronics Manufacturing Co. LTD., Japan).

Chapter 3 Underwater Low Adhesive Hydrogel-Coated Functionally Integrated Device by a One-Step Solution-Immersion Method for Oil–Water Separation

3.1 Introduction

In recent years, the frequent occurrence of oil spills has been a serious threat to marine and aquatic ecosystems. The environmental and economic demands also emphasize the need for materials which can effectively separate oil and water. In order to handle these environmental issues caused by oil spills, many kinds of oil–water separation methods have been developed to recover spilt oil from marine environments, such as physical diffusion, bioremediation, oil skimmers and so on [1-3]. Owing to the difference in interfacial effects for oil and water, utilizing the wetting behavior of solid surfaces to design oil–water separating materials has attracted a great deal of attention in fundamental research and for potential application in the field of oil–water separation. In the first report in 2004, Jiang and coworkers fabricated a superhydrophobic mesh for separation of oil and water [4]. Meanwhile, a series of oil–water separating materials with both superhydrophobic and superoleophilic properties have been fabricated via various methods [5-11].

However, conventional oil-water separation processes with superhydrophobic-superoleophilic materials are easily fouled, blocked up and even damaged by oils because of their intrinsic oleophilicity, resulting in a quick decrease in separation efficiency, flow rate, and film life, and even secondary pollution. These disadvantages have seriously restricted their practical application in oil-water separation. To solve these problems, a new strategy must urgently be found. Inspired by the underwater superoleophobicity of fish scales, several additional superhydrophilic-superoleophobic materials have been proposed [12-18] for oil-water separation. Compared with conventional

superhydrophobic-superoleophilic oil-water separation materials, these superhydrophilic and underwater superoleophobic materials [19-21] can allow water in filtration but prevent oil penetration and may solve oil fouling during the separating process very well. Despite much progress in this field, some of these superhydrophilic and underwater superoleophobic materials with micro-nano structures are easily destroyed under severe environmental conditions, thus resulting in the reduction of flow rate and film life. Meanwhile, some of these fabrication processes are usually time-consuming which may have limited their practical application and their production on a large scale.

The best strategy for the facile and simple method is to introduce hydrogel coating on the material surface and then realize the separation of oil-water mixtures. Jiang and coworkers designed and fabricated a novel superhydrophilic and underwater superoleophobic polyacrylamide (PAM) hydrogel-coated mesh and then successfully applied it to the separation of oil-water mixtures [15]. Because most superhydrophilic materials can only collect water on the oil surface, it is urgent for a device to be designed and produced which will enable the targeted recovery of water. The best strategy for the directional locomotion of an object on the oil surface is to introduce magnetically responsive materials into the system and then apply a magnetic field to drive the object to the targeted position. In the presence of an external magnetic field, this device can easily remove water droplets located at different places. To the best of our knowledge, there are few reports about the fabrication of functionally integrated device consisting of superhydrophilic and underwater superoleophobic coating to clean up and collect oil spills. Therefore, in this chapter, I have developed a facile and simple strategy to prepare a low-adhesive and hydrogel-coated functionally integrated device on magnetic nickel foam for highly efficient oil-water separation. For the asprepared device, the superhydrophilicity and underwater superoleophobicity of the hydrogel coating just allowed the water layer to in filtrate while the oil layer was prevented from passing through. In this way, the device could selectively and efficiently separate oil from a

variety of oil-water mixtures without external power. What is more, the as-prepared device can selectively absorb water droplet from the oil interface. In the presence of an external magnetic field, the as-prepared device can easily remove water droplets located at different places, remove and collect the little water into the interior of the device, exhibiting a directionality and selectivity. This novel method may provide a facile and simple strategy for separating complex oil-water mixtures in oil spill accidents.

3.2 Experimental

In this chapter, the commercially available nickel foams were functionalized by means of hydrogel coating with one-step solution-immersion method. By taking advantage of the superhydrophilic and underwater superoleophobic properties, the device was used to separate oil-water mixtures. The separation efficiency and reusability were investigated. What is more, because of the magnetic property of nickel foam, water absorbing on oil surface from a distance toward the targeted areas was tested.

3.3 Results and discussion

3.3.1 SEM analysis

Scanning electron microscope (SEM) images were used to evaluate the surface morphology of underwater low adhesive hydrogel-coated functionally integrated device both before and after modification. Fig. 3-1a showed a typical SEM image of nickel foam surface, the average diameter of pores was around 300 μm. Fig. 3-1b indicated a large-area of staggered holes covered with a thick and compact hydrogel layer, forming the superhydrophilic surface. The surface elements were detected by energy dispersive xray spectrom (EDX) before and after modification. From the corresponding EDX patterns, Ni element appeared and showed a stronger absorption in Fig. 3-1c, while as Fig. 3-1d showed, we can clearly observe the stronger signals of C, O, N after modification by hydrogel, which confirmed the presence of the PAM hydrogel layer.

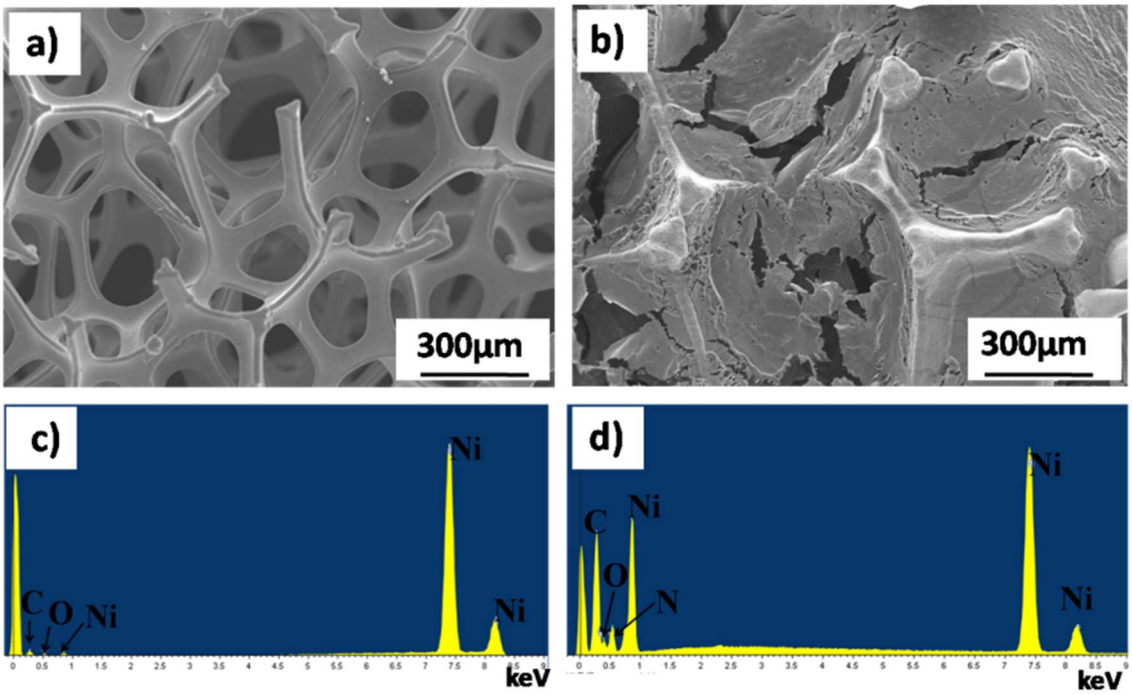

Fig. 3-1 SEM images of the nickel foam (a) before and (b) after modification by PAM hydrogel; the corresponding EDX patterns for (c) bare nickel foam and (d) modification by PAM hydrogel.

3.3.2 CA analysis

Surface morphology and chemical composition are two important factors which significantly affect the wettability of a solid surface. The chemical composition determines whether the surface is hydrophilic or not, while the morphological structure will amplify this surface property to superhydrophilicity or superhydrophobicity. Hydrogel with excellent water-absorbing and water-retaining capacities is one of the most typical hydrophilic materials and is considered to be promising candidate for designing novel water-removing materials for oil/water mixtures separation. I have developed a facile method for fabricating underwater low adhesive hydrogel-coated functionally integrated device. The CA measurement results showed that the water droplet CA on bare nickel foam surface was less than 90^{o}, indicated the hydrophilicity of surface, as shown in Fig. 3-2b. Obviously, a water droplet standing on the surface of nickel foam and cannot penetrate through spontaneously because of the negative capillary effect. However, the water droplet easily spreaded and penetrated the surface when it is in contact with the

surface coated by hydrogel, and the water droplet dropped down when more water was added. The surface was hydrophilic, with CA about 0º (Fig. 3-2a). So these phenomena indicated that superhydrophilicity had generated on the nickel foam surface after modification by hydrogel.

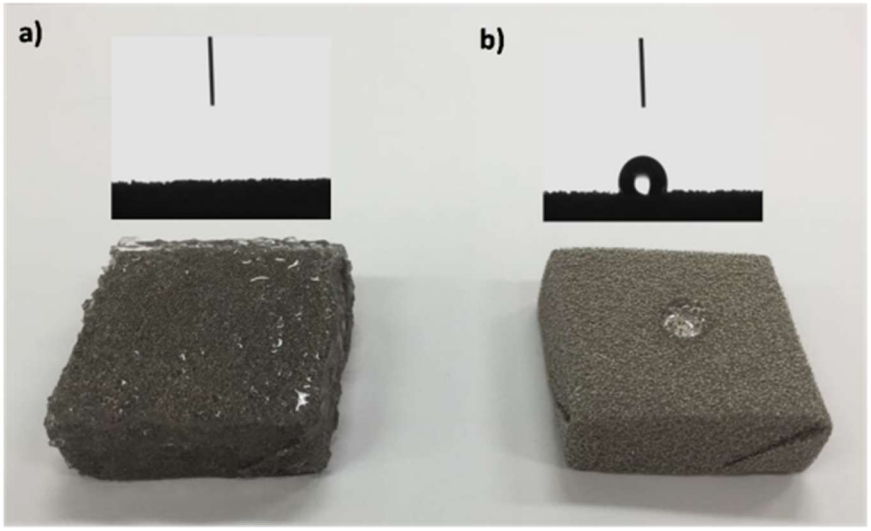

Fig. 3-2 CA and photographs of water droplets on different surfaces: (a) PAM hydrogel coated nickel foam and (b) bare nickel foam

It is well-known that superhydrophobic surface originate from the special formation of a water/air/solid system. According to the theory developed by Cassie et al. [22], stable air molecules exist on the surface of micro/nanostructures, forming a water/air/soild interface. This strategy will help us study the wetting behavior in the oil/water/soild system. When hydrogel coated on nickel foam contacted with the oil/water mixture, water molecules were trapped in the hydrogel coating, forming an oil/water/solid interface. This new composite interface showed superhydrophilic and underwater superoleophobic properties. To verify the surface wettability and low adhesive property underwater, the oil droplets were applied to the as-prepared hydrogel-coated functionally integrated device underwater. From Fig. 3-3a we can observe that a round oil droplet formed on the surface of the as-prepared device with an oil contact angle (OCA) of 150.1º, which indicated the underwater superoleophobicity of the surface. With slowly moving the injection syringe, we can take notice of the paralleled movement of the oil droplet without any residual oil

droplet on the surface. The shape of the oil droplet was spherical during the whole movement, which indicated the surface had a low adhesion property to the employed oil (Fig. 3-3b, c). To further study the oil wettability of the as-prepared device surface, another oil droplet was also utilized on the inclined surface. The OCA measurement results of as-prepared device with oil droplet sliding angle 3° ± 0.5° were presented in Fig. 3-3d-f. Accordingly, the oil/water mixture can be well separated via the hydrogel-coated functionally integrated device due to the different wettabilities of its surface including superhydrophilicity and underwater superoleophilicity.

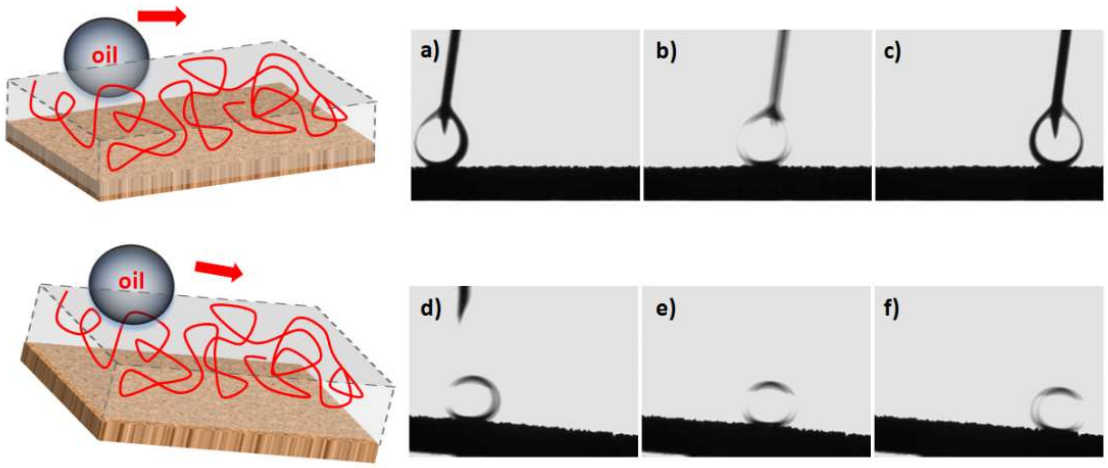

Fig. 3-3 The dynamic underwater oil adhesion measurement on as-prepared divice surface: (a-c) An oil droplet was applied to contact the surface and can be moved easily; (d-f) The slant surface showed an ultralow affinity to the oil droplet.

3.3.3 Oil-water separation

The oil/water mixtures were separated by as-prepared device, shown as Fig. 3-4a, b. Driven by gravity only, the superhydrophilic property of hydrogel allowed the water to pass through the device (Fig. 3-4c). Meanwhile, the oil was prevented from permeating into the hydrogel due to underwater superoleophobic and low adhesion properties. From the amplifying Fig. 3-4c**,** we can observe that the blue oil layer was still stored in the device. The volume of oil was measured to calculate the separation efficiency. By this way, the oil/water mixtures were separated successfully without any external force,

indicating its easy operation and low energy consumption.

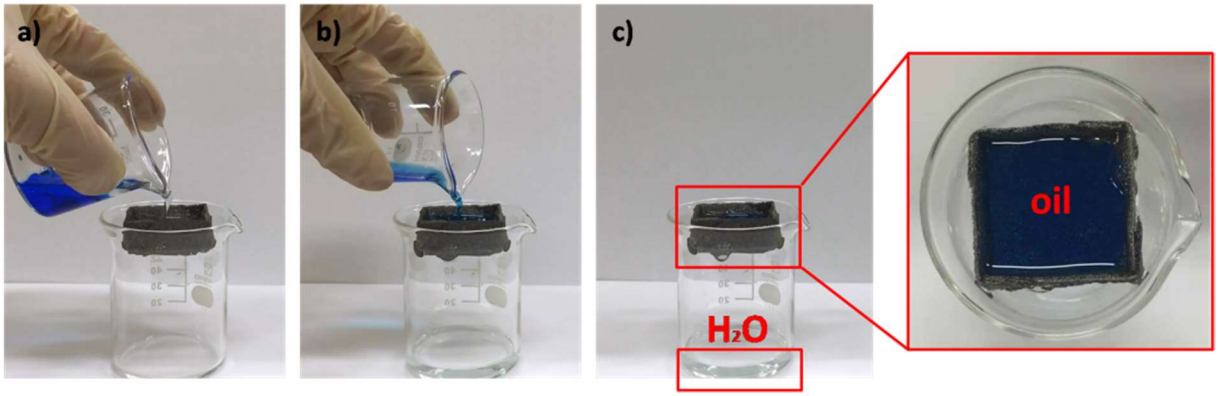

Fig. 3-4 The oil/water separation process: (a) A mixture of water and blue-dyed oil was poured into the device. (b) Water passed through the device, (c) while oil was prevented from permeating into the hydrogel and remains in the device.

In order to understand the separation efficiency of the as-prepared device, we have taken a dichloromethane-water mixture as an example to separate dichloromethane from water. A total of 5 mL dichloromethane labeled with blue dye (Fig. 3-5a and a') was added to a beaker containing 5 mL of water. Since the density of water was lower than that of dichloromethane, the added water finally floated on the dichloromethane surface (Fig. 3-5b). When we poured the dichloromethane-water mixture into the as-prepared device, water was soon taken up by the device, in filtrated through the walls, and finally gathered into the beaker due to gravitational effects (Fig. 3-5c). And then, the collected dichloromethane in the device was transferred to the original pipette, as shown in Fig. 3-5c'. According to the original added volume of the dyed dichloromethane (5 mL), the calculated collecting efficiency was 99.5%. As oil spill accidents occur frequently throughout the world, it is crucial to extend the application of the device for different oil-water mixtures, such as toluene, dichloromethane, canola oil and n-hexane. Separation efficiency was used to quantitatively describe the separation ability of device. It can be defined according to the ratio between the volume of collected oil after separation and that of original. As shown in Fig. 3-5d, the separation efficiencies of the as-prepared device for various oils were all above 98%, nearly no visible oil existed in the permeated

water, demonstrating the high efficiency of the as-prepared device in oil-water separation. What is more, the as-prepared device can be reused 6 times and still had high separation efficiency, for each time of separation, the collection efficiency of dichloromethane-water mixture was over 97%, which demonstrated its reproducibility, as shown in Fig. 3-5e. These results indicated that this novel superhydrophilic and underwater superoleophobic device was a potential candidate for oil-water separation, which would provide promising possibilities in industrial applications.

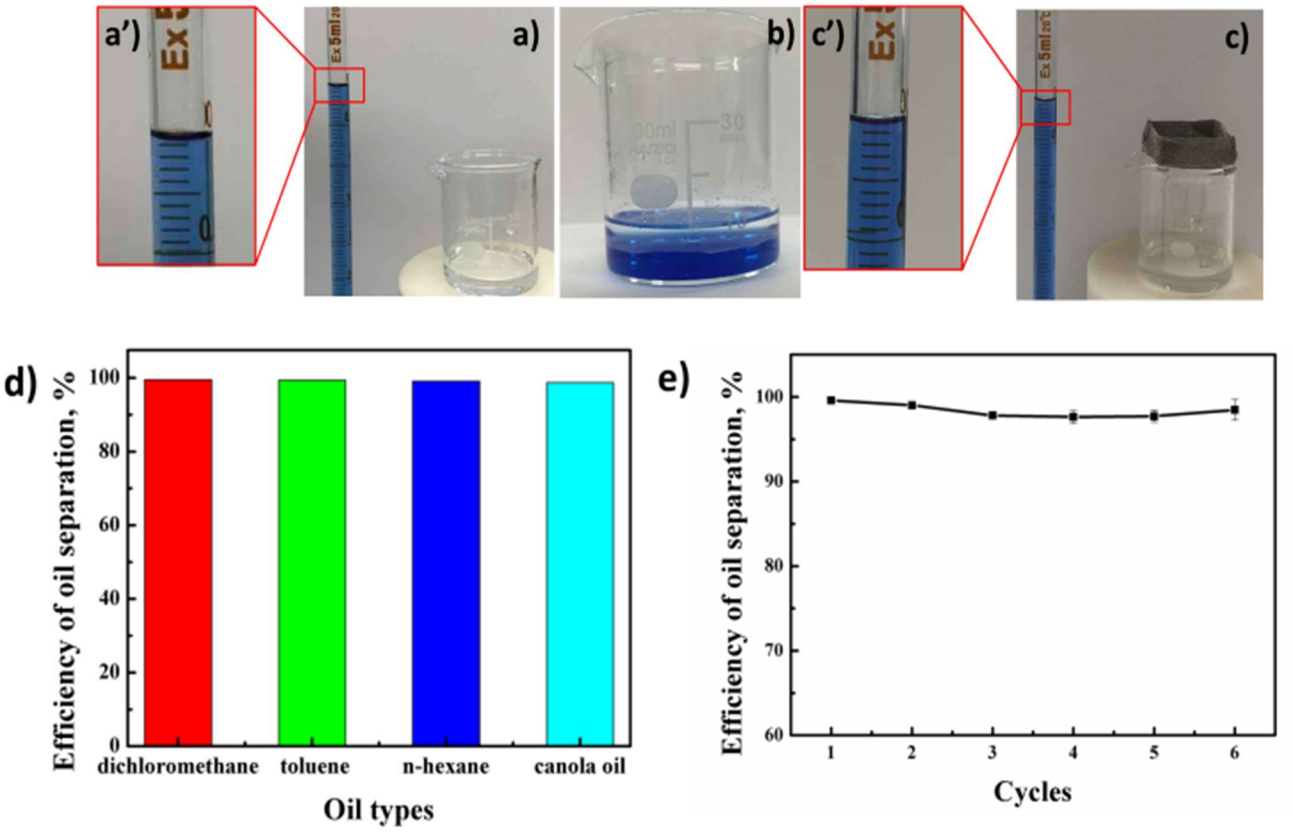

Fig. 3-5 The process (a-c) of evaluating the separation efficiency of the dichloromethane–water mixture by as-prepared device; The magnification of (a) and (c) indicate the volumes in the pipette; (d) Separation efficiency of the as-prepared device for different oil/water mixtures; (e) Recycled experiments for separating oil from water by as-prepared device.

For oil-water separation, a series of immiscible oil-water mixtures were poured onto

the as-prepared device. Water immediately permeated through the surface and oils were retained above. The oil contents in water before and after only one separation were measured by total organic carbon analyzer. During the course of the experiment, the solubility of oil in water is different with the oil type. The oil content in water also existed large difference. As shown in Fig. 3-6, before separation process, the oil contents were 702.5 ppm, 242.6 ppm, 180.1 ppm and 4607.7 ppm for dichloromethane, toluene, n-hexane and canola oil, respectively. The canola oil contains various water-soluble components such as amino acids which has led the highest oil content in water before separation. As shown in Fig. 3-7a, for the immiscible oil-water mixtures (dichloromethane, toluene, n-hexane), the oil contents were respectively 961.5 ppm, 267.5 ppm, 194.1 ppm. The results showed, after the separation process, the oil was almost separation from the water and there was almost no leakage in water. The water flow rates were calculated by measuring the time for different kinds of oil-water mixtures, as shown in Fig. 3-7a. The highest water flow rate of 0.425 and 0.3841 m h^{-1} were achieved for the hexane-water and dichloromethane-water mixtures, respectively. This result indicated that the type of oils had little effect on permeating flow rate. For canola oil, after making it and water stirred thoroughly, the oil-water mixtures need take a long time to stratify. As mentioned above, the canola oil contains various water-soluble components which have led a high oil content in water (5055 ppm) and a high-viscosity fluid ,therefore the water flow rate was relatively low (0.03667 mh^{-1}). In order to verify the repeatability of the as-prepared device, we had realized the test of the water flow rate for every cycle. During the six cycles experiments, the water flow rate was about 0.38 mh^{-1} and kept stable. This is because the as-prepared device only allows water to permeate, as shown in Fig. 3-7b.

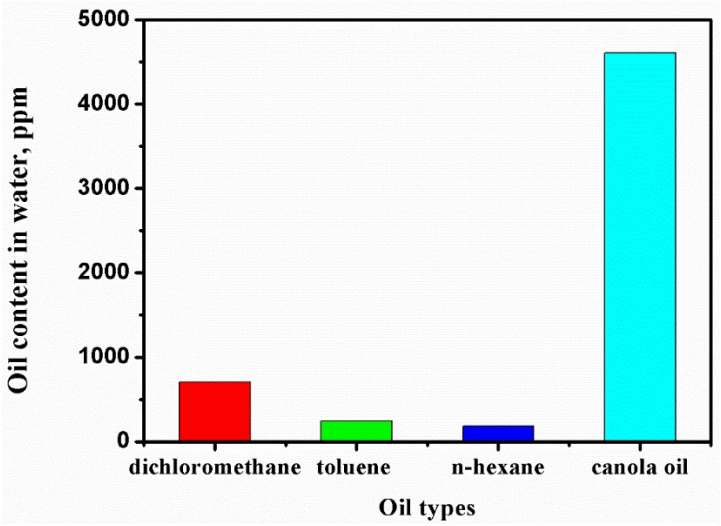

Fig. 3-6 Oil content in water of different oil types before oil-water separation

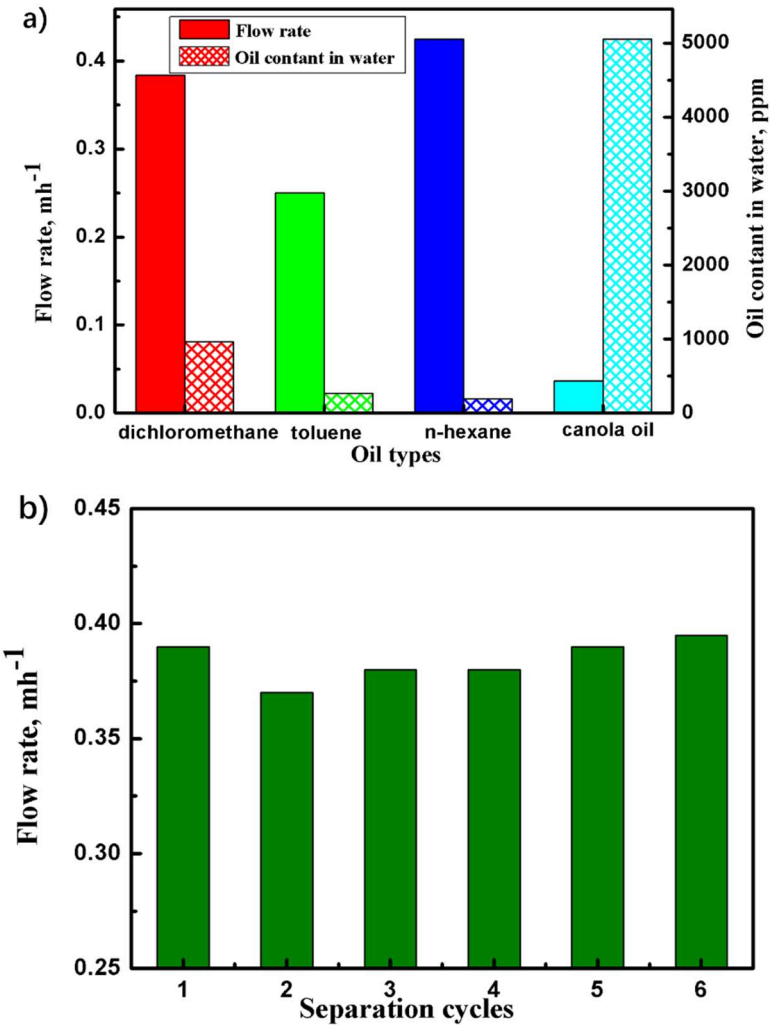

Fig. 3-7 Oil-water separation results of the as-prepared device. (a) Oil content and the water flow rate after permeating a series of immiscible oil–water mixtures. (b) Water flow rate for permeating oil–water mixture through the as-prepared device with

different cycle index.

Besides their ideal underwater superoleophobic property and high water-absorption capacity, the as-prepared device can also be actuated onto oil zones by means of a weak magnetic field. To confirm the hypothesis, we designed a system featuring a dichloromethane layer containing drops of dyed water at the surface of the beaker. The system was constructed by adding 0.1 mL of dyed water, whose density is lighter than dichloromethane, at different places at the surface of beaker (Fig. 3-8a). Afterwards, the as-prepared device was placed on the surface of the system. At the beginning, the as-prepared device was floating over the oil surface, as shown in Fig. 3-8a. In this case, the as-prepared device remained immobile and could not absorb the blue water automatically. To pull the as-prepared device directionally towards the dyed water, we applied an external magnetic field above the beaker. Guided by the movement of the magnet, the as-prepared device can directionally clean up the dyed water (Fig. 3-8b and c). When just coming into contact with the blue water droplets, the device quickly absorbed them. No blue water droplets were left on the surface (Fig. 3-8d), indicating the excellent capability of the device to directionally clean up the little water on the oil surface. The result demonstrated that the as-prepared device performed well, not only in the directional water collection, but also in the controlled magnetically responsive water absorption, exhibiting integrated functions. This design had broadened the application of as-prepared device in water-oil separation by the additional magnetic field. Meanwhile, the as-prepared device may be applied to closed-system to clean up little water, such as gas tanks, petroleum pipeline.

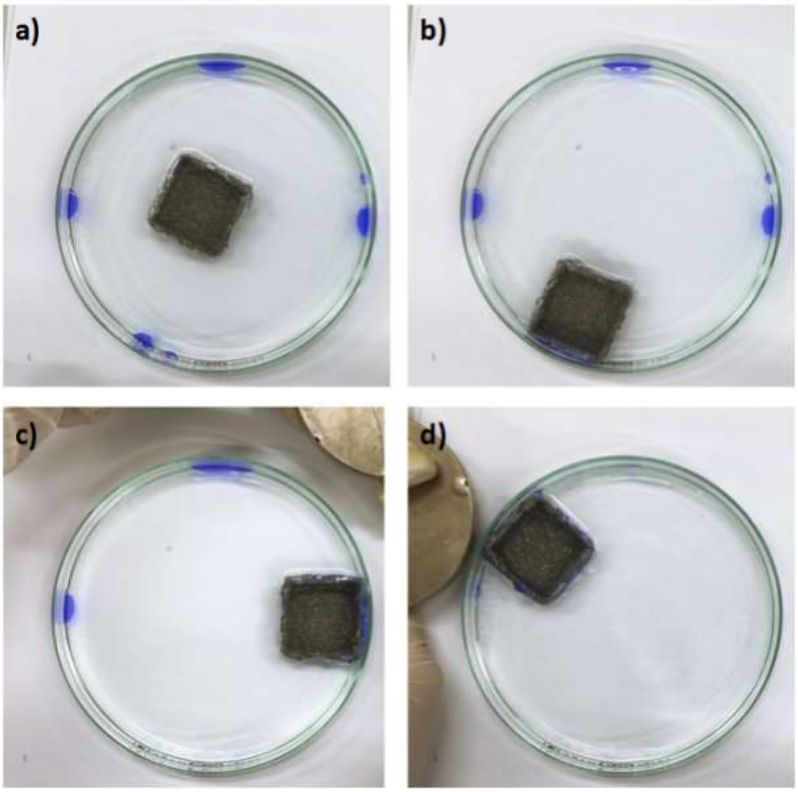

Fig. 3-8 (a) Dye-colored water on the surface of the dichloromethane in a watch glass; (b and c) subsequent removal of the little water by the magnetically driven the as-prepared device; (d) cleaned oil surface after the process.

3.4 Conclusions

In summary, the author has develop a facile method for fabricating underwater low adhesive hydrogel-coated functionally integrated device to separate oil from mixtures with water. In particular, the commercially available nickel foams are functionalized by means of hydrogel coating. Compared with other preparation methods, the nickel foams coated by hydrogel are also a promising approach in oil-water separation. The technique is simple and easy to be scaled up, while the employed materials are inexpensive and some of them can be recycled. Therefore, I propose the use of the developed systems in the selective removal of little water from oil surface by means of a magnetic field, underwater superoleophobic, and water absorbing nickel foams from a distance toward the targeted areas with minimal energy consumption. By taking advantage of the superhydrophilic and underwater superoleophobic properties, the author has realized the

effective separation of oil-water mixtures, which demonstrated a re-collecting efficiency as high as 99.5%. What is more, it also can be reused 6 times and still had high separation efficiency. The as-prepared device would provide a novel strategy for handling oil spills under various conditions and can be applied in other oil-water separating systems.

In this chapter, the author has fabricated the UWSOB material and investigated oil-water separation by UWSOB material. However, the surface of this separation device was soft, which would suffer from its poor mechanical properties. Meanwhile, the soft material of separation device has no obvious porous structure, the oil-water separation process depended on permeation of water which led to a slow flow rate. Therefore, I would like to investigated the oil-water separation performed with SHBOI material which holds not only superhydrophobicity and high separation efficiency but also excellent robustness.

References

[1] Hoff, R. Z. Bioremediation: An Overview of its Development and Uses for Oil Spill Cleanup. Mar. Pollut. Bull. 1993, 26, 476-481.

[2] Atlas, R. M. Microbial Hydrocarbon degradation-Bioremediation of Oil Spills. J. Chem. Technol. Biotechnol. 1991, 52, 149-156.

[3] Fingas, M. Oil spills and their cleanup. Chem. Ind. 1995, 24, 1005-1008.

[4] Feng, L.; Zhang, Z. Y.; Mai, Z. H.; Ma, Y. M.; Liu, B. Q.; Jiang, L.; Zhu, D. B. A superhydrophobic and superoleophilic coating mesh film for the separation of oil and water. Angew. Chem., Int. Ed. 2004, 43, 2012-2014.

[5] Darmanin, T.; Nicolas, M.; Guittard, F. Electrodeposited polymer films with both superhydrophobicity and superoleophilicity. Phys. Chem. Chem. Phys. 2008, 10, 4322-4326.

[6] Zhu, Q.; Chen, N.; Tao, F.; Pan, Q. M. Improving the lithium storage properties of Fe_2O_3@C nanoparticles by superoleophilic and superhydrophobic polysiloxane coatings. J. Mater. Chem. 2012, 22, 15894-15900.

[7] Li, J.; Shi, L.; Chen, Y.; Zhang, Y. B.; Guo, Z. G.; Su, B. L.; Liu, W. M. Stable superhydrophobic coatings from thiol-ligand nanocrystals and their application in oil/water separation. J. Mater. Chem. 2012, 22, 9774-9781.

[8] Liu, X. M.; He, J. H. One-Step Hydrothermal Creation of Hierarchical Microstructures toward Superhydrophilic and Superhydrophobic Surfaces. Langmuir. 2005, 25, 11822-11826.

[9] Cheng, Z. J.; Wang, J. W.; Lai, H.; Du, Y.; Hou, R.; Li, C.; Zhang, N. Q.; Sun, K. N. pH-Controllable On-Demand Oil/Water Separation on the Switchable Superhydrophobic-Superhydrophilic and Underwater Low-Adhesive Superoleophobic Copper Mesh Film. Langmuir. 2015, 31, 1393-1399.

[10] Ke, Q. P.; Jin, Y. X.; Jiang, P.; Yu, J. Oil/Water Separation Performances of Superhydrophobic and Superoleophilic Sponges. Langmuir. 2014, 30, 13137-13142.

[11] Yoon, H.; Na, S. H.; Choi, J. Y.; Latthe, S. S.; Swihart, M.T. Gravity-Driven Hybrid Membrane for Oleophobic–Superhydrophilic Oil–Water Separation and Water Purification by Graphene. Langmuir. 2014, 30, 11761-11769.

[12] Zhang, L. B.; Zhong, Y. J.; Cha, D. Y; Wang, P.; A self-cleaning underwater superoleophobic mesh for oil-water separation. Sci. Rep. 2013, 3, 2326-2330.

[13] Xu, L. P.; Zhao, J.; Su, B.; Liu, X. L.; Peng, J. T.; Liu, Y. B.; Liu, H. L.; Yang, G.; Jiang, L.; Wen, Y. Q.; Zhang, X. J; Wang, S. T. An ion-induced low-oil-adhesion organic/inorganic hybrid film for stable superoleophobicity in Seawater. Adv. Mater. 2013, 25, 606-611.

[14] Liu, X. L.; Zhou, J.; Xue, Z. X.; Gao, J.; Meng, J. X.; Wang, S. T.; Jiang, L. Clam's shell inspired high-energy inorganic coatings with underwater low adhesive superoleophobicity. Adv. Mater. 2012, 24, 3401-3405.

[15] Xue, Z. X.; Wang, S. T.; Lin, L.; Chen, L.; Liu, M. J.; Feng, L.; Jiang, L. A novel superhydrophilic and underwater superoleophobic hydrogel-coated mesh for oil/water separation. Adv. Mater. 2011, 23, 4270-4273.

[16] Liu, H. L.; Zhang, P. C.; Liu, M. J.; Wang, S. T.; Jiang, L. Organogel-based thin films for self-cleaning on various surfaces. Adv. Mater. 2013, 25, 4477-4481.

[17] Cai, Y.; Lin, L.; Xue, Z. X.; Liu, M. J.; Wang, S. T.; Jiang, L. Filefish-inspired surface design for anisotropic underwater oleophobicity. Adv. Funct. Mater. 2014, 24, 809-816.

[18] Zhang, F.; Zhang, W. B.; Shi, Z; Wang, D.; Jin, J.; Jiang, L. Nanowire-haired inorganic membranes with superhydrophilicity and underwater ultralow adhesive superoleophobicity for high-efficiency oil/water separation. Adv. Mater. 2013,25, 4192-4198.

[19] Gao, X. F.; Xu, L. P.; Xue, Z. X.; Feng, L.; Peng, J. T.; Wen, Y. Q.; Wang, S. T.; Zhang, X. J. Dual-scaled porous nitrocellulose membranes with underwater superoleophobicity for highly efficient oil/water separation. Adv. Mater. 2014, 26, 1771-1775.

[20] Jin, M. H.; Li, S. S.; Wang, J.; Xue, Z. X.; Liao, M. Y.; Wang, S. T. Underwater

superoleophilicity to superoleophobicity: role of trapped air. Chem. Commun. 2012, 48, 11745-11747.

[21] Xu, L. P.; Peng, J. T.; Liu, Y. B.; Wen, Y. Q.; Zhang, X. J.; Jiang, L.; Wang, S. T. Nacre-inspired design of mechanical stable coating with underwater superoleophobicity. ACS nano. 2013, 7, 5077-5083.

[22] Cassie, A. B. D.; Baxter, S. Wettability of porous surfaces. Trans. Faraday Soc.1944, 40, 546.

Chapter 4 Robust and Superhydrophobic Surface Modification by a “Paint+Adhesive” Method: Applications in Selfcleaning after Oil Contamination and Oil-Water Separation

4.1 Introduction

The wettability of solid surfaces is a renewed old topic which has impacted most fields of science and technology for a long time, from cave painting in the ancient to microfluidic devices in the modern [1]. In the past decades, bioinspired surfaces with superhydrophobicity that is one of the extreme states of surface wettability have been intensively explored and accelerated by discoveries of superwetting phenomena in nature [2-6]. The term superhydrophobicity was introduced in 1976 by Reick to describe hydrophobic particle coating made of hydrophobic fumed silicon dioxide, where water droplet maintains a contact angle (CA) $\theta > 150°$ and the force of adhesion is negligible.

In 1997, Barthlott and Neinhuis revealed that the superhydrophobicity and self-cleaning property of lotus leaves were caused by the microscaled papillae and the epicuticular wax, providing a monomicrostructure model [7]. Subsequently, Jiang et al. disclosed that there are micro- and nanoscaled hierarchical structures on the lotus leaf surface, that is, branch-like nanostructures on the top of micropapillae, which result in the superhydrophobicity [2]. Thus, the origin of superhydrophobicity of a lotus leaf becomes clear from a monoscaled model of microstructures to a dual-scaled model of hierarchical structures. These studies on superhydrophobicity activated the emerging applications of wettability from energy conversion, avoiding fluid drag in microfluidic devices, reducing fluid resistance for aquaculture devices, protection of electronic devices and oil−water separation [9-13]. In the following decade, lots of efforts have been proposed to develop

superhydrophobic surfaces, however, with the deepening of the research, robustness question of superhydrophobic surfaces was put on the more and more outstanding position, which was that the superhydrophobic surfaces were readily destroyed [14-20].

The superhydrophobic surfaces mostly shows a poor robustness, simultaneously depends on expensive and complicated roughness structures, which are inherently vulnerable to mechanical damages, sometimes abraded when there happens a tissue brushing.

However, superhydrophobicity and robustness are generally known to be conflicting properties. As roughness increasing, hydrophobicity increases, nevertheless, robustness decreases. As a result, the practical applications of superhydrophobic surfaces have so far been limited on the materials that require robustness. Consequently, realizing both superhydrophobicity and robustness simultaneously by a simple and cost-effective method is still a technical challenge at present. Conventional strategies used to enhance device robustness typically involve generating chemical bonding between superhydrophobic coating and substrate or cross-linking the coating layers. Zhou et al.[21] fabricated a elastomeric thin film by combining low surface energy substance and a rough surface which was composed by a nanocomposite structure and can endow film with highly durable superhydrophobicity. Alternative approaches to increase device durability include introducing self-healing capability to superhydrophobic device. For example, Li et al.[22] developed a self-healing superhydrophobic fiber which made of a rigidly flexible porous polymer with micro- and nanoscaled hierarchical structure, the fluoroalkylsilane was reacted in the pores. The fiber showed excellent self-healing property after oxygen plasma treatment. However the above works still depended on expensive and complex techniques.

Very recently, Lu et al.[23] developed a facile and simple method for fabricating superhydrophobic surfaces from various substrates. The process used dual-scale TiO2 nanoparticles coated with perfluorooctyltriethoxysilane. They created an ethanol based

suspension that can be sprayed onto surfaces and the water-repellent surface was generated.

After promoting the paint by adhesives, the painted surface achieved superhydrophobicity and robustness even after various kinds of damage. Similarly, Baron et al.[24] created a novel, facile and low-cost strategy to realize the superhydrophobicity on various substrates. They synthesized aluminum oxide nanoparticles modified by a new low surface energy substance-carboxylic acid with highly branched hydrocarbon chains. This low-cost and environmentally friendly low surface energy material could be used as a replacement of expensive and environmentally hazardous fluorocarbons. Then the aluminum oxide nanoparticles modified by carboxylic acid were sprayed onto the surface of substrate forming a superhydrophobic film. These works have provided an excellent idea for promoting the robustness and practicability of superhydrophobic surfaces.

Inspired by the above works, the author developed in this work a more versatile strategy to fabricate mechanically robust, self-cleaning and superhydrophobic surfaces for both soft and hard substrates. The author used low-cost, non-toxic and mono-scale nanoparticles of calcium carbonate which were coated with perfluorooctyltriethoxysilane. Then the silanized nanoparticles were made into a suspension that can be sprayed onto surfaces to create a superhydrophobic rough surface. For all kinds of substrates, spray adhesive was directly coated onto abluent substrates surfaces to promote the robustness, and then the “substrates + adhesive” surface was treated with the paint by spay-coating. These superhydrophobic surfaces were applicable on various substrates include both hard and soft materials, as well as showed remarkable robustness against knife scratch and sandpaper abrasion, while retaining their superhydrophobicity. What is more, the superhydrophobic surfaces have shown promising potential applications in self-cleaning and oil-water separation, and remained excellent oil-water separation efficiency even after reuses. It is believed that the superhydrophobic surfaces fabricated by this facile and simple strategy can be readily and robustly used in large-scale industrial applications

where maintain harsh and oily environments, such as external wall coating and oil-water separation material.

4.2 Experimental

In this chapter, a versatile and simple “paint+adhesive” method was used to fabricate superhydrophobic surfaces for both soft and hard substrates by a straightforward spraying. Its superhydrophobicity and selfcleaning property even under oil immersion were investigated. Meanwhile, the robustness against knife scratch and sandpaper abrasion were studied. By taking advantages of superhydrophobicity under oil immersion, this surface was used for oil-water separation, the separation efficiency and reusability was investigated.

4.3 Results and discussion

4.3.1 Surface modification and characterization

The robust self-cleaning surfaces were fabricated following the procedure shown in Fig. 4-1: firstly, the calcium carbonate nanoparticles with abundant hydroxyl were silanized with 1H, 1H, 2H, 2H-perfluorooctyltriethoxysilane in an absolute ethanol solution. Stable oxane bonds between silane and calcium carbonate nanoparticles formed after stirring for 3 h under room temperature, and the solution was finally a paint-like suspension. Meanwhile, hard substrates (glass slide, PTFE pad, wood, aluminium sheet and stainless steel mesh) were washed by dry ethanol/ethanol–deionized water (v/v 1:1)/deionized water sequentially for 15 min each time, following a drying process in an oven at 60 °C. And for soft substrates (paper and gauze), the surfaces were prepared by purging with sufficient nitrogen gas for 10 min at room temperature and ambient pressure. Then, to fabricate a robust surface, spray adhesive was used to promote the robustness of the painted superhydrophobic coatings: for all kinds of substrates, adhesive was directly kept spraying onto the abluent surfaces for 3s with a distance of 300 mm. Following, the paint-like suspension was sprayed onto the “substrates + adhesive” surfaces: a 0.8 mm

nozzle spray gun was used from the surfaces at a distance of 300 mm, the paint was sustained spraying for 3s with the pump output of 60 L/min under 0.78 Mpa. Finally, the residual solvent on robust self-cleaning surface was evaporated under atmosphere.

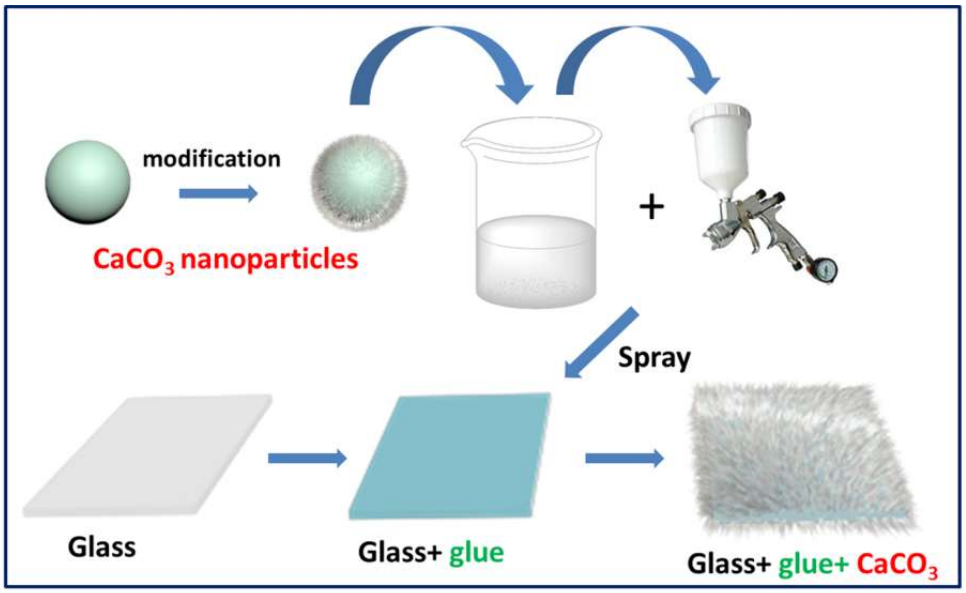

Fig. 4-1 Schematic illustration of the preparation process and properties of the robust self-cleaning surface.

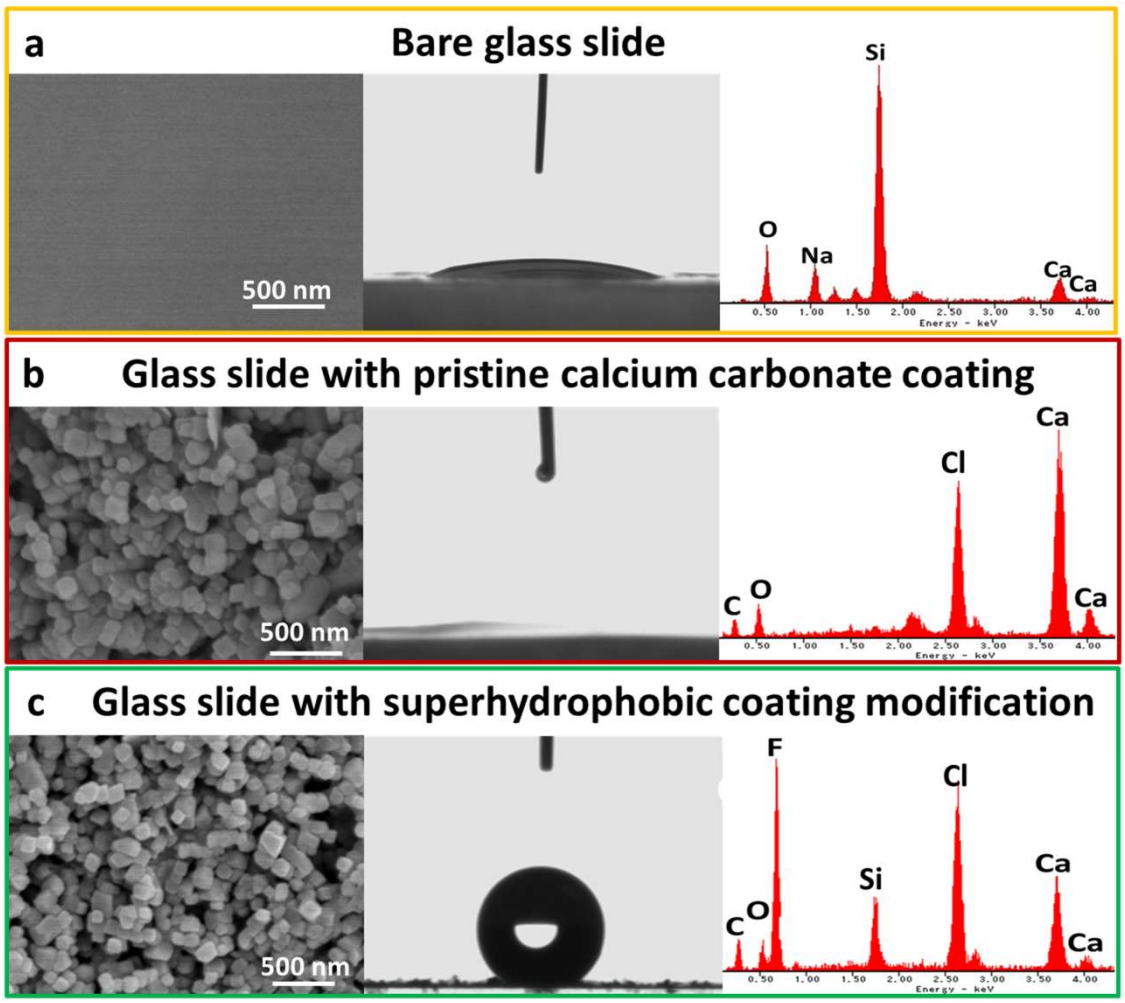

Fig. 4-2 The SEM images, CA and EDX measurements of different glass slide samples: (a) bare glass slide; (b) glass slide with pristine calcium carbonate coating; (c) glass slide with superhydrophobic coating modification.

Evident changes in wettability of the substrates surfaces occurred in the process of preparing the robust self-cleaning surfaces. The glass slide sample was tested as a representative, SEM, CA and EDX analysis was used to prove the superhydrophobic coatings modification.

As shown in Fig. 4-2a, the bare glass surface was washed by dry ethanol/ethanol-deionized water (v/v 1:1)/deionized water carefully, followed by SEM, CA and EDX analysis. The surface morphology in SEM image revealed the bare glass slide had a homogeneous and smooth surface, and signals of Na, Ca, Si and O elements, which

constituted glass primarily, were detected from the EDX analysis, ascertaining thorough cleaning of the surface by ethanol and water. Meanwhile, the bare glass surface emerged hydrophilicity due to the presence of hydroxy, and the CA of water was 44.3°. To fabricate the superhydrophilic sample, the abluent glass slide was coated by spray adhesive and pristine calcium carbonate nanoparticles successively. As shown in Fig. 4-2b, the SEM images revealed that the calcium carbonate nanoparticles showed a regular cubic in shape while being reasonably monodisperse, with the average diameters of 80 nm. Meanwhile, it can be observed that a rough surface formed by accumulating calcium carbonate nanoparticles evenly coated the glass slide. It is well-known that surface chemistry and surface morphology are two critical factors to obtain superhydrophobicity on a solid surface. Chemical composition would ensure the hydrophobicity of surfaces, while morphology would amplify hydrophobicity into superhydrophobicity. Rough surface with micro-nano structure is one of the most typical models which can amplify the wettability of the solid surface [24]. For example, as mentioned above, an abluent glass or freshly cleaved mica surfaces were simply naturally hydrophilic, but not superhydrophilic. Although water seemed spread on the surface with a few degrees, a flat homogeneous surface would not realize the superhydrophilicity (CA of 0°). However, it can be achieved on a rough surface accumulated by hydrophilic nanoparticles such as TiO_2 or $CaCO_3$. Similarly, the efforts made by Maguire-Boyle et al. [3] also provided a strong evidence for this theory. They fabricated a range of hydrophilic surfaces on silicon wafer coated with different carboxylic acids modified alumina nanoparticles. And the surface achieved the most hydrophilic one by being coated with cysteic acid modified alumina nanoparticles, which was in close proximity to superhydrophilic. Therefore, the CA analysis in Fig. 4-2b revealed the glass slide surface emerged a superhydrophilicity which can be confirmed by the CA of 0°. The surface can be easily wetted by water because the rough surface influenced on the wettability property of calcium carbonate nanoparticles seriously, i.e., the roughness structure enhanced the hydrophilic property of pristine calcium carbonate nanoparticles with abundant hydroxyl [1]. As shown in EDX

analysis of Fig. 4-2b, before the superhydrophobic modification step, Ca, O and C were the dominant elements on the surface. In contrast, after the promotion of robustness by spray adhesive and modification of superhydrophobic coating, obvious F, Si (belongs to 1H, 1H, 2H, 2H-perfluorooctyltriethoxysilane) and Cl (belongs to adhesive) signals could be detected by EDX analysis additionally (Fig. 4-2c). Meanwhile, the SEM image revealed the calcium carbonate nanoparticles silanized with 1H, 1H, 2H, 2H-perfluorooctyltriethoxysilane maintained the initial cubic shape while being reasonably monodisperse, with average diameters of 80 nm. Likewise, the nanoparticles accumulated into the rough surface which can be seen in the SEM images, however, with the presence of low surface energy substance 1H, 1H, 2H, 2H-perfluorooctyltriethoxysilane, the glass slide surface emerged a superhydrophobicity which can be confirmed by the CA of 151.7°. The surface simply cannot be wetted by water because the roughness structure amplified the hydrophobicity of 1H, 1H, 2H, 2H-perfluorooctyltriethoxysilane into superhydrophobicity.

4.3.2 Superhydrophobicity and self-cleaning property

To investigate the superhydrophobicity and robustness of the painted surfaces, Scarlet 4GE was dissolved into deionized water, and then a droplet of solution was dripped onto the surfaces, which was fixed to be a 20° tilting angle. Following, a knife was used to scratch the painted surfaces along a meshy path, finally by the water dropping test to confirm the robustness. The tests were presented graphically in Fig 4-3. The painted surfaces on various substrates showed water-proofing property and robustness from the knife-scratch tests. Fig. 4-3a was a demonstration of a red-dyed water droplet sliding off the painted glass slide surface. It can be concluded from the graphs that water moved easily off the superhydrophobic coating immediately.

To expand this novel superhydrophobic surface into large-scale industrial and daily applications, the superhydrophobic paint needs to be tested on different substrates in order to investigate the universal of this strategy. In Fig. 4-3b-g, we compared the

superhydrophobicity of the coatings on PTFE pad, wood, aluminium sheet, paper, gauze and stainless steel mesh substrates. Water droplets completely left the surfaces without wetting or even contaminating the surfaces, indicating that the surfaces were superhydrophobic, especially the soft substrates also gained the nonwetting property after treating with superhydrophobic paint. This was due to the low surface energy substance 1H, 1H, 2H, 2H-perfluorooctyltriethoxysilane, by combining with the roughness structure, a high ratio of trapped air appeared in the interface between solid and liquid, the water droplets can be suspended due to the multilevel discontinuous three-phase contact line, and low adhesion exists, which is similar to the case of lotus leaf.[25,26] Even after knife-scratch tests, the painted surfaces on all kinds of substrates still retained superhydrophobicity. Due to good compatibility of the superhydrophobic paint and spray adhesive, the superhydrophobic surfaces realized the robustness even though the inherent mechanical damage resistance was as weak as most superhydrophobic surfaces. As shown in Fig. 4-3(a_5-a_8, b_2-b_4, c_2-c_4, d_2-d_4, e_2-e_4, f_2-f_4 and g_2-g_4), the painted surfaces was still clean and dry even after knife-scratch and then water drop.

Fig. 4-3 The superhydrophobic coating painted surfaces of (a) glass slide, (b) PTFE pad, (c) wood, (d) aluminium sheet, (e) paper, (f) gauze substrates and (g) stainless steel mesh. Water droplets can move easily away from the superhydrophobic coating, and the painted surface retained its water-repellent property even after knife scratches.

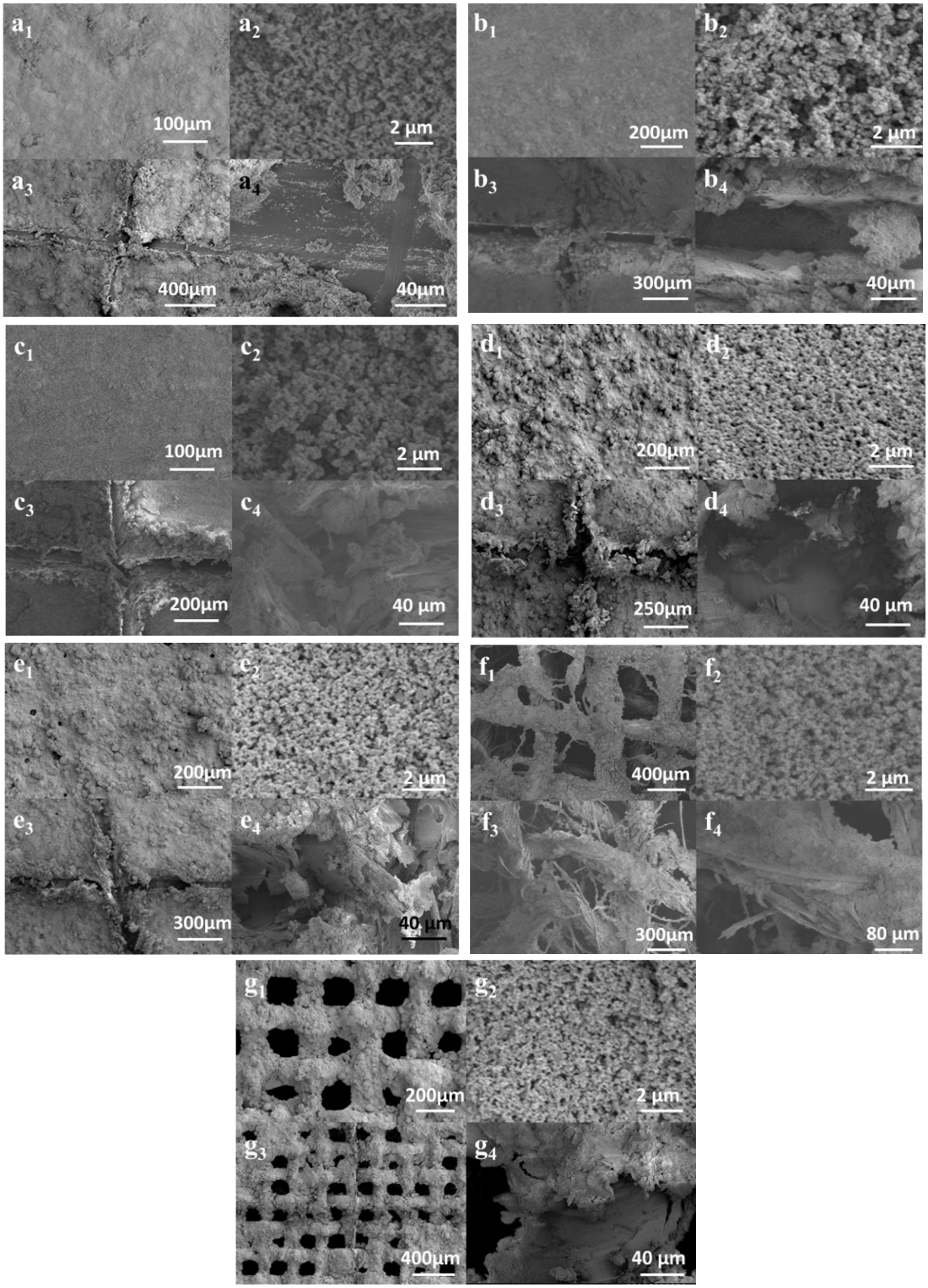

Fig. 4-4 SEM images taken before and after knife-scratch tests on the superhydrophobic coating painted surfaces of (a) glass slide, (b) PTFE pad, (c) wood, (d) aluminium sheet, (e) paper, (f) gauze substrates and (g) stainless steel mesh.

The SEM images of different substrates before and after knife-scratch tests were shown in Fig. 4-4. As can be seen, before knife-scratch tests (Fig. 4-4 a_1-a_2, b_1-b_2, c_1-c_2, d_1-d_2, e_1-e_2, f_1-f_2 and g_1-g_2), calcium carbonate nanoparticles evenly coated on the surfaces of various substrates, and rough surfaces formed by accumulating the nanoparticles. For all kinds of substrates, the painted surfaces did not lose their superhydrophobicity after knife-scratch tests (Fig. 4-4 a_3-a_4, b_3-b_4, c_3-c_4, d_3-d_4, e_3-e_4, f_3-f_4 and g_3-g_4). It can be observed that the scratch of knife showed about 80~100 μm wide, and the substrates exposed after knife- scratch. However, the width of scratch was far smaller than the size of water droplets, due to the atmospheric pressure, droplets crossed over the scratch without wetting the exposed substrates. Therefore, the painted surfaces still remained superhydrophobicity. Especially the gauze substrates also gained robustness against knife-scratch tests and remained superhydrophobicity, as can be seen in Fig. 4-4 f_3-f_4, the fiber of gauze was partially destroyed but superhydrophobic paint maintained the original appearance, which was because the surface roughness could be protected by its inherent flexibility and ability to reduce direct friction between coating and surface.

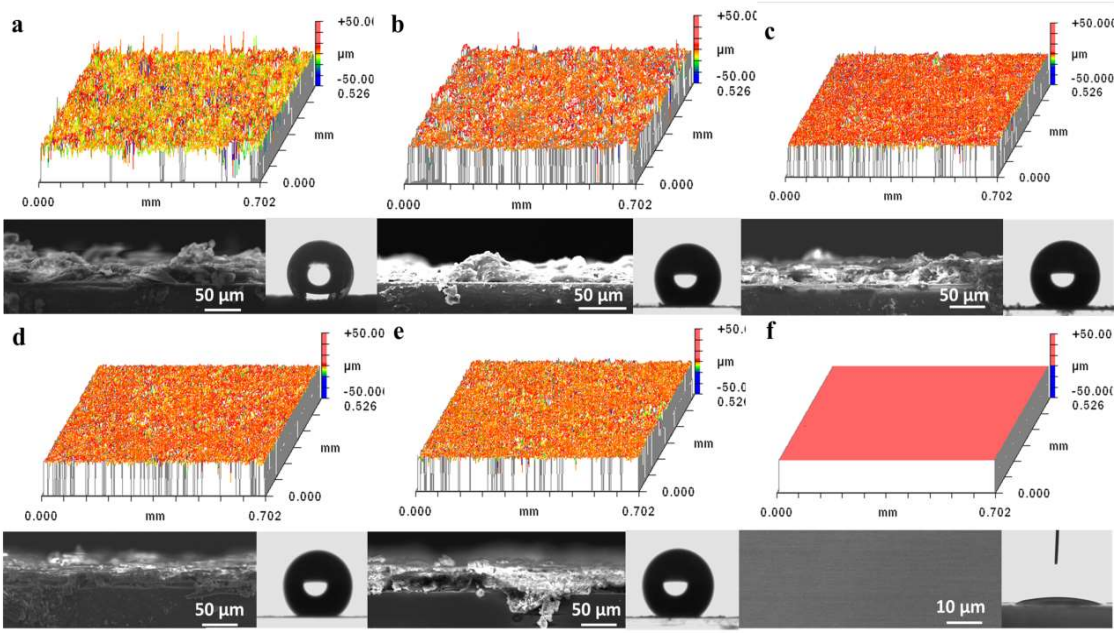

Fig. 4-5 The 3D optical surface images, SEM images and contact angle of the painted surfaces with different paint spray time. (a) 1 s; (b) 2 s; (c) 3 s; (d) 4 s; (e) 5 s; (f) glass slide.

To quantitatively investigate the effect of fabricating conditions on superhydrophobic surfaces, the spray time of superhydrophobic paint onto glass slides was regulated, and then the roughness and superhydrophobicity of surfaces was discussed. As shown in Fig. 4-5, paint spray time of 1 s, 2 s, 3 s, 4 s, 5 s and bare glass slide were studied, the roughness(Ra) showed obvious difference, which were 5807 nm, 3253 nm, 1894 nm, 1988 nm, 1862 nm and 0.485 nm. As the spray time increasing the Ra decreased, this was because that the roughness of adhesive sprayed on glass slide was large while the nanoparticles in superhydrophobic paint filled the interspace of adhesive forming a smoother surface. However, it was worth noting that the Ra of painted surfaces did not change and kept at about 1900 nm when the spray time rose to 3 s, which was the critical spray time for paint covering surface entirely. After completely coverage, the Ra value of surface tends to stable and showed the roughness accumulated by nanoparticles rather than adhesive. Meanwhile, the roughness had an effect on superhydrophobicity of surfaces, as the adhesive was covered by paint gradually, the contact angles increased and were 125.8°, 140.6°, 151.7°,150.7° and 151.4°, likewise, spray time of 3 s was the critical time for superhydrophobicity due to the complete coverage of surfaces. In addition, it can be observed from SEM images that the exposed adhesive was covered gradually by nanoparticles and the coverage tended to be tight.

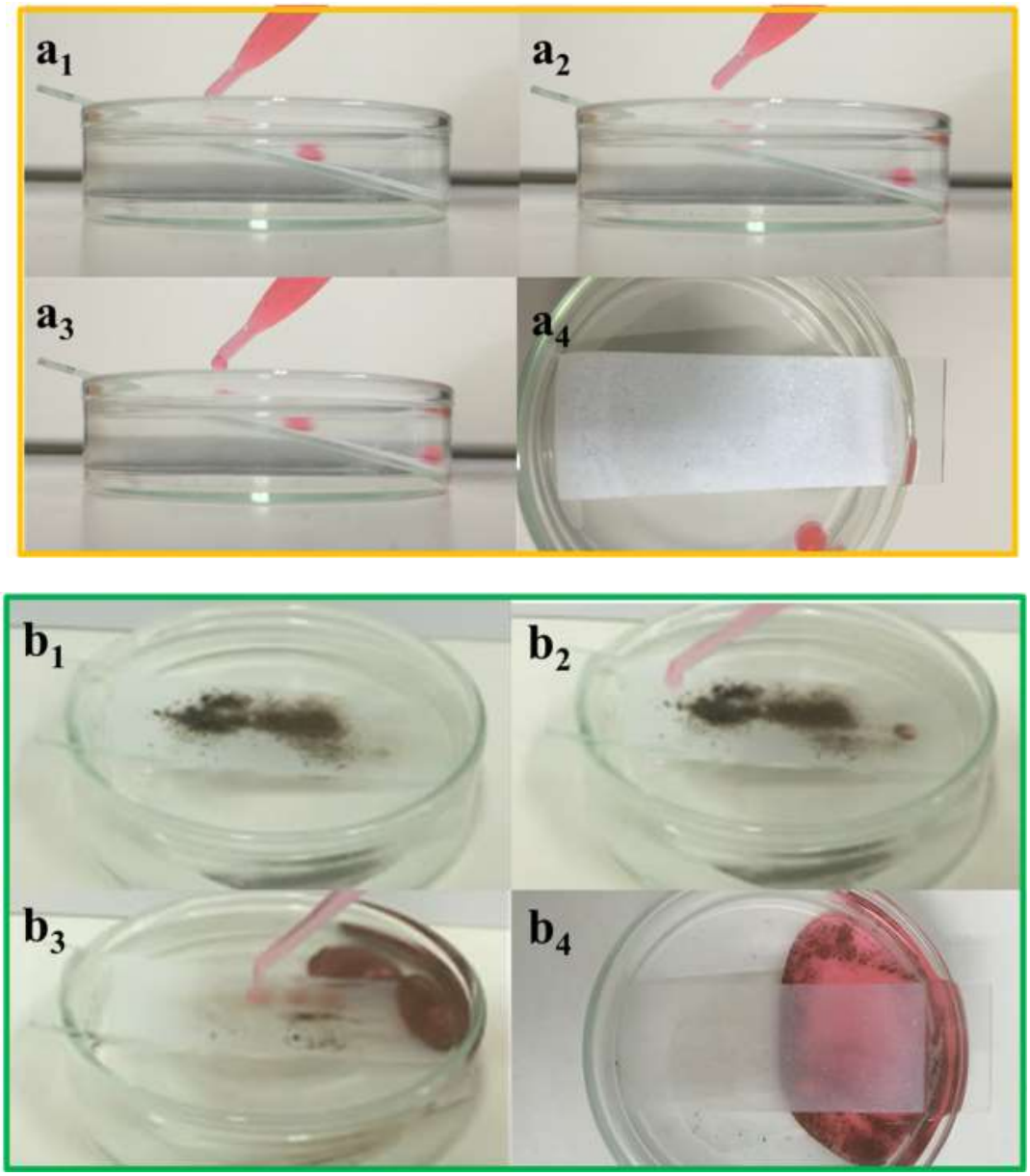

Fig. 4-6 Demonstration of the (a) superhydrophobicity and (b) self-cleaning property of dirt under oil (hexane) of the painted surface on glass slide.

There is few research has been reported on any superhydrophobicity or self-cleaning tests under oil immersion. Due to the lower surface tension of oil than that of water, the superhydrophobic surfaces were vulnerable to the penetration of oil, which resulted in losing their water repellency [27]. Superamphiphobic surfaces which repel both water and oil seems to be an effective solution to this problem [28, 29]. However, both self-cleaning from water repellency and a smooth coating of oil are imperative to many occasions, like bearings and gears lubrication. Under those situations, superamphiphobic

surfaces are going to be invalid due to its lubricating oils repellency characteristic.

The superhydrophobicity and self-cleaning tests of the painted surface under oil (hexane) were emerged graphically in Fig. 4-6a, a glass slide was employed as an example for these tests. As can be observed from Fig. 4-6a, water droplets still maintained "marbles" at the oil-solid interface without wetting the painted surface even immersed in oil, rather than forming a two-layer system, the droplets then rolled off, thus indicating that the surfaces retained their superhydrophobicity after being immersed in oil. Meanwhile, the superhydrophobic surface had a good self-cleaning and low adhesive property even immersed in oil, we showed in Fig. 4-6b, a dirt-removal test on the painted glass slide surface under oil immersion. The painted surface was fully immersed in oil and then dirt (dust and soil) was put onto the surface. To test the dirt-removal property, water was dropped onto the painted surface so as to remove the dirt. Obviously, the water droplets can move easily away from the surface while taking off dirt, which meant the superhydrophobic paint can prevent the infiltration of water and the contamination of dirt.

When the painted surface was immersed in oil, the oil gradually penetrated into the surface because of its superhydrophobicity and worked as a lubricating fluid. Due to dual supporting by both lubricating fluid and inherent superhydrophobicity, water droplets still remained marble-shape. Likewisely, the self-cleaning behavior immersed in oil could also be explained by this mechanism [30-32]. Dirt could be easily wiped off by passing water over the surface. Precisely because of these reasons, the painted surface retained its superhydrophobicity and self-cleaning property even if being immersed in oil. It is believed that the paint with excellent superhydrophobicity and self-cleaning property can be extensively applied on various materials, especially for those substrates vulnerable to pollution, such as those used for clothes and external wall.

4.3.3 Robustness

The main cause limits widespread application of superhydrophobic coatings lies in the low level of surface robustness and the surface roughness is usually micro- or nano-scale

that is mechanically weak and easily gets abrasion [18]. Gauze and paper would be used as soft substrate to protect surface roughness since they hold inherent flexibility and be able to cushion direct impacts occurring on coating and surface [37]. However, micro-nanostructures on hard substrates are apt to be destructive or removed. As this work has proposed a new method that utilize adhesive for adhering superhydrophobic coatings on substrates, detailed and robust adhesive can be applied increasingly and superhydrophobic surfaces, which has the feature of inherent weak robustness, then can be coped with well.

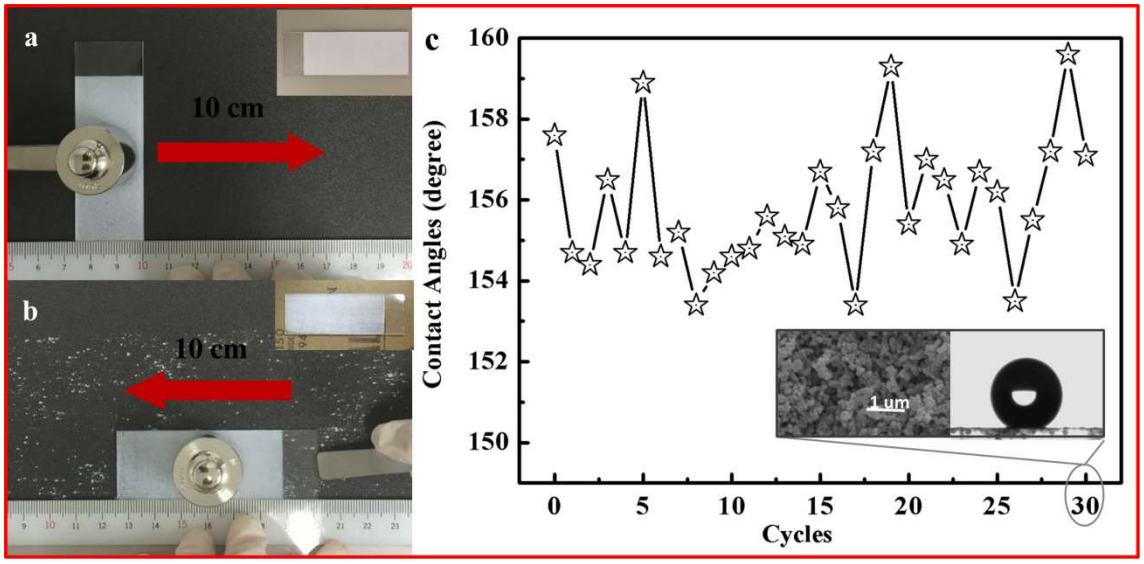

Fig. 4-7 Sandpaper abrasion tests. (a and b) One cycle of the sandpaper abrasion test. (c) Plot of mechanical abrasion cycles and water contact angles after each abrasion test.

For the further study on robustness of painted surfaces, a glass slide sample was used for the sandpaper abrasion tests and shown in Fig. 4-7. The glass sample was placed face-down to sandpaper under a weight at 100 g and moved longitudinally for 10 cm along the ruler (Fig. 4-7a). Following, the sample was rotated by 90° in situ and then moved transversely for 10 cm along the ruler (Fig. 4-7b). This procedure guaranteed the surface was abraded both longitudinally and transversely, which could be defined as one abrasion cycle. The optical photographs before and after 30 cycles of sandpaper abrasion tests were shown in the inset of Fig. 4-7a and b, respectively. It can be observed that the white

superhydrophobic coating was not peeled off from the glass substrates. Meanwhile, water contact angles after each abrasion cycle were shown in Fig. 4-7c, and it can be seen that the static water contact angles were between 153° and 160°, indicating the painted surface retained superhydrophobicity after sandpaper abrasion tests. The SEM image and contact angle of the painted surface after 30 cycles of sandpaper abrasion tests was shown in the inset. As can be seen, even after 30 cycles of sandpaper abrasion, the painted surface still remained abundant calcium carbonate nanoparticles and the contact angle was 157.1° verifying the robustness and superhydrophobicity once again.

Comparison with knife-scratch tests, sandpaper abrasion test was a more powerful damage. Even so, after different damages, the painted surface still remained superhydrophobicity, indicated the robustness of the superhydrophobic paint was efficiently enhanced.

In order to employ the sprayed surfaces to more widely application, it is very necessary to investigate the effect of permanent immersion in water on the surfaces. I have immersed the superhydrophobic surfaces into water for 120 h, then the weight of the sample was investigated.

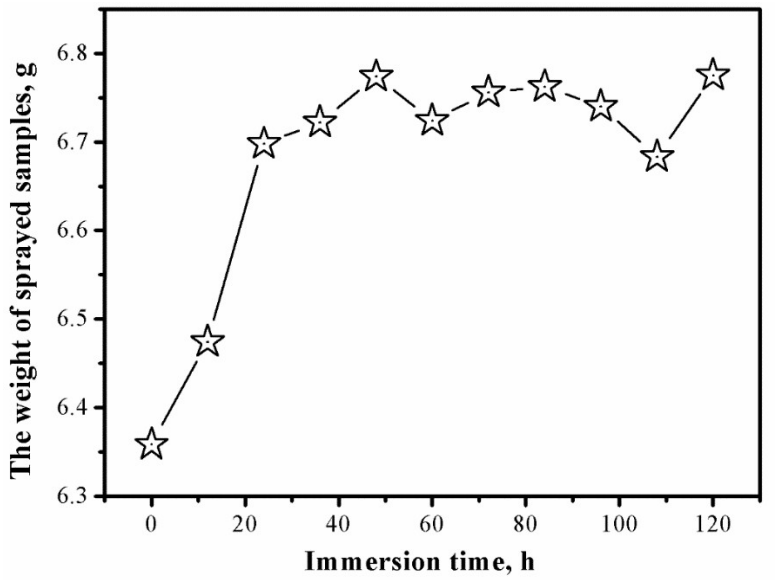

Fig. 4-8 The weight-change of sprayed superhydrophobic surfaces immersed in water for 60 h.

As can be seen from Fig. 4-8, before immersion in water, the weight of the sprayed sample was 6.3854 g. At the first stage of immersion, the sample absorbed water and the weight had a slightly increase. However, when the immersion time reached 36 h the weight became stable and was about 6.75 g which indicated the sample has reached saturated adsorption of water. For reasons of this phenomenon, the superhydrophobic calcium carbonate nanoparticles on topside of the sprayed sample would not absorb water because it held the repellency of water and was solid nanoparticle, therefore, the weight-change should be attributed to the water adsorption of sprayed adhesive. The superhydrophobicity of sprayed sample after immersion had also proved this point.

4.3.4 Oil-water separation

The superhydrophobic paint can also be utilized as an oil-water separation membrane on mesh owing to its durable superhydrophobicity under oil. Therefore, we used the same "superhydrophobic paint +adhesives" method to coat the paint on a stainless steel mesh, then the painted mesh was used to separate oil-water mixture. Dichloromethane-water mixture was used as a representative to investigate the oil-water separation efficiency of the separation device, and the separation efficiency was studied as shown in Fig. 4-9, 10 and 11.

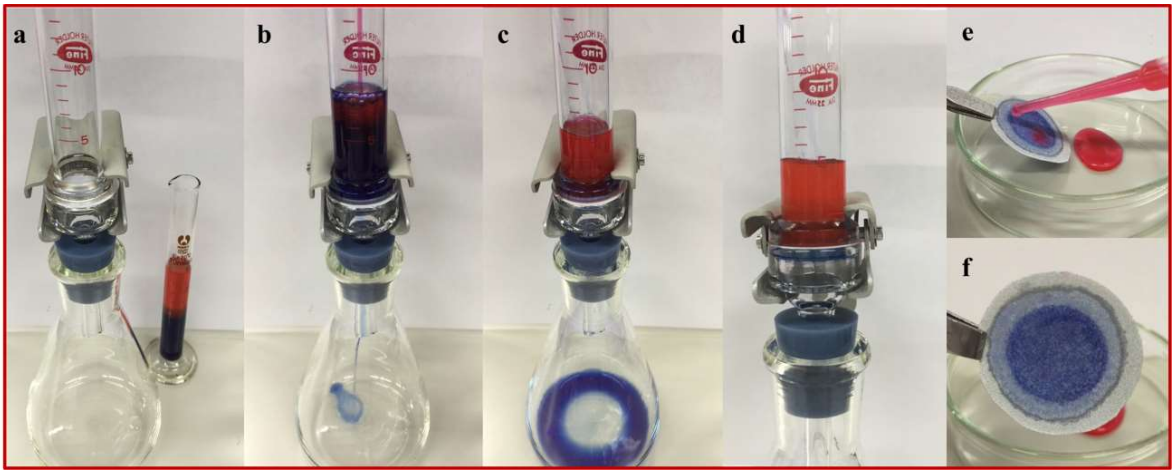

Fig. 4-9 A selective oil-water separation using the painted stainless steel mesh: (a) The oil-water mixture and separation device were prepared, then (b) the mixture was poured into the device. (c) Oil passed through the painted stainless steel mesh, (d) while water was prevented from flowing down and retained above. After separation test, (e and f) the painted stainless steel mesh was still superhydrophobic and the water droplets completely left the surface without wetting or even contaminating the surface.

After fabricating the painted mesh by “superhydrophobic paint +adhesives” method and demonstrating the superhydrophobicity, a rounded painted mesh was placed between a split type funnel formed an oil-water separation device, then the device was placed on the top of a flask as shown in Fig. 4-9a. Meanwhile, the oil-water mixture was prepared by mixing the same volume (5 mL) of blue-dyed dichloromethane and red-dyed deionized water, forming separated upper and bottom layers. Then the oil-water mixture was poured rapidly into device, dichloromethane soon sank to the bottom of the device because its density was higher than that of water. Driven by gravity only, blue-dyed dichloromethane was immediately taken up by the device, penetrated through the painted mesh, and finally swirled into the flask (Fig. 4-9b and c). There was not any leaked water in flask, this was because the superhydrophobicity of the painted mesh even if was immersed in oil. It was emerged in Fig. 4-9d that the red water layer was still remained in the device. In addition, after the oil-water separation course, painted mesh was taken out from the device and tested superhydrophobicity. As can be seen in Fig. 4-9e and f, water droplets did not wet

or even contaminate the surface, reconfirmed that the painted surface would remain superhydrophobicity even under oil immersion. Meanwhile, this phenomenon implied that the as-prepared device could be reused.

The theory created by Cassie et al. [38], has been well-known as a classic theory, which indicates the superhydrophobicity formed from the water-air-solid interface. The air molecules locked in micro-nanostructures, water and rough surface form the water-air-solid system. Similarly, the wetting behavior in water-oil-solid system could also be explained by this strategy. The oil-water mixture was separated successfully only depended on gravity by taking advantage of the feature of superhydrophobic surface, which has indicated easy operation and low energy consumption of the strategy.

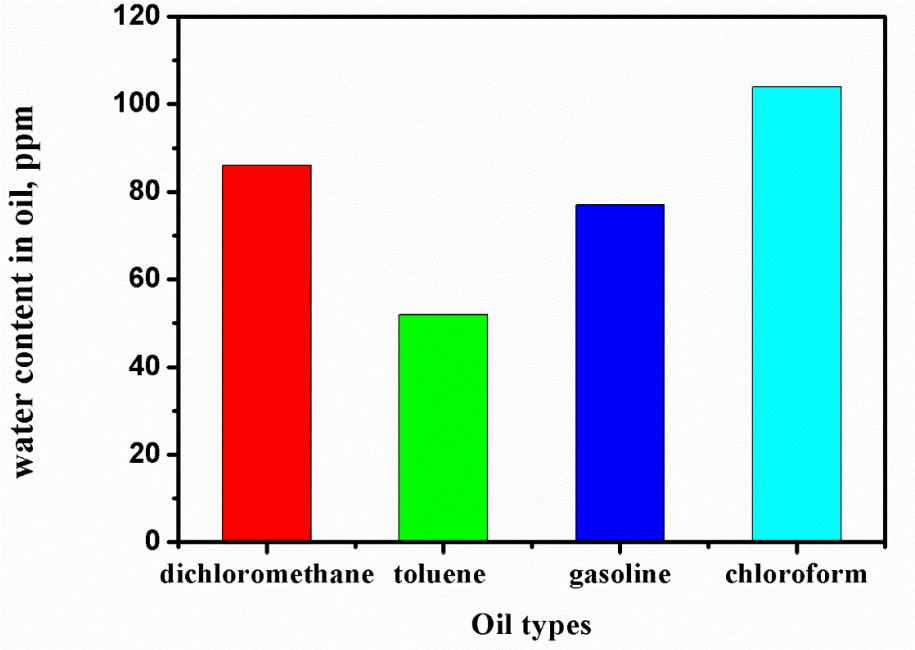

Fig. 4-10 Water content in oil of different oil types before oil-water separation

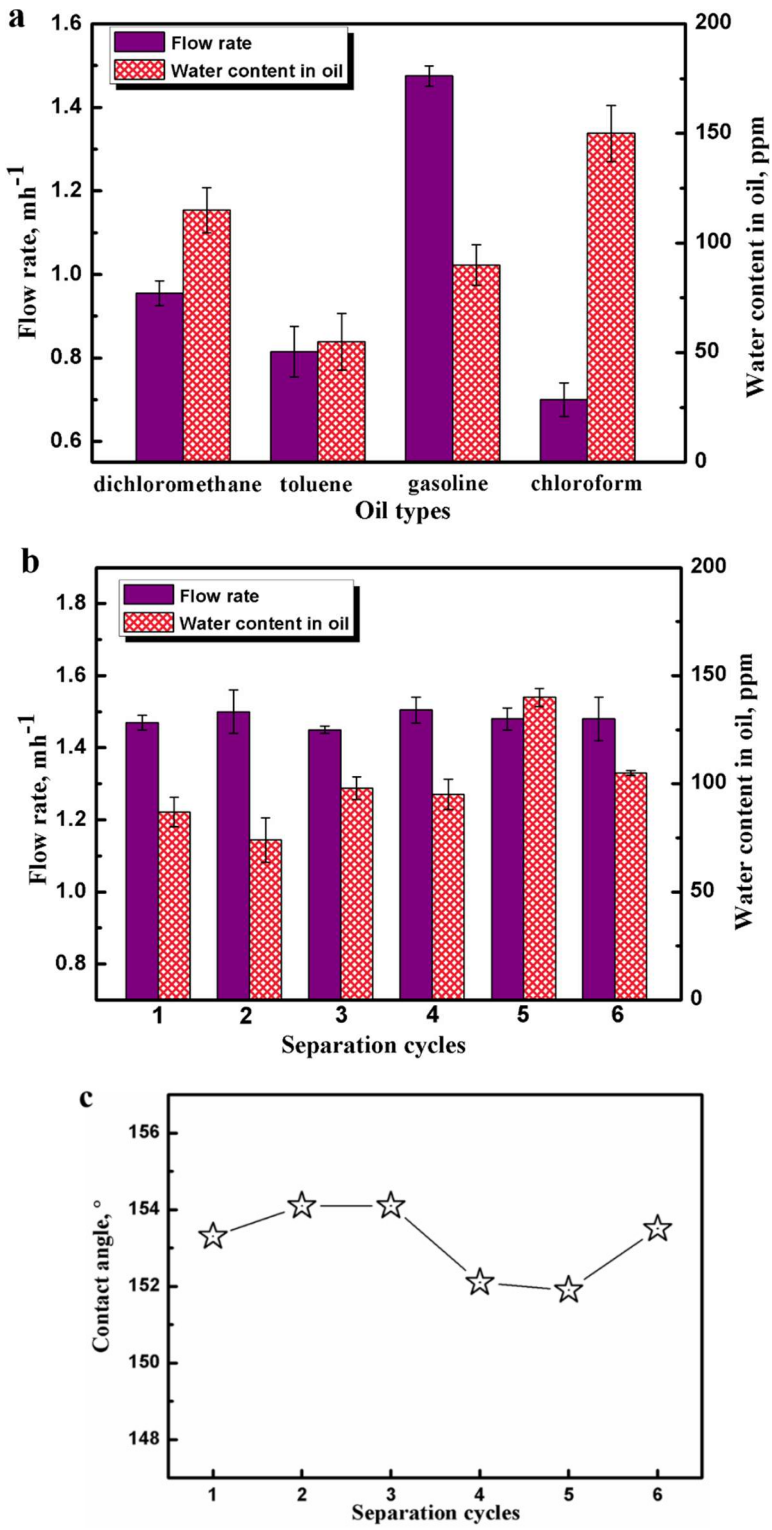

Fig. 4-11 Oil-water separation results of the as-prepared device. (a) Water content in oil and oil flow rate for penetrating a series of immiscible oil-water mixtures. (b) Water content in oil and oil flow rate for penetrating gasoline-water mixture through the as-prepared device with different cycle index. (c) Plots of separation cycles for gasoline-water mixture and water contact angles after each cycle.

It is very important to spread the application of as-prepared device to different oil-water mixtures because of the oil spill accidents throughout the world, such as dichloromethane toluene, gasoline and chloroform. Separation property of the as-prepared device could be quantitatively described according to the separation efficiency, which was defined by water content in oil after separation. To investigate the oil-water separation, four kinds of mixtures were separated by the as-prepared device. Oil instantly penetrated through the painted mesh while water was retained above. The water content in oil before and after first separation was measured by Karl Fischer Moisture Titrator. As can be seen from Fig. 4-10, for different oil-water mixtures, water content in oil differed from one another significantly before separation, because the solubility of oil in water exist large difference. The water contents in oil (dichloromethane, toluene, gasoline and chloroform) before separation were respectively 86 ppm, 52 ppm, 77 ppm and 104 ppm. The chloroform has a better compatibility with water, therefore, after simply mixing, the water content in chloroform was relatively high (104 ppm). As can be observed in Fig. 4-11a, the values of water content in oil (dichloromethane, toluene, gasoline and chloroform) were respectively 115 ppm, 55 ppm, 90 ppm and 150 ppm. This result showed that the water was almost separated from oil and there was almost no leakage in oil. As mentioned above, the water content in chloroform after separation was relatively high (150 ppm) because of its better compatibility with water. Meanwhile, the oil flow rates were calculated by measuring the passing time of oil phase and shown in the same figure. The highest flow rate of 1.475 and 0.955 mh^{-1} were achieved from the gasoline-water and dichloromethane-water mixtures, respectively, indicating the oil kinds had great influence on penetrating flow rate. For chloroform, after stirring its mixture thoroughly, the oil-water mixture took a longer time to stratify because of its better water-soluble and relatively high viscosity. As a result, the water content in chloroform was high (150 ppm) and the oil flow rate was relatively low (0.701 mh^{-1}). Next, the as-prepared device was reused to separate gasoline-water mixture for 6 times to verify its repeatability, and we had realized the tests of water content and oil flow rate for every circle. During the 6 cycle tests, the oil flow rate was

about 1.475 mh^{-1} and kept stable, and for each time of separation, the water content in oil was below 140 ppm (Fig. 4-11b), which was because the superhydrophobic painted mesh only allowed oil penetrating. In addition, the CA of painted stainless steel mesh after each separation cycle was shown in Fig. 4-11c, it was observed that the static water contact angles were between 151° and 155°, indicating the painted surface still retained superhydrophobicity even after 6 cycles separation. The results demonstrated that the superhydrophobic surfaces performed well, not only in the self-cleaning property and robustness, but also in oil-water separation application, exhibiting integrated functions.

4.4 Conclusions

In summary, the author have developed a versatile and simple strategy to fabricate robust, self-cleaning and superhydrophobic surfaces for both soft and hard substrates by a straightforward spraying method. This superhydrophobic surface remained its superhydrophobicity and self-cleaning property even under oil immersion. Meanwhile, it showed remarkable robustness against knife scratch and sandpaper abrasion. In particular, the surface still retained its superhydrophobicity even after 30 abrasion cycles with sandpaper. Because of the superhydrophobicity under oil immersion, this surface could also be used for oil-water separation as well as showed excellent separation efficiency. Further, the oil-water separation device has realized 6 times reuses and still remained excellent oil-water separation efficiency. It is believed that the superhydrophobic surface can be simply, flexibly, and robustly used in large-scale industrial applications where maintain harsh and oily environments, such as external wall coating and oil-water separation material.

Excellent robustness has been realized by utilizing the “paint+adhesive” method, the prepared surfaces had not only robustness, self-cleaning and superhydrophobicity but also outstanding separation efficiency. These excellent properties were depended on robust and satisfactory roughness structure. However, roughness structure scatters the light which affects transparence of the prepared device seriously. Therefore, the applications

of superhydrophobic materials have suffered from the limits of poor transparence. In next chapter, I would like to develop a not only robust and superhydrophobic but also transparent surface, meanwhile, this surface would be used in oil-water separation and the separation efficiency would be investigated. This kind of novel surface would be used in touch screen of telephone where transparence and robustness are both significant. Furthermore, this transparent, robust and superhydrophobic surface can be also fabricated on transparent materials, thus visible oil-water separation can be developed. Oil-water separation would be easier to manage.

References

[1] Wang, S. T.; Liu, K. S.; Yao, X.; Jiang, L. Bioinspired Surfaces with Superwettability: New Insight on Theory, Design, and Applcations. Chem. Rev. 2015, 115, 8230-8293.

[2] Feng, L.; Li, S. H.; Li, Y. S.; Li, H. J.; Zhang, L. J.; Zhai, J.; Song, Y. L.; Liu, B. Q.; Jiang, L.; Zhu, D. B. Super-Hydrophobic Surfaces: from Natural to Artificial. Adv. Mater. 2002, 14, 1857-1860.

[3] Maguire-Boyle, S. J.; Barron, A. R. A New Functionalization Strategy for Oil/Water Separation Membranes. J. Membr. Sci. 2011, 382, 107-115.

[4] Alexander, S.; Eastoe, J.; Lord, A. M.; Guittard, F.; Barron, A. R. Branched Hydrocarbon Low Surface Energy Materials for Superhydrophobic Nanoparticle Derived Surfaces. ACS Appl. Mater. Interfaces. 2016, 8, 660-666.

[5] Gao, X. F.; Yan, X.; Yao, X.; Xu, L.; Zhang, K.; Zhang, J. H.; Yang, B.; Jiang, L. The Dry-Style Antifogging Properties of Mosquito Compound Eyes and Artificial Analogues Prepared by Soft Lithography. Adv. Mater. 2007, 19, 2213-2217.

[6] Ye, C. Q.; Li, M. Z.; Hu, J. P.; Cheng, Q. F.; Jiang, L.; Song, Y. L. Highly Reflective Superhydrophobic White Coating Inspired by Poplar Leaf Hairs toward an Effective “Cool Roof”. Energy Environ. Sci. 2011, 4, 3364-3367.

[8] Barthlott, W.; Neinhuis, C. Purity of The Sacred Lotus, or Escape from Contamination In Biological Surfaces. Planta. 1997, 202, 1-8.

[9] Nosonovsky, M.; Bhushan, B. Energy Transitions in Superhydrophobicity: Low Adhesion, Easy Flow and Bouncing. J. Phys.: Condens. Matter. 2008, 20, 395005.

[10] Pan, Q.; Wang, M.; Wang, H. Separating Small amount of Water and Hydrophobic Solvents by Novel Superhydrophobic Copper Meshes. Appl. Surf. Sci. 2008, 254, 6002-6006.

[11] Mishchenko, L.; Hatton, B.; Bahadur, V.; Taylor, J. A.; Krupenkin, T.; Aizenberg, J. Design of Ice-Free Nanostructured Surfaces Based on Repulsion of Impacting Water Droplets. ACS Nano. 2010, 4, 7699-7707.

[12] Shi, F.; Niu, J.; Liu, J.; Liu, F.; Wang, Z.; Feng, X. Q.; Zhang, X. Towards Understanding Why a Superhydrophobic Coating is Needed by Water Striders. Adv. Mater. 2007, 19, 2257-2261.

[13] Ou, J.; Rothstein, J. P. Direct Velocity Measurements of the Flow Past Drag-Reducing Ultrahydrophobic Surfaces. Phys. Fluids. 2005, 17, 103606.

[14] Ju, G. N.; Cheng, M. J.; Shi, F. A PH-Responsive Smart Surface for the Continuous Separation of Oil/Water/Oil Ternary Mixtures. NPG Asia Mater. 2014, 6, e111.

[15] Cheng, M. J.; Ju, G. N.; Jiang, C.; Zhang, Y. J.; Shi, F. Magnetically Directed Clean-Up of Underwater Oil Spills Through a Functionally Integrated Device. J. Mater. Chem. A. 2013, 1, 13411-13416.

[16] Ju, G. N.; Li, D. L.; Zhang, Y. J. Magnetically Driven Functionally Integrated Device for Continuous and Efficient Collection of Oil Droplets From Water. RSC Adv. 2016, 6, 20559-20564.

[17] Chen, B. Y.; Ju, G. N.; Sakai, E.; Qiu, J. H. Underwater Low Adhesive Hydrogel-Coated Functionally Integrated Device by One-Step Solution-Immersion Method for Oil-water Separation. RSC Adv. 2015, 5, 87055-87060.

[18] Zimmermann, J.; Reifler, F. A.; Fortunato, G.; Gerhardt, L. C.; Seeger, S. A Simple, One Step Approach to Durable and Robust Superhydrophobic Textiles. Adv. Funct. Mater. 2008, 18, 3662-3669.

[19] Zhu, L.; Shi, P.; Xue, J.; Wang, Y. Y.; Chen, Q. M.; Ding, J. F.; Wang, Q. J. Superhydrophobic Stability of Nanotube Array Surfaces under Impact and Static Forces. ACS Appl. Mater. Interfaces. 2014, 11, 8073-8079.

[20] Zhu, Q.; Chu, Y.; Wang, Z. K.; Chen, N.; Lin, L.; Liu, F. T.; Pan, Q. M. Robust Superhydrophobic Polyurethane Sponge as a Highly Reusable Oil-Absorption Material. J. Mater. Chem. A. 2013, 1, 5386-5393.

[21] Zhou, H.; Wang, H.; Niu, H.; Gestos, A.; Wang, X.; Lin, T. Fluoroalkyl Silane Modified Silicone Rubber/Nanoparticle Composite: a Super Durable, Robust Superhydrophobic Fabric Coating. Adv. Mater. 2012, 24, 2409-2412.

[22] Li, Y.; Li, L.; Sun, J. Bioinspired Self-Healing Superhydrophobic Coatings. Angew. Chem. 2010, 122, 6265-6269.

[23] Lu, Y.; Sathasivam, S.; Song, J. L.; Crick, C. R.; Carmalt, C. J.; Parkin, I. P. Robust Self-Cleaning Surfaces that Function When Exposed to Either Air or Oil. Science. 2015, 347, 1332-1335.

[24] Nosonovsky, M. Materials Science: Slippery When Wetted. Nature. 2011, 477, 412-413.

[25] Patankar, N. A. On The Modeling of Hhydrophobic Contact Angles on Rough Surfaces. Langmuir. 2003, 19, 1249-1253.

[26] Guo, P.; Zheng, Y. M.; Wen, M. X.; Song, C.; Lin, Y. C.; Jiang, L. Icephobic/ Anti-icing Properties of Micro/ Nanostructured Surfaces. Adv. Mater. 2012, 24, 2642-2648.

[27] Tuteja, A.; Choi, W.; Ma, M.; Mabry, J. M.; Mazzella, S. A.; Rutledge, G. C.; McKinley, G. H.; Cohen, R. E. Designing Superoleophobic Surfaces. Science. 2007, 318, 1618-1622.

[28] Deng, X.; Mammen, L.; Butt, H. J.; Vollmer, D. Candle Soot as a Template for a Transparent Robust Superamphiphobic Coating. Science. 2012, 335, 67-70.

[29] Tutelage, A.; Choi, W.; Mabry, J. M.; McKinley, G. H.; Cohen, R. E. Robust Omniphobic Surfaces. Proc. Natl. Acad. Sci. U.S.A. 2008, 105, 18200-18205.

[30] Guldin, S.; Kohn, P.; Stefik, M.; Song, J. H.; Divitini, G.; Ecarla, F., Ducati, C.; Wiesner, U.; Steiner, U. Self-Cleaning Antireflective Optical Coatings. Nano Lett. 2013, 11, 5329-5335.

[31] Fürstner, R.; Barthlott, W.; Neinhuis, C.; Walzel, P. Wetting and Self-Cleaning Properties of Artificial Superhydrophobic Surfaces. Langmuir. 2005, 21, 956-961.

[32] Yang, Y.; Deng, Y. H.; Tong, Z.; Wang, C. H. Renewable Lignin-Based Xerogels with Self-Cleaning Properties and Superhydrophobicity. ACS Sustainable Chem. Eng. 2014, 7, 1729-1733.

[37] Im, M.; Im, H.; Lee, J.-H.; Yoon, J.-B.; Choi, Y.-K. A Robust Superhydrophobic and Superoleophobic Surface with Inverse-Trapezoidal Microstructures on a Large

Transparent Flexible Substrate. Soft Matter. 2010, 6, 1401-1404.

[38] Cassie, A.B.D.; Baxter, S. Wettability of Porous Surfaces. Trans. Faraday Soc. 1944, 40, 546-551.

Chapter 5 Candle Soot as a Template for Transparent, Robust and Superhydrophobic Surface and its Application in Oil-Water Separation

5.1 Introduction

The wettability of solid surfaces is a renewed old topic which has impacted most fields of science and technology for a long time, from cave painting in the ancient to microfluidic devices in the modern.[1] In past decades, bioinspired surfaces with superhydrophobicity that is one of the extreme states of surface wettability have been intensively explored and accelerated by discoveries of superwetting phenomena in nature.[2-6] The term superhydrophobicity was introduced in 1976 by Reick to describe hydrophobic particle coating made of hydrophobic fumed silicon dioxide, where a water droplet maintains a contact angle (CA) $\theta > 150°$ and the force of adhesion is negligible.

In 1997, Barthlott and Neinhuis revealed that the superhydrophobicity and self-cleaning property of lotus leaves were caused by microscaled papillae and epicuticular wax, providing a mono-microstructure model.[7] Subsequently, Jiang et al. disclosed that there are micro- and nanoscaled hierarchical structures on the lotus leaf surface, that is, branch-like nanostructures on top of the micropapillae, which result in the superhydrophobicity.[2] Thus, the origin of superhydrophobicity of a lotus leaf becomes clear from a monoscaled model of microstructures to a dual-scaled model of hierarchical structures. These studies on superhydrophobicity activated the emerging applications of wettability from energy conversion, avoiding fluid drag in microfluidic devices, reducing fluid resistance for aquaculture devices, protection of electronic devices, and oil−water separation.[8-12] However, with deepening of the research, the robustness question of superhydrophobic surfaces was put into a more outstanding position, which was that the superhydrophobic surfaces were readily destroyed.[13-19] Conventional

superhydrophobic surfaces mostly depend on expensive, sophisticated, and fragile roughness structures, which are inherently vulnerable to mechanical damage and sometimes abraded when tissue brushing happens. In the meantime, roughness structure as a critical factor to obtain superhydrophobicity on solid surface has always prevented the surfaces from transparence seriously.[20] Therefore, poor robustness and transparence has turned into the bottleneck for large-scale industrial applications of the superhydrophobic surfaces.

To handle this problem, many efforts have been devoted to realizing the superhydrophobic surfaces with both robustness and transparence simultaneously by a simple and cost-effective method. Ebert et al. [21] used deep reactive ion etching to create rough surfaces on PDMS substrates using a O_2/CF_4 plasma. Surfaces then underwent an additional treatment with either octafluorocyclobutane (C_4F_8) plasma or vapor deposition of perfluorooctyltrichlorosilane following surface activation with O_2 plasma. The effects of surface roughness and the additional surface modifications were examined with respect to the contact angle, contact angle hysteresis, and optical transmittance. To examine wear resistance, a sliding wear experiment was performed using an atomic force microscope. Rao et al. [22] synthesized optically transparent superhydrophobic silica films at room temperature using sol-gel process by a simple dip coating technique. The molar ratio of MTMS:MeOH:H_2O was kept constant at 1:10.56:4.16, respectively. Methyl groups were introduced in the silica film by post-synthesis grafting from two solutions using trimethylchlorosilane (TMCS) and hexamethyldisilazane (HMDZ) silylating agents in hexane solvent, individually. The TMCS modified films exhibited a very high water contact angle ($166\pm2°$) in comparison to the HMDZ ($138\pm2°$) modified films, indicating the water repellent behavior of the surface. However, the above works still depended on expensive and complex techniques.

Very recently, Xu Deng et al.[23] designed an easily fabricated, transparent, and oil-rebounding superamphiphobic coating. A porous deposit of candle soot was coated with

a silica shell. The black coating became transparent after calcination. After silanization, the coating was superamphiphobic and remained so even after its top layer was damaged by sand impingement.

Inspired by this work, the author described a versatile and simple strategy to fabricate robust, transparent and superhydrophobic coatings. The surface to be coated, in our case a quartz wafer, was held above the flame of a paraffin candle. Deposition of a soot layer turned the wafer black. This candle soot layer had roughness structure and superhydrophobicity. However, this structure was fragile because of its physical particle-particle interactions were weak. When water rolled off the surface, the drop carried soot particles away with it until almost all the soot deposition was removed. Inspired by this promising morphology of soot, we made use of chemical vapor deposition of $SiCl_4$. Similar to a Stöber reaction, a filmy silica shell was formed by hydrolysis and condensation. Calcining the hybrid soot-silica shell in air caused combustion of the carbon core, while the silica shell kept its roughness and network texture. To reduce the surface energy, the hydrophilic silica shell coated substrate was modified with a semifluorinated silane by chemical vapor deposition. After that, the surface obtained remarkble robustness, transparence and superhydrophobicity. What is more, the superhydrophobic surface showed promising potential applications in oil-water separation and retained excellent oil−water separation efficiency even after reuses. It is believed that this superhydrophobic surface can be simply, flexibly, and robustly used in large-scale industrial applications where maintain harsh, transparent and oily environments, such as external wall coating, touch screen and oil-water separation material.

5.2 Experimental

In this chapter, I describe a simple way to make robust, transparent, superhydrophobic coatings. The surface to be coated, in our case a quartz wafer, is held above the flame of a paraffin candle. Deposition of a soot layer turns the wafer black. This soot surface has

roughness structure and superhydrophobicity. However, the structure is fragile because the particle-particle interactions are only physical and are weak. When water rolls off the surface, the drop carries soot particles with it until almost all of the soot deposit is removed. Inspired by the promising morphology of soot, we made use of chemical vapor deposition (CVD) of $SiCl_4$. Similar to a Stöber reaction, silica is formed by hydrolysis and condensation. Calcinating the hybrid carbon/silica network in air caused combustion of the carbon core, but the layer kept its roughness and network texture. To reduce the surface energy, the hydrophilic silica shells were coated with a semifluorinated silane by CVD. After CVD, the surface obtained superhydrophobicity. This surface can also been used in oil-water separation.

5.3 Results and discussion

5.3.1 Surface modification and characterization

Highly transparent and superhydrophobic robust coating was fabricated following the procedure depicted in Fig. 5-1: firstly, a quartz wafer was washed by dry ethanol/ethanol–deionized water (v/v 1:1)/deionized water sequentially for 15 min each time, following a drying process in an oven at 60°C. Then, the abluent wafer was held in the flame of a candle until a soot layer a few micrometers thick was deposited. Subsequently, the soot coated substrate was placed in a desiccator together with an open glass dish containing about 1 ml of $SiCl_4$. The desiccator was closed again and chemical vapor deposition of $SiCl_4$ was carried out for 2 h. Similar to a Stöber reaction, a silica shell was formed as a coating on candle soot by hydrolysis and condensation of $SiCl_4$. Consequently, the quartz wafer coated by candle soot and silica shell was calcinated in air. The silica coating prepared by Stöber reaction was porous. During calcination, candle soot composed of carbon polymer thermally degraded and diffused through the silica coating. After calcination of the soot-silica shell coated substrate at 600°C for 30 min in air, a superhydrophilic and hollow silica shell was obtained on the quartz wafer. To

transform it into superhydrophobic, the silica shell coated substrate with abundant hydroxyl was performed chemical vapor deposition in a desiccator together with an open glass dish containing about 1ml of Trichloro(1H, 1H, 2H, 2H-perfluorooctyl)silane, stable oxane bonds between silane and silica shell formed by left for 2h at 60°C, the silica shell finally achieved superhydrophobicity.

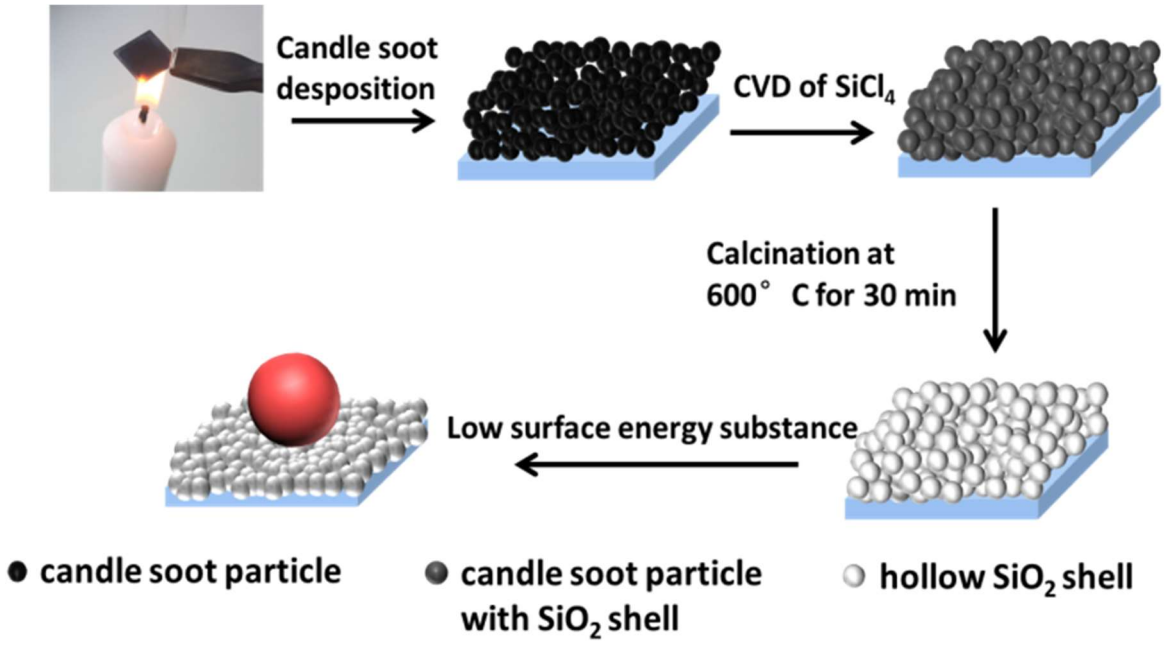

Fig. 5-1 Schematic illustration of the preparation process and properties of the transparent, roubust and superhydrophobic surface.

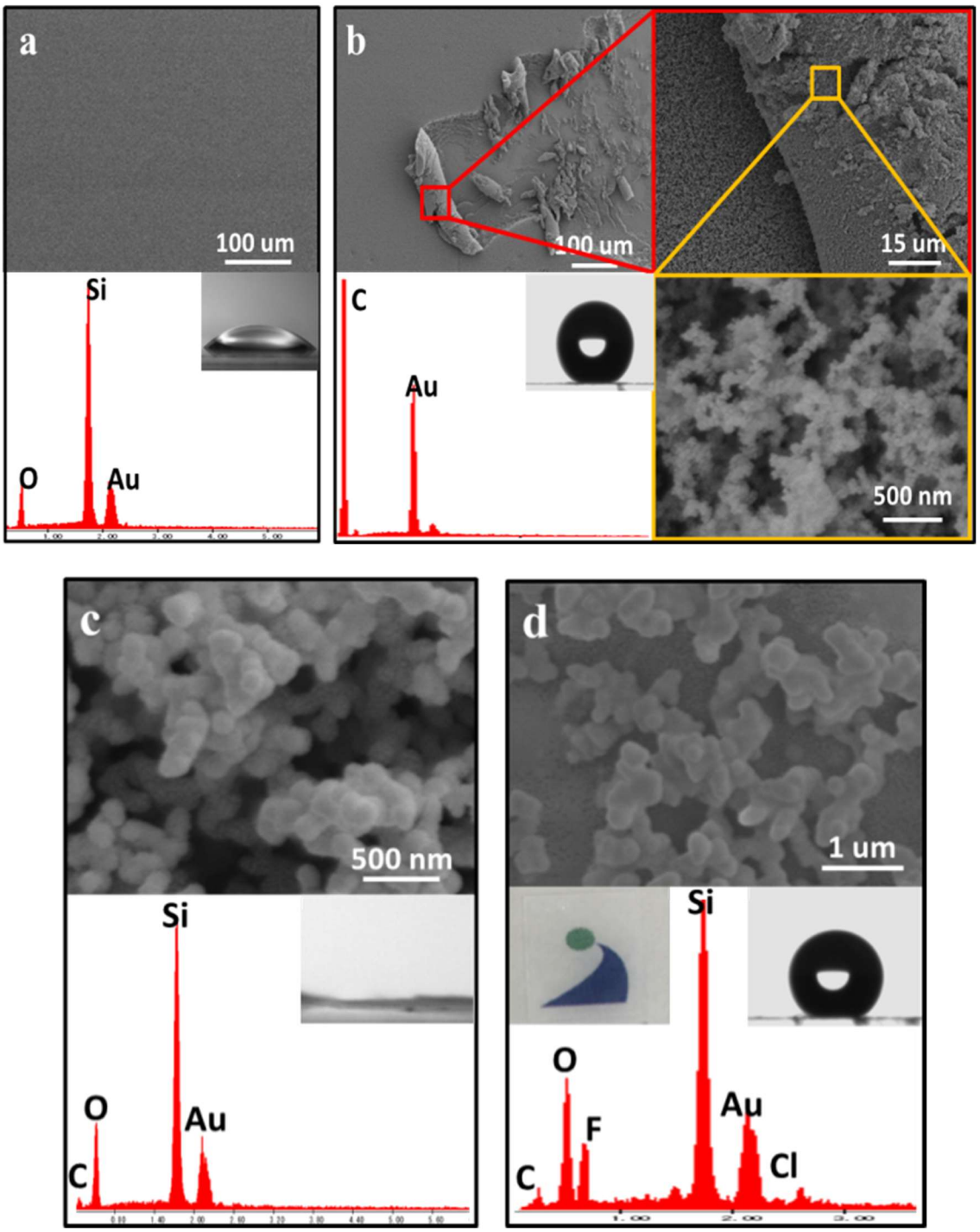

Fig. 5-2 The SEM images, CA and EDX measurements of different glass slide samples: (a) bare quartz wafer; (b) quartz wafer with a candle soot layer; (c) quartz wafer coated by candle soot and silica shell; (d) quartz wafer with superhydrophobic silica shell.

Evident changes in wettability of the substrates surfaces occurred in the process of preparing highly transparent and superhydrophobic robust coating. The quartz wafer sample was tested as a representative, SEM, CA and EDX analysis was used to prove the

modification.

As shown in Fig. 5-2a, the bare quartz wafer was washed by dry ethanol/ethanol-deionized water (v/v 1:1)/deionized water carefully, followed by SEM, CA and EDX analysis. The surface morphology in SEM image revealed the bare quartz wafer had a homogeneous and smooth surface, and signals of Si and O elements only, which constituted quartz primarily, were detected from the EDX analysis, ascertaining thorough cleaning of the surface by ethanol and water. Meanwhile, the bare quartz surface emerged hydrophilicity due to the presence of hydroxy, and the CA of water was 40.7°. To fabricate the candle soot template, the abluent quartz wafer was held in the flame of a candle for 3-5 s until a black soot layer a few micrometers thick was deposited. As shown in Fig. 5-2b, the SEM images revealed that the soot consisted of carbon particles with a regular diameter of 30 to 40 nm, forming a loose, porous layer. Meanwhile, it can be observed that a rough surface formed by accumulating candle soot nanoparticles evenly on the quartz wafer. It is well-known that surface chemistry and surface morphology are two critical factors to obtain superhydrophobicity on a solid surface. Chemical composition would ensure the hydrophobicity of surfaces, while morphology would amplify hydrophobicity into superhydrophobicity. Rough surface with micro-nano structure is one of the most typical models which can amplify the wettability of the solid surface.[24] For example, the surface of abluent plastic plate were simply naturally hydrophobic, but not superhydrophobic. Although water seemed cannot wet the surface, a flat homogeneous surface would not realize the superhydrophobicity (CA above 150°). However, it can be achieved on a rough surface accumulated by hydrophobic nanoparticles such as candle soot nanoparticles, hydrophobic candle soot particles accumulated on quartz wafer forming a roughness structure, which amplified hydrophobicity into superhydrophobicity. Therefore, a water drop gently deposited on the hydrophobic candle soot coated surface showed a contact angle above 150° and rolled off easily, demonstrating the surface's superhydrophobicity. However, the soot deposition layer was fragile because the physical

particle-particle interactions were too weak. When water rolled off the surface, droplet carried soot particles away with it until almost all the deposition was removed and then the surface underwent a wettability transition. Inspired by this promising morphology and superwettability of candle soot deposition layer, we adopted a novel approach to coat the soot layer with a silica shell, making use of chemical vapor deposition of $SiCl_4$. The soot-coated substrate was placed in a desiccator together with an open glass dish containing about 1 ml of $SiCl_4$. After 2 h, the soot particles were coated by a silica shell due to the hydrolysis and condensation of $SiCl_4$. Meanwhile, as can be observed in Fig. 5-2c obviously, the average diameter of soot particles increased slightly after deposition, but the primary morphology of soot layer was maintained, i. e., the roughness structure of candle soot layer was not destroyed by chemical vapor deposition of $SiCl_4$. Therefore, as mentioned above, due to the hydrophilicity of silica and roughness structure provided by candle soot layer, the silica shell achieved superhyrophilicity (CA of 0°). Calcining the soot-silica shell coated substrates at 600°C for 30 min in air caused combustion of the candle soot layer (Fig. 5-2d). Only isolated chains of soot particles, which were not linked in silica shell, broke during calcination. Nevertheless, the hollow silica shell was retained and still kept its roughness structure and porous texture. To reduce the surface energy, the superhydrophilic silica shell was modified by Trichloro(1H, 1H, 2H, 2H-perfluorooctyl)silane via chemical vapor deposition method. After modification, a water drop placed on top of the coating formed a static contact angle of 152.1°. Owing to the extremely low adhesion of the surface to water, it was difficult to deposit water drops, because they immediately rolled off.

For applications on glass surfaces such as goggles or touch screens, the superhydrophobic coating needs to be transparent and mechanically robust. The silica shell coated on candle soot had a shell thickness well below the wavelength of visible light, such thin shells are highly transparent. After calcination of the black carbon template, candle soot nanoparticles disappeared and air filled the void. Therefore, the

silica shell coated substrate was white, while, when liquid (e. g. water or ethanol) fill in the void, the substrate was transparent (Fig. 5-2d).

5.3.2 Robustness

In outdoor applications, superhydrophobic surfaces need to survive harsh conditions. To investigate the mechanical resistance of our coating, sand impact tests were performed. Sand grained 300 to 500 um in diameter impinged the surface from a height of 40 cm, crresponding to an impinging energy of 1.1×10^{-4} J per grain. The silica shells were not sufficiently robust to completely resist sand impact as shown in Fig. 5-3. As time increased at initial stage, a cave formed on the impacted area (Fig. 5-3a and b), after 210s, the silica shell was removed and the substrate was exposed (Fig. 5-3c and d). However, zooming into the cave almost unaltered the micro-morphology. Owing to the silica shell's self-similarity, the surface kept its superhydrophobicity until the silica shell was completely removed after extended impact. The mechanical durability depended on the amount of sand impinging per unit of time, the size of the grains, the height of fall, and the thickness of the silica shell. The mechanical stability would increase with the thickness of the silica shell, but at the expense of the coating's transparency.

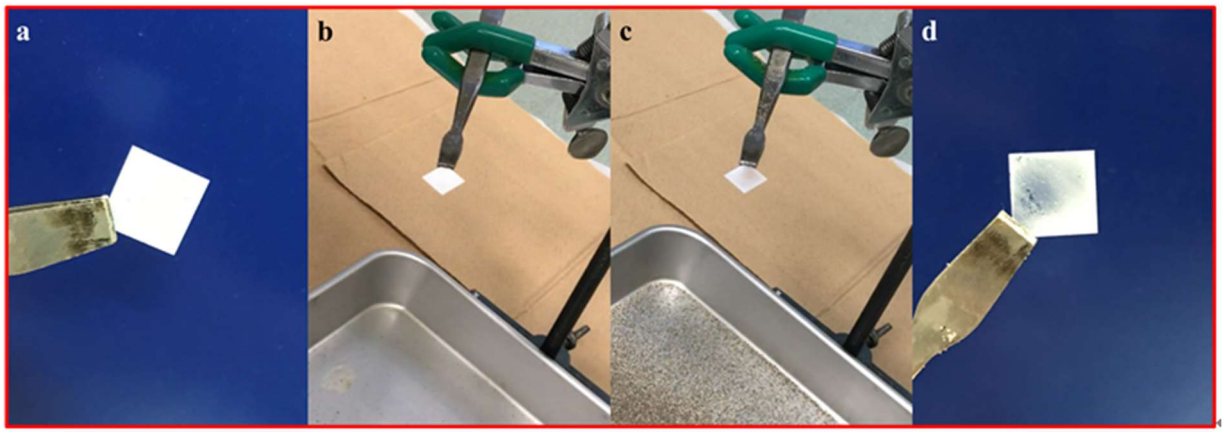

Fig. 5-3 The robustness quantified by sand abrasion: (a) silica shell coated quartz wafer before sand abrasion, (b) and (c) silica shell coated quartz wafer during sand abrasion, (d) silica shell coated quartz wafer after sand abrasion.

5.3.3 Oil-water separation

The superhydrophobic silica shell can also be utilized as an oil−water separation membrane on mesh owing to its durable superhydrophobicity under oil. Therefore, we used the method mentioned above to modify a superhydrophobic silica shell on a stainless steel mesh; then the modified mesh was used to separate an oil−water mixture. Dichloromethane−water mixture was used as a representative to investigate the oil−water separation efficiency of the separation device, and the separation efficiency was studied as shown in Fig. 5-4,5 and 6.

After fabricating the modified mesh as separation device and demonstrating the superhydrophobicity, the as-prepared device was placed between a split type funnel forming an oil-water separation device; then the device was placed on the top of a flask as shown in Fig. 5-4a. Meanwhile, the oil−water mixture was prepared by mixing the same volume (5 mL) of blue-dyed dichloromethane and red-dyed deionized water, forming separated top and bottom layers. Then the oil−water mixture was poured rapidly into the device; dichloromethane soon sank to the bottom of the device because its density was higher than that of water. Driven by gravity only, blue-dyed dichloromethane was immediately taken up by the device, penetrated through the modified mesh, and finally swirled into the flask (Fig. 5-4b and c). There was not any leaked water in the flask; this was because of the superhydrophobicity of the modified mesh even if it was immersed in oil. It was shown in Fig. 5-4d that the red water layer was still retained in the device. In addition, after the oil-water separation course, modified mesh was taken out from the device and the superhydrophobicity was tested. Water droplets did not wet or even contaminate the surface, reconfirming that the modified surface would retain superhydrophobicity even after oil-water separation. Meanwhile, this phenomenon implied that the as-prepared device could be reused.

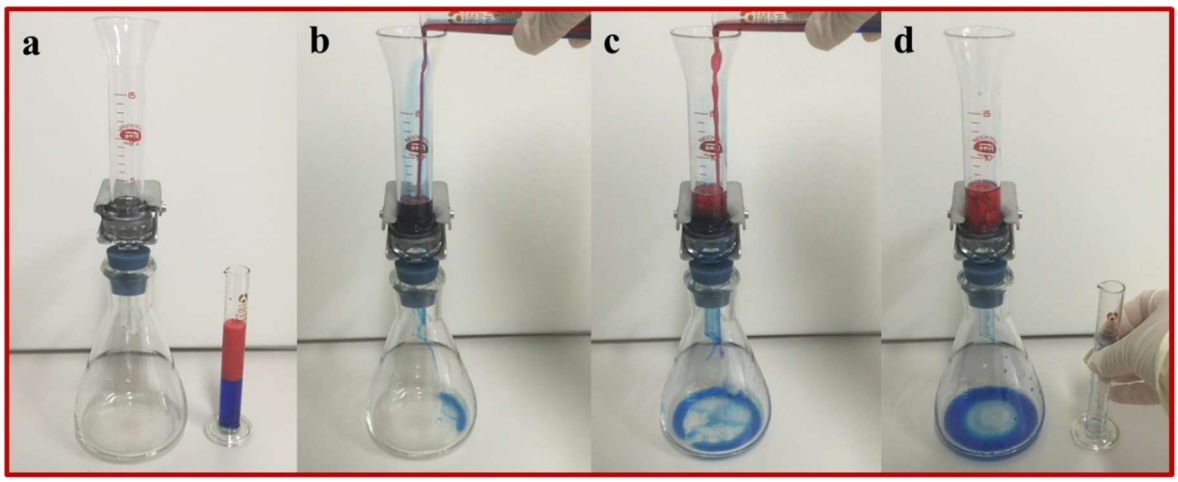

Fig. 5-4 A selective oil-water separation using the modified stainless steel mesh: (a) The oil water mixture and separation device were prepared, then (b) the mixture was poured into the device. (c) Oil passed through the modified stainless steel mesh, (d) while water was prevented from flowing down and retained above.

The theory created by Cassie and Baxter,[25] has been well-known as a classic theory, which indicates the superhydrophobicity formed from the water-air-solid interface. The air molecules locked in micro-nanostructures, water, and rough surface form the water-air-solid system. Similarly, the wetting behavior in the water-oil-solid system could also be explained by this strategy. The oil-water mixture was separated successfully only dependent on gravity by taking advantage of the feature of the superhydrophobic surface, which has indicated easy operation and low energy consumption of this strategy.

It is very important to spread the application of the asprepared device to different oil-water mixtures because of the oil spill accidents throughout the world, such as dichloromethane, toluene, gasoline, and chloroform. The separation property of the as-prepared device could be quantitatively described according to the separation efficiency, which was defined by water content in oil after separation. To investigate the oil-water separation, four kinds of mixtures were separated by the as-prepared device. Oil instantly penetrated through the modified mesh while water was retained above. The water content in oil after first separation was measured by Karl Fischer moisture titrator. As can be seen from Fig. 5-5, for different oil-water mixtures, water content in oil differed from one

another significantly before separation, because the solubility of oil in water exist large difference. The water contents in oil (dichloromethane, toluene, gasoline and chloroform) before separation were respectively 52 ppm, 48 ppm, 77 ppm and 99 ppm. Because of the better compatibility with water, chloroform showed a relatively high water content in oil. As can be observed in Fig. 5-6a, the values of water content in oil (dichloromethane, toluene, gasoline and chloroform) were respectively 770 ppm, 262 ppm, 133 ppm and 148 ppm. The water contents in oil of all the oil types showed substantial growth after separation, but the growth range differed from each other. Among all of the oil types, the water content growth range of dichloromethane showed the maximum value and that of chloroform showed the minimum value. This was because the different surface tension of dichloromethane and chloroform. The chloroform has relatively high viscosity and surface tension, when permeating through the separation device, chloroform coated on the inorganic modified mesh forming a chloroform liquid membrane due to its superoleophilicity. And then, the chloroform membrane with high surface tension performed a better bearing capacity of water compared with other oils where water was hard to leak through the device. For dichloromethane, the result was the opposite-dichloromethane performed relatively low bearing capacity of water due to its low surface tension. Therefore, the water content in dichloromethane after separation was high. Meanwhile, the flow rates of oil were calculated by measuring the passing time of the oil phase and shown in the same figure. The highest flow rates of 1.4 and 0.991 mh^{-1} were achieved from the gasoline-water and toluene-water mixtures, respectively, indicating the oil kinds had great influence on the penetrating rate. For chloroform, after stirring its mixture thoroughly, the oil-water mixture took a longer time to stratify. As a result, the oil flow rate was relatively low (0.586 mh^{-1}). Next, the as-prepared device was reused to separate a gasoline-water mixture for 6 times to verify its repeatability, and we had realized the tests of water content and flow rate for every circle. During the 6 cycle tests, the flow rate was about 1.0 mh^{-1} (Fig. 5-6b) and remained stable, and for each cycle of separation, the water content in oil was below 300 ppm (Fig. 5-6b), which was because

the superhydrophobic modified mesh only allowed oil penetrating. The results demonstrated that the superhydrophobic surfaces performed well, not only in the robustness and transparence but also in oil-water separation application, exhibiting integrated functions.

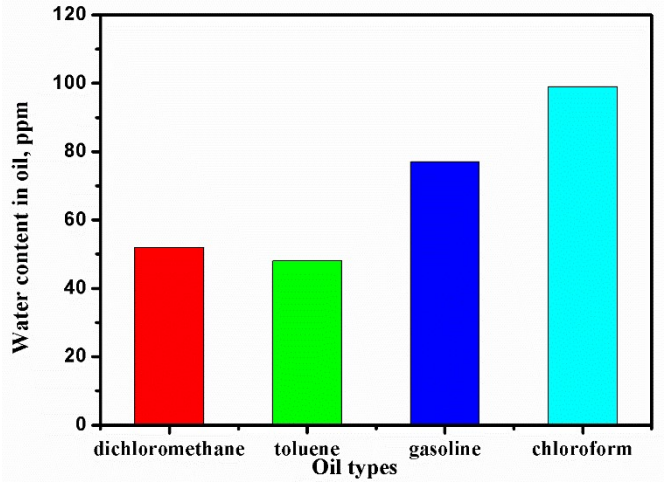

Fig. 5-5 Water content in oil of different oil types before oil-water separation

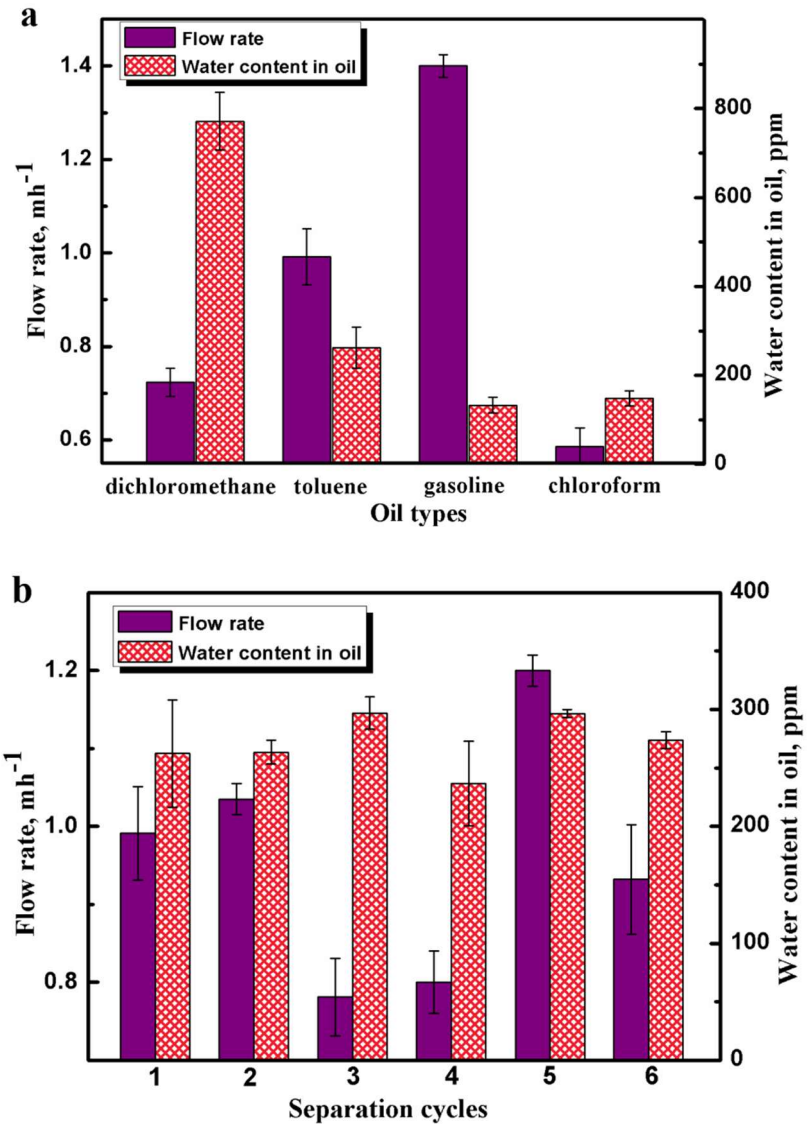

Fig.5-6 Oil-water separation results of the as-prepared device. (a) Water content in oil and flow rate for penetrating a series of immiscible oil-water mixtures. (b) Water content in oil and oil flow rate for penetrating gasoline-water mixture through the as-prepared device with different cycle index.

5.4 Conclusions

In summary, the author have developed a versatile and simple strategy to fabricate robust, transparent and superhydrophobic surface on quartz wafer and stainless steel mesh by a straightforward template method. Candle soot was used as rough surface template and then the roughness structure was reinforced by a filmy silica shell through the

chemical vapor deposition of $SiCl_4$. Further, the soot-silica shell coated substrate was calcined to remove template. Finally, the silica shell surface was modified into superhydrophobic and used for oil-water separation. The wettability of substrate surface before and after modification was tested. Meanwhile, the robustness, transparence and oil-water separation efficiency were investigated. The results revealed that the robust, transparent and superhydrophobic surface was successfully fabricated and the CA was 152.1°. The reinforced surface showed robustness against 210s sand abrasion with height of 40cm. In addition, the oil-water separation device revealed excellent separation efficiency and reusability in oil-water separation. The oil-water separation device has realized 6 times reuses and still remained excellent oil-water separation efficiency. It is believed that this superhydrophobic surface can be simply, flexibly, and robustly used in large-scale industrial applications where maintain harsh, transparent and oily environments, such as external wall coating, touch screen and oil-water separation material.

References

[1] Wang, S. T.; Liu, K. S.; Yao, X.; Jiang, L. Bioinspired Surfaces with Superwettability: New Insight on Theory, Design, and Applcations. Chem. Rev. 2015, 115, 8230−8293.

[2] Feng, L.; Li, S. H.; Li, Y. S.; Li, H. J.; Zhang, L. J.; Zhai, J.; Song, Y. L.; Liu, B. Q.; Jiang, L.; Zhu, D. B. Super-Hydrophobic Surfaces: from Natural to Artificial. Adv. Mater. 2002, 14, 1857−1860.

[3] Maguire-Boyle, S. J.; Barron, A. R. A New Functionalization Strategy for Oil/Water Separation Membranes. J. Membr. Sci. 2011, 382, 107−115.

[4] Alexander, S.; Eastoe, J.; Lord, A. M.; Guittard, F.; Barron, A. R. Branched Hydrocarbon Low Surface Energy Materials for Superhydrophobic Nanoparticle Derived Surfaces. ACS Appl. Mater. Interfaces 2016, 8, 660−666.

[5] Gao, X. F.; Yan, X.; Yao, X.; Xu, L.; Zhang, K.; Zhang, J. H.; Yang, B.; Jiang, L. The Dry-Style Antifogging Properties of Mosquito Compound Eyes and Artificial Analogues Prepared by Soft Lithography. Adv. Mater. 2007, 19, 2213−2217.

[6] Ye, C. Q.; Li, M. Z.; Hu, J. P.; Cheng, Q. F.; Jiang, L.; Song, Y. L. Highly Reflective Superhydrophobic White Coating Inspired by Poplar Leaf Hairs toward an Effective “Cool Roof. Energy Environ. Sci. 2011, 4, 3364−3367.

[7] Barthlott, W.; Neinhuis, C. Purity of The Sacred Lotus, or Escape from Contamination In Biological Surfaces. Planta. 1997, 202, 1−8.

[8] Nosonovsky, M.; Bhushan, B. Energy Transitions in Superhydrophobicity: Low Adhesion, Easy Flow and Bouncing. J. Phys.: Condens. Matter. 2008, 20, 395005.

[9] Pan, Q.; Wang, M.; Wang, H. Separating Small amount of Water and Hydrophobic Solvents by Novel Superhydrophobic Copper Meshes. Appl. Surf. Sci. 2008, 254, 6002−6006.

[10] Mishchenko, L.; Hatton, B.; Bahadur, V.; Taylor, J. A.; Krupenkin, T.; Aizenberg, J. Design of Ice-Free Nanostructured Surfaces Based on Repulsion of Impacting Water Droplets. ACS Nano 2010, 4, 7699−7707.

[11] Shi, F.; Niu, J.; Liu, J.; Liu, F.; Wang, Z.; Feng, X. Q.; Zhang, X. Towards Understanding Why a Superhydrophobic Coating is Needed by Water Striders. Adv. Mater. 2007, 19, 2257−2261.

[12] Ou, J.; Rothstein, J. P. Direct Velocity Measurements of the Flow Past Drag-Reducing Ultrahydrophobic Surfaces. Phys. Fluids 2005, 17, 103606.

[13] Ju, G. N.; Cheng, M. J.; Shi, F. A PH-Responsive Smart Surface for the Continuous Separation of Oil/Water/Oil Ternary Mixtures. NPG Asia Mater. 2014, 6, e111.

[14] Cheng, M. J.; Ju, G. N.; Jiang, C.; Zhang, Y. J.; Shi, F. Magnetically Directed Clean-Up of Underwater Oil Spills Through a Functionally Integrated Device. J. Mater. Chem. A. 2013, 1, 13411−13416.

[15] Ju, G. N.; Li, D. L.; Zhang, Y. J. Magnetically Driven Functionally Integrated Device for Continuous and Efficient Collection of Oil Droplets From Water. RSC Adv. 2016, 6, 20559−20564.

[16] Chen, B. Y.; Ju, G. N.; Sakai, E.; Qiu, J. H. Underwater Low Adhesive Hydrogel-Coated Functionally Integrated Device by One- Step Solution-Immersion Method for Oil-water Separation. RSC Adv. 2015, 5, 87055−87060.

[17] Zimmermann, J.; Reifler, F. A.; Fortunato, G.; Gerhardt, L. C.; Seeger, S. A Simple, One Step Approach to Durable and Robust Superhydrophobic Textiles. Adv. Funct. Mater. 2008, 18, 3662−3669.

[18] Zhu, L.; Shi, P.; Xue, J.; Wang, Y. Y.; Chen, Q. M.; Ding, J. F.; Wang, Q. J. Superhydrophobic Stability of Nanotube Array Surfaces under Impact and Static Forces. ACS Appl. Mater. Interfaces 2014, 6, 8073−8079.

[19] Zhu, Q.; Chu, Y.; Wang, Z. K.; Chen, N.; Lin, L.; Liu, F. T.; Pan, Q. M. Robust Superhydrophobic Polyurethane Sponge as a Highly Reusable Oil-Absorption Material. J. Mater. Chem. A 2013, 1, 5386−5393.

[20] Park, E. J.; Sim, J. K.; Jeong, M. G.Transparent and superhydrophobic films prepared with polydimethylsiloxane-coated silica nanoparticles. RSC Adv. 2013, 3, 12571-12576

[21] Ebert, D.; Bhushan, B. Transparent, superhydrophobic, and wear-resistant surfaces

using deep reactive ion etching on PDMS substrates. J. Colloid Interface Sci., 2016, 481, 82-90.

[22] Rao, A. V.; Latthe,; Nadargi, D. Y. Preparation of MTMS based transparent superhydrophobic silica films by sol–gel method. J. Colloid Interface Sci., 2009, 2, 484-490.

[24] Patankar, N. A. On The Modeling of Hhydrophobic Contact Angles on Rough Surfaces. Langmuir 2003, 19, 1249−1253.

[25] Cassie, A. B. D.; Baxter, S. Wettability of Porous Surfaces. Trans. Faraday Soc. 1944, 40, 546−551.

Chapter 6 Conclusions

To handle serious oil spills, many strategies have been proposed to design novel materials for oil–water separation. In the past decades, bioinspired surfaces with superwettability have been explored and utilized in oil-water separation. The underwater superoleophobic and superhydrophobic-superoleophilic materials were usually used for oil-water separation. However, their application has been limited because the complex fabricating process, fragile roughness structure, easy to be polluted and lose efficacy. Therefore, this study has aimed on developing simple and versatile strategies to fabricate low cost and robust oil-water separation devices with superwettability.

In Chapter 1, the research backgrounds, fundamental understandings of superwettability, research significance and research purpose were particularly described.

In Chapter 2, the experimental section was presented. The experimental materials, methods and characterizations were particularly described in this chapter.

In Chapter 3, the author develop a facile method for fabricating underwater low adhesive hydrogel-coated functionally integrated device to separate oil from mixtures with water. In particular, the commercially available nickel foams are functionalized by means of hydrogel coating. Compared with other preparation methods, the nickel foams coated by hydrogel are also a promising approach in oil-water separation. The technique is simple and easy to be scaled up, while the employed materials are inexpensive and some of them can be recycled. Therefore, I propose the use of the developed systems in the selective removal of little water from oil surface by means of a magnetic field, underwater superoleophobic, and water absorbing nickel foams from a distance toward the targeted areas with minimal energy consumption. By taking advantage of the superhydrophilic and underwater superoleophobic properties, I have realized the effective separation of oil-water mixtures, which demonstrated a re-collecting efficiency as high as 99.5%. What is more, it also can be reused 6 times and still had high separation

efficiency. The as-prepared device would provide a novel strategy for handling oil spills under various conditions and can be applied in other oil-water separating systems.

In Chapter 4, the author have developed a versatile and simple strategy to fabricate robust, self-cleaning and superhydrophobic surfaces for both soft and hard substrates by a straightforward spraying method. This superhydrophobic surface remained its superhydrophobicity and self-cleaning property even under oil immersion. Meanwhile, it showed remarkable robustness against knife scratch and sandpaper abrasion. In particular, the surface still retained its superhydrophobicity even after 30 abrasion cycles with sandpaper. Because of the superhydrophobicity under oil immersion, this surface could also be used for oil-water separation as well as showed excellent separation efficiency. Further, the oil-water separation device has realized 6 times reuses and still remained excellent oil-water separation efficiency. It is believed that the superhydrophobic surface can be simply, flexibly, and robustly used in large-scale industrial applications where maintain harsh and oily environments, such as external wall coating and oil-water separation material.

In Chapter 5, the author have developed a simple strategy to fabricate robust, transparent and superhydrophobic surface used for oil-water separation. Candle soot was used as rough surface template and then the roughness structure was reinforced through chemical vapor deposition of $SiCl_4$. Further, the surface was modified into superhydrophobic and used for oil-water separation. The wettability of substrate surface before and after modification was tested. Meanwhile, the robustness and oil-water separation efficiency were investigated. The results revealed that the robust, transparent and superhydrophobic surface was successfully fabricated and the CA was 151.6°. The reinforced surface showed robustness against 210s sand abrasion with height of 40cm. Further, the oil-water separation device revealed excellent separation efficiency and reusability in oil-water separation. The oil-water separation device has realized 6 times reuses and still remained excellent oil-water separation efficiency.

In chapter 6, general conclusions of the research were made.

Publications

Ⅰ．審査付投稿論文

[1] **Baiyi Chen**, Jianhui Qiu, Eiichi Sakai, Nobuhiro Kanazawa, Ruilu Liang, Huixia Feng. Robust and Superhydrophobic Surface Modification by a “Paint + Adhesive” Method: Applications in Self-Cleaning after Oil Contamination and Oil-Water Separation. ACS Applied Materials & Interfaces, 8 (2016) 17659−17667, (IF=7.145)

[2] **Baiyi Chen**, Guannan Ju, Eiichi Sakai, Jianhui Qiu. Underwater low adhesive hydrogel-coated functionally integrated device by a one-step solution-immersion method for oil-water separation. RSC Advances, 5 (2015) 87055-87060, (IF=3.289)

[3] **Baiyi Chen**, Jianhui Qiu, Huixia Feng. Synthesis and application of bilayer-surfactant-enveloped Fe_3O_4 nanoparticles: water-based bilayer-surfactant-enveloped ferrofluids. International Journal of Minerals, Metallurgy and Materials, 23 (2016) 234-240, (IF=0.882)

[4] Feng Huixia, **Chen Baiyi**, Zhang Deyi, Zhang Jianqiang, Tan Lin. Preparation and characterization of the cobalt ferrite nano-particles by reverse coprecipitation. Journal of Magnetism and Magnetic Materials, 356 (2014) 68-72, (IF=2.357)

[5] Huixia Feng, Bin Wang, Lin Tan, Nali Chen, Nuoxin Wang, **Baiyi Chen**. Polypyrrole/hexadecylpyridinium chloride-modified graphite oxide composites: Fabrication, characterization, and application in supercapacitors. Journal of Power Sources, 246 (2014) 621-628, (IF=6.333)

注：博士論文研究関連：2 編（（1）～（2））、その他：3 編（（3）～（5））

Ⅱ．国際会議論文・発表

[1] **Baiyi Chen**, Jianhui Qiu, Eiichi Sakai, Kazushi Itou, Huixia Feng, Nobuhiro Kanazawa. A novel functionally integrated device with durable and robust superhydrophobicity and its application in oil-water separation. 2016 12th China-Japan Joint Conference on Composite Materials (CJJCC), Kochi, Japan, September

14-18, 2016.

[2] **Baiyi Chen**, Haodao Mo, Jianhui Qiu, Kazushi Itou, Eiichi Sakai, Nobuhiro Kanazawa. Candle Soot as a Template for Transparent, Durable and Superhydrophobic Surface and its Application in Oil-Water Separation. 2016 12th China-Japan Joint Conference on Composite Materials (CJJCC), Kochi, Japan, September 14-18, 2016.

注：博士論文研究関連：2編

Ⅲ. 国内学会

[1] **陳 柏屹**、邱　建輝、境　英一. 水系二重層界面活性剤による Fe_3O_4 ナノ粒子の合成および磁流体への応用. 2014 年 9 月日本複合材料学会第 39 回複合材料シンポジウム、秋田市、講演論文集.

[2] **陳 柏屹**、邱　建輝、境　英一. 細孔構造制御したメソポーラスシリカの合成およびセルラーゼの固定化. 2015 年 9 月日本機械学会東北支部第 51 期秋季講演会、いわき市、講演論文集.

注：博士論文研究関連：0 編

Acknowledgements

I am very glad to express my thanks to a number of people without whom this study could not be possible. First and foremost, I would like to thank my advisor, Professor in Department of Machine Intelligence and Systems Engineering, Faculty of Systems Science and Technology, Akita Prefectural University, Dr. Jianhui Qiu. He imparted the knowledge of material science to me. And during the three years study period, his elaborated guidance, considerable encouragement and invaluable discussion make my research of great achievement and my study life unforgettable.

My deepest appreciation goes to the professors in Department of Machine Intelligence and Systems Engineering, Faculty of Systems Science and Technology at Akita Prefectural University, Dr. Mamoru Mizuno, Dr. Nobuhiro Kanazawa and Professor in Department of Mechanical Engineering and Robotics, Faculty of Textile Science and Technology at Shinshu University, Dr. Qingqing Ni for the comments and suggestions, whose advices have inestimable value for my research.

I sincerely appreciate the professors in Faculty of Systems Science and Technology at Akita Prefectural University, Dr. Kazushi Ito and Dr. Eiichi Sakai for the actual help and suggestions, whose advices have inestimable value for my research.

I appreciate the technical support from Dr. Jingming Wang, Dr. Ruilu Liang and Dr. Takao Komiyama in Akita Prefectural University. Thanks for the people who are paying attention to me for my study and life; Professor at Lanzhou University of Technology, Dr. Huixia Feng. And thanks also go to my peer research group members as well as all my surrounding friends, for their honest assistance to my research and warm care in daily life.

Baiyi Chen

2017.02